2005-01-01

Characterisation of an Acrylamide-based Photopolymer for Holographic Data Storage

Hosam Sherif
Technological University Dublin

Characterisation of an acrylamide-based photopolymer for holographic data storage

By

Hosam Sherif BSc

A thesis submitted to the Dublin Institute of Technology, for the degree of Master of Philosophy (MPhil)

School of Physics

Dublin Institute of Technology

Kevin Street, Dublin 8

2005

ABSTRACT

An acrylamide-based photopolymer, formulated in the Centre for Industrial and Engineering Optics, was investigated as a recording material for holographic data storage applications. Holographic data storage (HDS) is an optical storage technique, which theoretically allows densities as high as tens of TB/cm^2 with data transfer rates of many GB/s. HDS has unique advantages, such as the ability to perform parallel data searches (associative recall) and implement novel encryption techniques.

At present, many materials have been investigated to determine their suitability for use as HDS media. As yet, no one material possesses all the properties that are required to realise the huge benefits that HDS has to offer, these being large dynamic range, good optical quality, high sensitivity and resolution, temporal and dimensional stability, and low scattering. To aid in the characterisation of two of these properties, dynamic range and temporal stability, a test system for multiplexing plane gratings was developed. The system was designed to be modular so that its capabilities could be expanded upon at a later time, both in terms of optical setup and control software.

The test system has the ability to multiplex sets of holographic gratings with equalised diffraction efficiency using either angular or peristrophic multiplexing or a combination of the two techniques. This enables the photopolymer's dynamic range to be determined for many different formulations of photopolymer. In addition, it is possible to investigate the photopolymer's temporal stability in terms of material shrinkage and

diffraction efficiency by studying variations in the Bragg selectivity curve. The results of the dynamic range studies and temporal stability studies are presented in this thesis.

Finally, work was carried out to investigate the possibility of storing bit data pages (2-dimensional binary patterns) in the photopolymer. A phase-code multiplexing system was used to determine the necessary energy levels required to record data pages in the photopolymer. The recording period i.e. the period of time that it is possible to record data pages of good quality in the material, was also determined. All bit data page research was conducted in the Angewandte Physik, Westfälische Wilhelms-Universität, Germany.

DECLARATION

I certify that this thesis which I now submit for examination for the award of MPhil, is entirely my own work and has not been taken from the work of others save and to the extent that such work has been cited and acknowledged within the text of my work.

This thesis was prepared according to the regulations for postgraduate studies by research of the Dublin Institute of Technology and has not been submitted in whole or in part for an award in any other Institute or University.

The work reported on in this thesis conforms to the principles and requirements of the Institute's guidelines for ethics in research.

The Institute has permission to keep, or lend or to copy this thesis in whole or in part, on condition that any such use of the material or the thesis be duly acknowledged.

Signature Hosam Shaig Date 02/02/06

ACKNOWLEDGEMENTS

First and foremost, I would like to express my gratitude to Dr. Izabela Naydenova and Dr. Vincent Toal, my supervisors, for all the help and encouragement they gave me over the past two years. They were always generous in sharing their knowledge and time as well as providing me with the necessary guidance to bring this thesis to fruition. In addition, I would like to thank Dr. Suzanne Martin who gave me support and technical advice.

I would also like to thank my research colleagues from the Centre for Industrial and Engineering Optics, Sridhar Reddy-Guntaka, Raghavendra Jallapuram, Colm McGinn, Michael O'Hora, and everyone else from the IEO for their friendship and many coffee breaks shared. To this list, I would like to add everyone in the FOCAS building for their good-humoured attitudes and making my time in FOCAS an enjoyable one.

Additionally, I would like to thank the technical staff from the School of Physics and FOCAS building, which if it was not for their help I would have ran aground many a time. In particular, I would like to express my gratitude to Joe Keogh for his technical expertise. Furthermore, I would like to thank James Callis and Andrew Hartnett for their computer and networking assistance.

My sincerest thanks to Gernot Berger and Prof. Dr. Cornelia Denz of the Angewandte Physik, Westfälische Wilhelms-Universität in Muenster for allowing me the opportunity to work with their group and to use their facilities.

I would also like to thank my friends and family for all the encouragement and motivation they gave me throughout my academic career, and for being there for me whenever I needed.

Finally, I would like to acknowledge the DIT Faculty of Science for awarding me a Postgraduate Scholarship, the *FOCAS Institute* for providing laboratory facilities and office space, and COST Action P8 *Materials and Systems for Optical Data Storage and Processing* for funding my short-term scientific mission in Muenster, Germany.

CONTENTS

CHAPTER 1

1. Introduction

Due to the growing amounts of digital information generated each year [1] and the limitations of existing storage devices, there is increased pressure to develop new storage technologies that can keep pace with this growth.

At present, the storage capacities of optical and magnetic technologies such as DVDs (Digital Versatile Disks) and hard drives are increasing on a yearly basis [2, 3]. Both technologies rely on storing each data bit as variations of either optical or magnetic properties of the surface of the storage medium. Consequently, as the areal density of the bits increases, so too does the storage capacity of the medium.

There is reason to believe that this increase in storage capacity may not continue much longer. For instance, diffraction effects limit the bit size that can be resolved on an optical disk [2]. Currently the only means of increasing storage is to reduce the wavelength of light used, as is the case with HD-DVD [4] and Blu-ray [5] disks. Similar restrictions apply to hard drives, the main restriction being due to the superparamagnetism effect (SPE) [3] limiting the size of a magnetic dipole constituting one bit while remaining stable over time. It is for the reasons outlined above that alternative storage technologies must be developed.

Holographic data storage (HDS) may be one such technology. Not only does HDS have the potential for storing large amounts of data [6], it also has numerous advantages (see section 1.2), which are not possible to implement with current storage methods. What sets HDS apart from these technologies is that the entire volume of the recording medium is used to store information. Another benefit of HDS is that data pages can be multiplexed (superimposed) into the same volume of a medium allowing for the parallel recording and readout of data, thus achieving high data transfer rates with short access times [7].

The number of data pages that can be multiplexed is highly dependent on the angular selectivity, which in turn is dependent upon media properties and the recording geometry used. Angular selectivity is a measure of the range of angles by which the medium can be rotated relative to the readout beam whilst still fulfilling the Bragg condition. The higher the selectivity, the smaller the angular range that satisfies this condition. High selectivity is desirable as it allows a large set of data pages to be recorded when an angular multiplexing approach is employed. Each data page can be angularly shifted by smaller rotations from neighbouring pages. Since the Bragg condition for each page is only fulfilled for a much smaller angular range, the pages do not interfere negatively with one another.

The data pages themselves are encoded into the recording beam using a spatial light modulator (SLM), this being most commonly an addressable liquid crystal display consisting of a 2D array of elements. An example of a data page that would be imaged on an SLM can be seen below, figure 1.1.

Figure 1.1: The image above shows an example of a typical data page. This one consists of 60 x 80 bits represented by bright and dark squares.

The data written to, and read out from a holographic recording material is parallel as each page is essentially a two-dimensional data channel encoded into a laser beam. Thus, the read out latency of a HDS system is partially based on the sum of the times it takes for the readout beam to reach the medium, transverse it, and for the read out data to be imaged on the detector. While latency is dependent on the speed of light, the number of pixels encoded into each data page determines the throughput. This implies that throughput can be greatly increased by increasing the number of pixels of the SLM and imaging detector array.

The advent of commercial HDS systems and photopolymer media developed by companies such as InPhase Technologies, Optware, and Aprilis Inc., [8-10] indicates that the technology is no longer merely confined to optical benches. Now emphasis is on investigating different materials to find the optimum medium for this new technology. Many photopolymer materials have been investigated for their suitability as HDS media [11-15]. The work presented below was carried out to assess this material's performance in its current formulation and when doped with zeolite nanoparticles. This was done for photopolymer layers of different thicknesses.

A purpose built test system was developed to aid in the assessment of the photopolymer characteristics. The test system is computer controlled by means of software written using LabVIEW 7.0, which along with the self-developing capabilities of the photopolymer enables a high degree of automation in the experimental process. The system was used to determine the photopolymer's suitability in terms of dynamic range (amount by which the refractive index can be modulated). This was done by multiplexing a number of gratings in the same volume of layer. The material's temporal and dimensional stability were studied too.

The majority of the photopolymer characterisation carried out in this thesis was based on how gratings recorded under near identical experimental conditions varied depending on photopolymer composition and thickness. Diffraction gratings of a single spatial frequency were used for characterisation, as they are one of the simplest and well understood features that can be recorded holographically, i.e. a sinusoidal interference pattern consisting of a single spatial frequency.

1.1 Principles of optical and magnetic storage technologies

The advent of magnetic storage drives, such as the RAMAC (random-access method of accounting and control) disk drive developed by IBM [16] was a landmark event in terms of modern digital storage. Up until then, most digital data was stored on punch cards and to a lesser extent magnetic tape. This was an important transition as data could be stored in a relatively compact and portable form and could be made rewritable.

Magnetic storage having the potential for many technological and engineering improvements, enabled the capacity and reliability of these devices to dramatically increase over the past fifty years. However, it is uncertain whether constant technological advancements can be maintained much longer. For one, the phenomenon of superparamagnetism [17] may soon become a limiting factor as to how small the discrete magnetic domains in the hard disk platter can become before they start being randomly flipped by thermal fluctuations. The thermal energy required to flip the direction of the magnetic domain is the crystalline anisotropy energy [18]. As the domain size decreases so too do the crystalline anisotropy energy and the temperature at which superparamagnetism effects take place. This temperature depends on the properties of the magnetic coating in addition to the crystalline size.

Another widely used method to store information is optical data storage, examples of which are the ubiquitous CD and DVD. The successors to the DVD format come in the form of HD-DVD and Blu-ray disks. These disks can store 15 and 25 GB of information in a single layer, respectively. This is a marked improvement compared with the 4.7 GB capacity of single-sided single-layered DVDs. The increase in capacity is a result of HD-DVD and Blu-ray drives using a laser diode, which can be focused to a much

smaller spot size thus allowing readout of smaller features on the disk surface. The wavelength of the laser, 405 nm in this case, and the numerical aperture of the lens determine the minimum spot size to which the laser can be focused [2]. The future of this "land and pit" optical storage approach depends largely on whether smaller wavelength lasers and higher numerical apertures can be used, along with the successful use of *near field* optical techniques. Without these improvements being implemented, effects such as the diffraction limit may put a cap on the further increase of optical storage capacities.

1.2 Advantages of holographic data storage systems

Besides having the potential to store vast amounts of data [19-20], holographic data storage opens up the possibility of optically performing tasks that would otherwise be carried out electronically in a computer processor. These include associative and fuzzy recall [20] for conducting database searches, data encryption, and arithmetic operations. All of these tasks with the exception of fuzzy recall have been demonstrated using a phase-code multiplexing system developed by Denz et al. [21]. The advantage of performing a database search optically by the method of associative recall is that it is parallel. Every data page recorded is searched simultaneously and at the speed it takes light to traverse the particular holographic storage medium; this can be seen in figure 1.2.

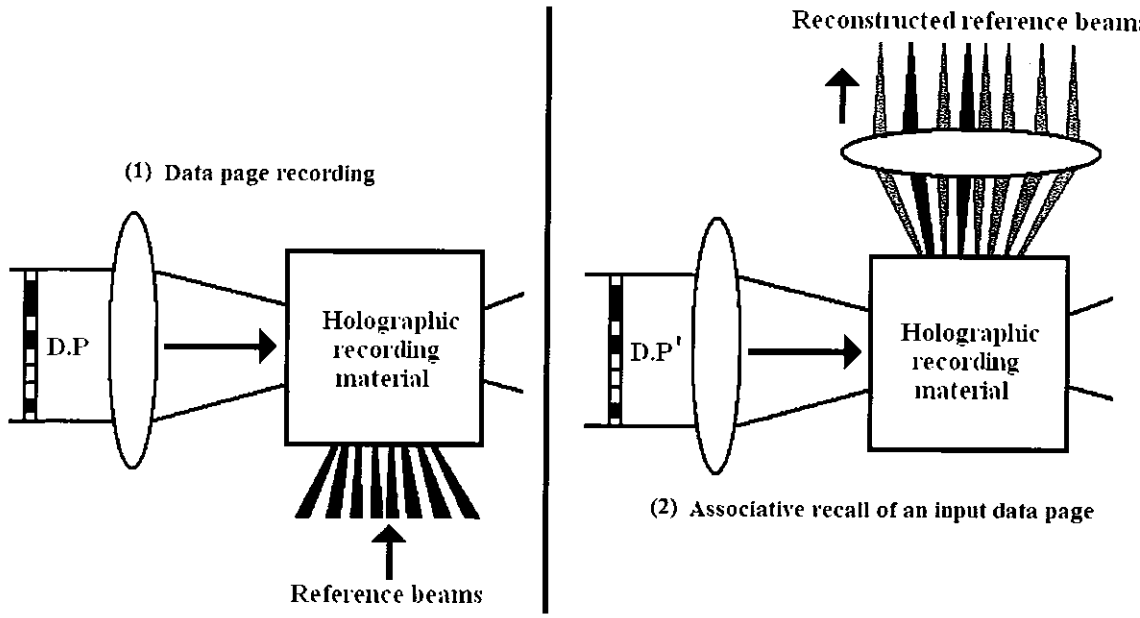

Figure 1.2: Database search performed using associative recall in a phase code multiplexing system. In (1), D.P. is a stored data page, which is recorded as a hologram with a set of phase-coded reference beams. In (2), a data page D.P.' is used to address the medium. If D.P.' resembles any stored data page in the volume the reference beams used to record it will be partially reconstructed, the intensity of the reconstructed beams are proportional to the similarity between D.P.' and the stored data pages.

To conduct a search, a complete or partial data page query (D.P.') is used to address the medium. Reference beams that were used to record similar pages to the query data page will be reconstructed with varying intensities depending on the degree of similarity between the query data page and that of the pages stored within the medium. The intensities of the reconstructed reference beams are therefore an indicator of the degree of similarity between the corresponding pages and the page in question and give information regarding the page's location in the storage medium. To access one of the matches, the appropriate reference beam angle (if the system relies on the technique of angular multiplexing) or the correct phase-code (if it relies on phase multiplexing) must be used. This search method works equally well with analogue images and therefore can be used to create an image archive. For instance, if a number of images are multiplexed into a storage medium, a small portion of one of those images could be used to

determine the location of the corresponding image in the database as well as the locations of other similar images [22].

Fuzzy recall is a data-encoding search method developed by Ashley et al. [20]. It is another content-addressable search method similar to the previous example, but differs in that a small portion of the SLM is used to encode attributes relating to the data page or image. A portion of the SLM is divided into 1D pixel tracks that encode specific attributes pertaining to the data page/image as a block of bright pixels. It is the position of the block along the 1D track that determines the value encoded into it. This produces what can be equated to a bright "slider" on a dark 1D track. To conduct a search the storage medium is addressed from the side of the storage medium that the object beam would normally be reconstructed. This means that the object beam is now used to reconstruct the reference beams. The "fuzzy" aspect of the search is due to the query being encoded as a pixel block in a 1D track. If the query slider and the stored slider block overlap completely, the reference beam that was used to record the corresponding data page/image will be reconstructed and will have maximum intensity. If there is only a partial overlap, the reference beam will have a lower intensity relating to the amount of overlap between query and stored slider. An example of how a fuzzy search could be carried out can be seen in figure 1.3. Many different attributes may be encoded as sliders for each data page/image.

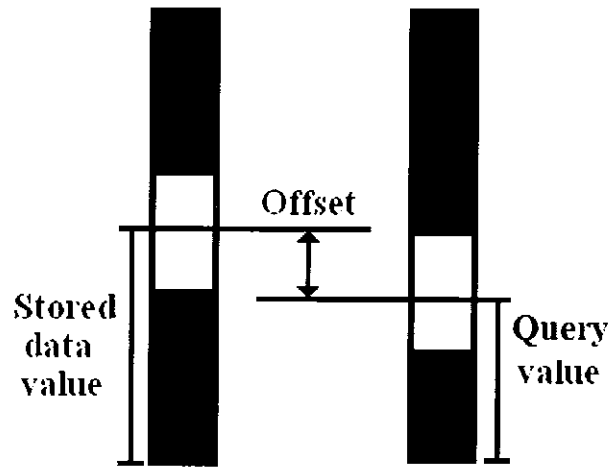

Figure 1.3: The area of overlap between the bright region on the stored data track and the query track will determine the correlation between the stored page/image and the user query.

In addition, HDS provides the possibility of performing optical arithmetic operations between stored data pages [23]. This enables image or data processing to be carried out at the data readout stage rather than just being the preserve of the computer processor, see figure 1.4. Sets of pages can be added, subtracted or inverted, these being equivalent to the logical operations OR, XOR, and NOT respectively. Using phase-code multiplexing techniques, these operations can be carried out by reducing the selectivity of the reference phase-code in such a way as to allow more than one page to be reconstructed simultaneously. For instance to perform addition (OR) of two pages it is necessary to use only a subset of a phase-code, one that is exclusively common to both data pages. Subtraction (XOR) is carried out in a similar manner but this time the medium is referenced with an inverted phase-code, one that is π radians out of phase. To invert (NOT) a data page it is required that a plane wave hologram be stored as a separate page along with the other data pages. To carry out the inversion it is a matter of subtracting the relevant page from a fully bright page. It should be noted that the combined operations of NOT and OR are equivalent to a NOR operation. It has been shown that all other logical operations can be carried out using specific combinations of

NOR operations [24]. This leads to the possibility of carrying out quite complex tasks during the readout stage.

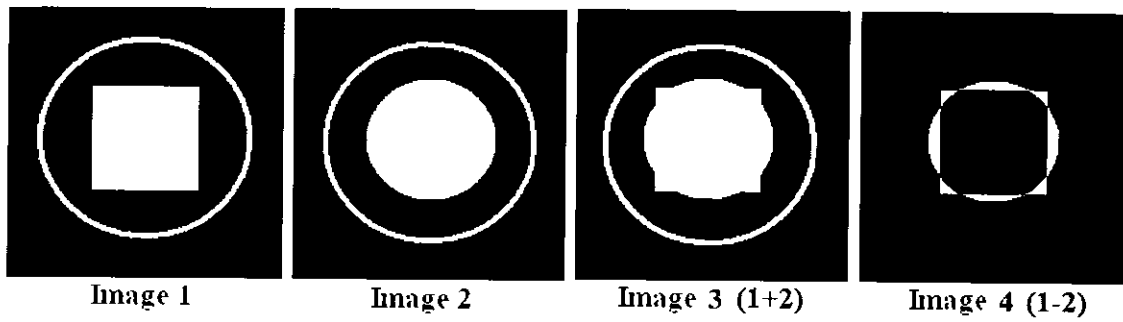

Figure 1.4: Optical arithmetic operations performed on two holographic images, images 1 and 2, by means of HDS. Image 3 shows the result of adding images 1 and 2 together; likewise image 4 shows the result of subtracting image 1 from 2.

Another advantage of HDS is that it allows for unique methods of data encryption [25 - 27]. One such method takes advantage of the ability of phase-code multiplexing by applying optical arithmetic operations between data pages as discussed previously. The information to be encrypted is distributed throughout all the recorded data pages using a combination of OR, XOR, and NOT operations. Even if the data pages can be accessed, the information encrypted in them will not be accessible unless the correct sequence of arithmetic operations is known. Decrypting the information entails reducing the selectivity of the phase-codes during readout so that the necessary arithmetic operations can be performed between the data pages as described in the previous paragraph. This means the decryption key comprises information relating to the operations used to encrypt the pages and the sequence of these operations. The probability of "cracking" this form of encryption depends on the number of data pages stored, i.e. the number of combinations of the phase-codes used. The probability of decryption is described in eqn. 1.1 [25],

$$P_a(N) = \left[\sum_{i=0}^{n-1} 2^i \binom{N}{2^i} \right]^{-1} \qquad (1.1)$$

where $N = 2^n$ is the number of data pages recorded.

N	64	256	512
P_a (N)	1.7×10^{-20}	1.4×10^{-78}	8.8×10^{-156}

Table 1.1: Probability of decrypting information stored for various numbers of holograms recorded. A greater number of holograms result in a lower probability of decryption.

A second method involves encrypting the location of the data pages rather than the pages themselves. To achieve this, the phase-codes used to encode the reference beams are distorted by the addition of a random phase mask in the reference beam arm. To access the pages, the phase mask must remain in place during both recording and reconstruction of the pages. If the phase mask is taken out of the system and the phase-codes are used to address the storage medium, all that is retrieved are meaningless pages composed of partial segments of all the data pages. The phase mask acts as a key that encodes the correct locations of the pages and must be in place for proper reconstruction of the data. The probability of decrypting this code and effectively determining the correct phase mask to use is given by equation 1.2 [25],

$$P_r(N) = k.\frac{(N/k)!^k}{N!} \qquad (1.2)$$

N is the number of data pages stored in the medium and k is a measure of how close the phase values have to be matched. If k = 5, then a precision of ± (π/5)/2 in the phase value is sufficient for correct reconstruction. The probabilities for decrypting 64 to 512 data pages are tabulated below.

N	64	256	512
P_a (N)	2.8×10^{-41}	2.7×10^{-174}	1.2×10^{-352}

Table 1.2: Probability of decrypting code and determining correct phase mask, when k is equal to 5.

1.3 Objectives

As stated previously, the objective of this work is to characterise various formulations of an acrylamide-based photopolymer developed in the Centre for Industrial and Engineering Optics (CIEO), Dublin Institute of Technology, for use as a HDS medium.

Achieving this objective entails the design and construction of a test system consisting of optical components, electronic hardware, and software written using the LabVIEW programming language. The system is to be automated to the level where multiplexing experiments can be conducted in a matter of minutes per experiment as opposed to hours. This reduction in experimental time is due in part to the software being able to control various instruments such as rotational stages, electronic shutters, and perform data acquisition using a PCI DAQ card.

The software interface should be intuitive with the capability of displaying experimental results in an appropriate and easily interpretable graphical manner. Since several separate types of experiment are to be conducted using the test system, the software needs to reflect this by being modular thus allowing the user the ability to freely switch between different experimental modes. When a new experimental procedure needs to be conducted, the software should be written in a way that additional LabVIEW code can be incorporated in a modular fashion that does not interfere with the functionality of the other software components.

Finally, the feasibility of recording data pages in the photopolymer will be investigated by means of a phase-code multiplexing system. This incorporates a SLM and CCD array for recording and playing back data pages.

1.4 Summary

Since the development of optical and magnetic media, storage capacity has been steadily increasing. Unfortunately, this increase is not sustainable. Fundamental limitations such as the superparamagnetism effect and the diffraction limit will eventually abate this increase in capacity. Holographic data storage is a technology being developed with the intention of superseding current storage technologies. It gives rise to capacities on the order of terabytes/cm^2, with data transfer rates of tens of Gigabytes/s. In addition to this vast increase in capacity, HDS has a number of unique advantages compared with present day technologies. This is due to the highly parallel way in which data is stored. Advantages include associative and fuzzy searching, simultaneous arithmetic operations, and novel encryption methods. The huge benefits of HDS have resulted in a number of companies being established with the goal of

commercialising the technology. Each of these companies is developing their own HDS systems and accompanying photopolymer-based storage media. It is the aim of this work to develop a test system to aid in characterisation of a photopolymer developed in the Centre for Industrial and Engineering Optics, with the goal of optimising its formulation specifically for HDS applications.

1.5 References

[1] P. Lyman, H. R. Varian, "How much info 2003", www.sims.berkeley.edu/research/projects/how-much-info-2003/.

[2] H. Coufal, G. Burr, "Optical data storage", International Trends in Optics, 2002.

[3] D. A. Thompson, J. S. Best, "The future of magnetic data storage technology", IBM Journal of Research and Development, Vol. 44 No. 3 May 2000.

[4] HD-DVD Promotion Group, http://www.hddvdprg.com/, 2005.

[5] Blu-ray Disc Founders, "Blu-ray disc format, 4 Key Technologies" http://www.blu-raydisc.com/assets/downloadablefile/4_keytechnologies-12835.pdf Aug. 2004.

[6] D. Psaltis, F. Mok, "Holographic Memories," Scientific American, 273, No. 5, 70, 1995.

[7] R. M. Shelby, J. A. Hoffnagle, G. W. Burr, C. M. Jefferson, M. -P. Bernal, H. Coufal, R. K. Grygier, H. Gunther, R. M. Macfarlane, and G. T. Sincerbox, "Pixel–matched holographic data storage with megabit pages", Optics Letters, 22(19): 1509–1511, 1997.

[8] InPhase Technologies homepage, http://www.inphase-tech.com/, 2005.

[9] Optware homepage, http://www.optware.co.jp/english/index_tech.htm, 2005.

[10] Aprilis Inc. homepage, http://www.aprilisinc.com/, 2005.

[11] L. Dhar, A. Hale, H. E. Katz, M. L. Schilling, M. G. Schones, F. C. Schilling, "Recording media that exhibit high dynamic range for digital holographic data storage", Optics Letters, Vol. 24, No. 7, April 1999.

[12] A. Pu, K. Curtis, D. Psaltis, "Exposure schedule for multiplexing holograms in photopolymer films", Optical Engineering, 35 (10): 2824-2829 Oct 1996.

[13] R. T. Ingwall, D. Waldman, "CROP photopolymers for hologram recording", Holography, 11, 2, December 2000.

[14] K. Y. Hsu, S. H. Lin, Y. -N. Hsiao, W. T. Whang, "Experimental characterization of phenanthrenequinone-doped poly (methylmethacrylate) photopolymer for volume holographic storage", Optical Engineering, 42(5) 1390-1396 May 2003.

[15] H. Sherif, I. Naydenova, S. Martin, C. McGinn, and V. Toal "Characterization of an acrylamide-based photopolymer for data storage utilizing holographic angular multiplexing", Journal of Optics A: Pure Applied Optics, 7, 255-260, 2005.

[16] M. L. Lesser, J. W. Haanstra, "The Random-Access Memory Accounting Machine-I. System Organization of the IBM 305", IBM Journal of Research and Development, 1, 62-71, 1957.

[17] M. Albrecht and G. Schatz: "Magnetic nanostructures: The next generation of magnetic data storage?", NanoS 1, 19, 2005.

[18] L. Ranno, "Applications: Information storage", Ecole Franco-Rounmaine: Magnétisme des systèmes nanoscopiques et structures hybrides - Brasov, 2003.

[19] G. W. Burr, E. Mecher, T. Juchem, H. Coufal, C. M. Jefferson, M. Jurich, F. Gallego, K. Meerholz, N. Hampp, J. A. Hoffnagle, R. M. Macfarlane, R. M. Shelby, "Progress in read-write fast-access volume holographic data storage", SPIE Conference on Three- and Four- Dimensional optical Data Storage, 4459-52, July 2001.

[20] J. Ashley, M. -P. Bernal, G. W. Burr, H. Coufal, H. Guenther, J. A. Hoffnagle, C. M. Jefferson, B. Marcus, R. M. Macfarlane, R. M. Shelby, and G. T. Sincerbox "Holographic Data Storage", IBM Journal of Research and Development, Vol. 44, No. 3, May 2000.

[21] C. Denz, K. -O. Müller, F. Visinka, T. Tschudi, "A Demonstration Platform for Phase-Coded Multiplexing" Published in "Holographic Data Storage", H. Coufal, D. Psaltis, G. Sincerbox (Eds.), Springer, S. 419-428, 2000.

[22] G. Berger, C. Denz, S. S. Orlov, B. Phillips, L. Hesselink, "Associative recall in a volume holographic storage system based on phase-code multiplexing", Applied Physics B, 73, 839-845, 2001.

[23] K. –O. Müller, C. Denz, T. Rauch, T. Heimann, T. Tschudi, "High capacity holographic data storage based on phase-coded multiplexing", Optical Memory and Neural Networks, Vol. 7, No. 1, 1998.

[24] T. L. Floyd, "Digital Fundamentals" 7th Ed., Prentice Hall International, Inc. 237-239, 2000.

[25] G. Berger, K. -O. Müller, C. Denz, I. Földvári, Á. Péter, "Digital data storage in a phase-encoded holographic memory system: data quality and security", In: Advanced Optical Storage, H.J. Coufal, ed., SPIE Proc. 4988, 2003.

[26] X. Tan, O. Matoba, T. Shimura, K. Kuroda, B. Javidi, "Secure optical storage that uses fully phase encryption", Applied Optics, Vol. 39, No. 35, Dec. 2000.

[27] X. Tan, O. Matoba, T. Shimura, K. Kuroda, "Improvement in holographic storage capacity by use of double-random phase encryption", Applied Optics, Vol. 40, No. 26, 4721-4727, Sept. 2001.

CHAPTER 2

2. Principles of holography

This chapter briefly discusses the history and principles of recording plane wave holograms and how different types of holograms are categorised. Since the holographic gratings recorded in the photopolymer for this work are phase holograms, descriptions of transmission and reflection phase holograms are also given attention.

The field of holography can be traced back to research conducted by Bragg [1] in x-ray crystallography. Bragg had been able to form the image of a crystal lattice by means of diffraction from the photographically recorded x-ray diffraction pattern of the lattice, thus leading to the development of the Bragg x-ray microscope.

Bragg's method was limited as the phase information naturally occurring within light was discarded. Therefore, the method could only be used for certain types of objects, such as crystal lattices, for which the absolute phase of the diffracted field could be predicted. It took the insight of Dennis Gabor in 1948 [2] to extend Bragg's work. He reasoned that the phase of the diffracted wave could be determined by comparison with a standard reference wave, his aim being to increase the resolution of electron microscopy. Gabor proposed recording the scattered electron field of an object irradiated with electrons and then reconstructing the image from this record with visible light. In order to demonstrate this he used light waves to record the image thus paving the way for optical holography.

2.1 Holographic theory

The fundamental differences between holography and photography are best understood by examining each separately.

In the case of photography, a two-dimensional intensity distribution of a three-dimensional scene is recorded in a light sensitive medium. All information pertaining to the relative phases (i.e. optical path differences between the light waves from different points in the scene) is lost. In general, each scene consists of a large amount of reflecting and radiating points of light. The waves from each of these individual points contribute to a complete wavefront. An optical lens is used to convert this intricate wavefront into an image of the radiating object. The photographic image thus, consists of differing intensity regions, but carries no optical path information.

Holography differs from photography in that the optically formed image is not recorded, rather the complete object wave is [3]. The wave is recorded in such a way that subsequent illumination of the record serves to reconstruct the original object wave, even when the original object is absent. When reconstructed, the image is practically indistinguishable from the original, maintaining both phase and amplitude information of the original scene.

Since photographic media can only record variations of light intensity, a method for converting phase and amplitude information into variations of light intensity is required. This is achieved by recording the resulting interference pattern of two waves, one wave being the object wave of interest and the second a reference wave. The reference wave is usually an easily reproducible plane or spherical wave. The intensity of any given

point in the interference pattern will contain information regarding both the phase and amplitude of the object and reference waves. By subsequently illuminating the photographically recorded interference pattern with the reference wave, light is diffracted in such a way that the object wave is reconstructed.

2.2 Types of holograms

Conceptually, holograms can be categorised as being either thick or thin, based on the relationship between the fringe spacing of the holographically recorded grating and the thickness of the recording medium. If the fringe spacing is relatively small compared with the grating thickness, the hologram is considered thick and is known as a *volume hologram*. Conversely, if the fringe spacing is large compared with the thickness, the hologram is regarded as being thin.

A criterion that determines whether a hologram is thick or thin is known as the Q *parameter* [3]. This is defined in equation 2.1 as,

$$Q = \frac{2\pi\lambda_0 d}{n_0 \Lambda^2} \qquad (2.1)$$

where λ_0 is the wavelength of light, d is the thickness of the layer, n_0 is the refractive index, and Λ is the spatial period of the grating. In general, values of $Q < 1$ imply that the layer is thin, while values of $Q > 1$ correspond to thick layers. This is only a general rule because instances contradicting this definition have been demonstrated [4].

Thick holographic layers, more commonly referred to as volume holograms, can be used to record reflection and transmission holograms. The photosensitive layer thickness is sufficiently large that fringe planes can be recorded parallel to the layer plane. Reflection holograms are recorded by illuminating a holographic medium from opposite sides, whilst a transmission hologram is recorded by having two beams incident on the layer from the same side.

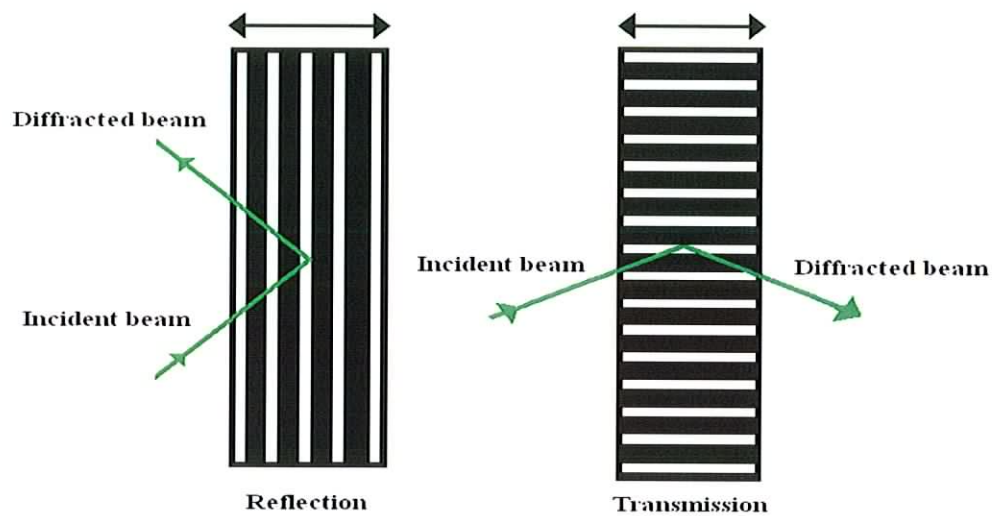

Figure 2.1: Example of fringe patterns occurring in reflection and transmission holographic gratings.

A hologram can be recorded as a variation of the transmittance of the material, leading to an amplitude hologram. Likewise, it may be recorded as a variation of the refractive index, leading to a phase hologram. As a result, six main classifications of hologram exist, table 2.1.

	Transmission hologram	**Reflection hologram**	**Thin hologram**
Amplitude	Transmission amplitude	Reflection amplitude	Thin amplitude
Phase	Transmission phase	Reflection phase	Thin phase

Table 2.1: Six main hologram classifications.

Both transmission and reflection phase holograms are described in more detail in sections 2.2.1 and 2.2.2 respectively.

2.2.1 Transmission phase holograms

Holograms recorded in thick recording media (thick being approximately tens of microns) can be classified either as being transmission amplitude/phase holograms or reflection amplitude/phase holograms [3], see table 2.1. The term *transmission* indicates that the reference beam must be transmitted through the hologram in order for the image to be reconstructed.

Initially, the recording medium has uniform refractive index. However, after recording, a variation of the refractive index develops in the direction perpendicular to the interference surfaces. As a result, the interference surfaces are also perpendicular to the hologram plane, figure 2.1. This fringe orientation arises because the two interfering wavefronts make equal but opposite angles normal to the surface of the photosensitive layer and are incident from the same side of the layer. In order to reconstruct a hologram with maximum diffraction of the incident reference wave, the reference wave must pass through the recording medium at the same angle as during recording.

Adjusting the bisector angle of the incident beams so that it is no longer normal to the layer, results in a slanted fringe pattern being formed. Recording slanted fringes in a layer can be beneficial as it enables changes in the layer thickness before and after grating recording to be determined. This is due to the dependency of the slant angle of the grating on layer thickness. Therefore reconstructing the grating with maximum diffraction efficiency will require that the reference beam angle be changed with respect

to the grating. In section 6.3, slanted gratings are used to characterise the shrinkage of various photopolymer layers.

2.2.2 Reflection phase holograms

Unlike a hologram recorded in transmission mode whose fringes are perpendicular to the layer, reflection holograms are recorded with fringes parallel to the layer, figure 2.1. This type of hologram is recorded by illuminating the layer with two beams incident from opposite sides of the layer. Consequently, the object beam is reconstructed on the same side of the layer as the reference beam used to reconstruct it. The image is virtual and is seen by the viewer to be located on the opposite side of the layer.

Reflection holograms have the property that they can be reconstructed by means of white light. The fringe pattern recorded in the holographic material has a spatial period that is determined by the wavelength of laser light used to record it. When the material is illuminated with white light, only light of the same wavelength as used to record the hologram is reflected. All other wavelength components are transmitted through the medium.

2.3 Summary

Holography is a relatively new field of optics, originating from research conducted by Bragg in x-ray crystallography and Dennis Gabor's work on increasing the resolution of electron microscopes. Holography differs from photography in that holograms retain both the phase and amplitude information of a recorded wavefront emanating from an object, unlike photographs which merely record the amplitude variations of the light from an object. Thus holograms have the ability to reproduce a 3D image, which is indistinguishable from the original object. The object is recorded using two beams, one to illuminate it and a reference beam to interfere with the object beam, thus creating an interference pattern in the medium. When the hologram is illuminated with light of appropriate wavelength, the object wave is reconstructed.

There are a number of different ways of categorising holograms. One of the chief distinctions is determined by the mode of recording. If a spatially varying phase shift or variation in the amplitude of the light passing through the hologram occurs upon illumination, a phase or amplitude hologram is recorded. Holograms can also be regarded as being *thick* or *thin*, depending on the ratio of the hologram's thickness to the fringe spacing. If the fringe spacing is large compared with the hologram it is considered *thin* and vice versa. Lastly, holograms can be recorded in either reflection or transmission mode. A reflection hologram is formed when the fringes making up the hologram are recorded parallel to the layer, whilst a transmission hologram has fringes perpendicular to the layer. Gratings having slanted fringes with respect the layer normal can also be recorded. In section 6.3, slanted gratings are utilised to quantify layer shrinkage. For the purposes of this work all photopolymer characterisation was carried out using thick phase transmission holograms.

2.4 References

[1] W. L. Bragg, "The X-Ray Microscope", Nature, Vol. 149, 470-471, No. 3782, April, 1942.

[2] P. Hariharan, "Optical Holography, Principles, techniques and applications" 2nd Ed. Cambridge University Press, 1996.

[3] E. Hecht, "Optics" 3rd Ed. Addison-Wesley, 1998.

[4] R. Alferness, "Analysis of propagation at the second-order Bragg angle of a thick holographic grating", Journal of the Optical Society of America, 66, 353-62, 1976.

CHAPTER 3

3. HDS materials and recording techniques

The first HDS systems were demonstrated by Anderson et al. in 1968 [1] and by Langdon et al. in 1970 [2]. Each system consisted of an array of 32 x 32 holograms with each hologram being composed of 1024 bits of data. The capacity of both these systems was approximately 0.125 MB. Since then, technological advances such as the development of highly coherent laser diodes, high resolution liquid crystal SLMs, and megapixel detector arrays have significantly increased the potential storage capacities and data transfer rates of HDS systems. Holographic media research, carried out in parallel with these hardware advances, has led to the development of new materials that are highly stable, sensitive, and have improved dynamic range. Storage densities of 250 bits/μm^{-2} with access times of microseconds and transfer rates of 20 GB/s have been demonstrated in such materials [3].

In this chapter an overview of the present state of holographic data storage is discussed. Two different data storage systems, WORM (write-once read-many) and *erasable write-once-read-many times*, and the types of materials most commonly used for each system are detailed in sections 3.1 and 3.2 respectively. Some of the main advantages and disadvantages of using photopolymer materials for HDS are discussed in section 3.1.1. In section 3.3 particular attention is paid to the photopolymer system developed by the Centre of Industrial and Engineering Optics in the Dublin Institute of Technology. The photopolymer was characterised by means of the test system

specifically developed for that purpose. The most common methods of multiplexing holographic information are then elaborated upon in section 3.4. This is of interest as the increase in capacity provided by HDS is mainly due to multiple 2D data pages being multiplexed (superimposed) in the same volume of holographic recording material. Finally, HDS systems and photopolymer materials that are nearing commercialisation are examined in section 3.5.

3.1 Photopolymer WORM systems

The two most common types of holographic materials used for HDS are photopolymer systems such as the one characterised for this work [4], as well as photorefractive crystals like iron-doped lithium niobate and bismuth telluride [5, 6]. Photopolymer systems tend to be used for WORM media [7] whereas *erasable write-once-read-many times* systems have been predominately implemented using photorefractive crystals [8].

WORM storage has been a valuable method of storing data for a very long time; a book is an obvious example of a WORM storage device. An example from the digital domain would be a CD or DVD-ROM. These devices are mass produced with digital data already recorded on them. This data can be read back at a later stage but not changed or overwritten in any way.

A photopolymer WORM material such as the one investigated in this thesis enables a hologram to be stored in the material's volume by means of localised photopolymerisation [4]. When an optical interference pattern is imaged in the material, sites of constructive interference produce a polymerisation of monomers in that region. A reduction in the density of the material at dark regions is observed as well. This

reduction is attributed to monomer diffusion from these dark regions into brighter regions, aiding in further polymer chain formation. A corresponding change in the refractive index and absorption coefficient of the material occurs as a result. The spatial change in absorption of the material produces an amplitude hologram. This is of little concern with regard to this thesis, as subsequent bleaching of the photopolymer eliminates this amplitude hologram. What is of most significance is the spatial variation of the refractive index as this is what ultimately produces a transmission phase hologram.

3.1.1 Advantages and disadvantages of photopolymer systems

Photopolymer materials exhibit a number of properties making them suitable for HDS. For example, they can be moulded into any shape unlike photorefractive crystals. This has the commercial benefit that a HDS medium can be moulded to be dimensionally equivalent to the ubiquitous CD/DVD format. A HDS system designed to read such a format could conceivably be backward compatible with these other optical formats. This approach has been taken by Optware and Aprilis in designing their new HDS system architecture and media. Besides offering flexibility in media design, photopolymer materials can be made cheaply and in bulk like these other optical formats.

Another material requirement for a HDS media is that the recording process must be relatively straightforward without the need for post-processing. Photopolymers fulfil this need because they can be self-developing without needing to be dried after recording. In contrast, holographic recording materials such as silver halide or dichromated gelatin [9], both require wet processing followed by drying.

Photopolymer materials are also noted for having high dynamic ranges, whereby the greater the possible refractive index modulation the greater the achievable dynamic range. Since the majority of HDS systems rely on multiplexing to achieve high storage capacities, a higher dynamic range means more holograms can be multiplexed into the same volume of material.

The photopolymer developed in the Centre for Industrial and Engineering Optics is characterised by high sensitivity (1400 cm/J). High sensitivity is an attribute any potential holographic data medium will need in order to facilitate fast writing speeds. If the sensitivity is low, longer exposure times and higher recording intensities are needed to produce holograms with the desired diffraction efficiency.

Photopolymer materials have the additional benefit that their chemistry can be formulated quite readily to achieve long shelf life and archival characteristics. Adjusting or adding dopants can optimise the photopolymer system depending on the particular requirements of the storage system.

A disadvantage many photopolymer systems suffer from is dimensional instability such as material shrinkage, which in turn can lead to low readout fidelity; this is elucidated in section 4.2.2. Another drawback of photopolymer systems is that until now, most have been developed for WORM memory applications, where data is written to the material once and then read out many times. This is not suitable for dynamic memory applications such as PCs and computer servers where data is constantly being stored, updated, or deleted. Recording in this way requires a photopolymer that can be written to and read from many times. A WORM photopolymer system is not completely disadvantageous though, as this approach is the method of choice for media and

software distribution. Proprietary information is printed onto the CD or DVD-ROM in bulk and can then be accessed at a later stage but not recorded over.

3.2 *Erasable write-once read-many times* photorefractive crystals

A second important group of materials often used for HDS are inorganic photorefractive crystals doped with either rare earth metals or transition metals such as manganese, iron, cerium etc. [5]. The most commonly used photorefractive crystal is iron doped lithium niobate [10]. Crystals such as strontium barium niobate, bismuth telluride, barium titanate, to name but a few, have also been investigated as potential candidates for use as holographic materials [11].

The photorefractive effect is the physical mechanism that enables these materials to store holographic information [5]. When an interference pattern is created in the bulk of the crystal by means of two writing beams, electrons in the bright fringe regions are raised into the conduction band where they redistribute. This redistribution of charge carriers tends toward dark fringe regions where the electrons are trapped at crystal defects. Therefore, a net diffusion of electrons from light to dark areas of the material occurs. This spatial modulation of the electric field in turn leads to a corresponding local change in the refractive index. Redistribution of electrons back into the conduction band is possible with further illumination of spatially uniform light. This restores the local refraction index to the mean value, effectively erasing any hologram recorded in the crystal [12].

Photorefractive crystals have a number of characteristics that make them well suited as holographic storage media. These include: real-time response, ability to be doped, dimensional stability, and good optical quality [13]. A drawback of photorefractive crystals is that they exhibit the undesirable property of having a slow recording rate, which is usually a factor of 5-50 times slower than the readout rate at a given lasing power [14].

Erasing or altering a particular data page in a set of multiplexed pages is a non-trivial matter, further adding to the materials disadvantages and thus making them better suited for use in erasable WORM system. Data-books can be written in a crystal and read out as necessary, but when a page in a particular book needs to be updated, the whole book would have to be rerecorded with the changes made [12].

3.3 Photopolymer developed at the Centre for Industrial and Engineering Optics

The photopolymer developed in the Centre for Industrial and Engineering Optics is an acrylamide-based self-developing dry layer [4]. It consists of a polyvinylalcohol binder in which a monomer, an electron donor, and dye sensitizer are dissolved. Erythrosine B is used as the dye sensitizer as it is sensitive to the recording wavelength of the lasers used. When a dye molecule absorbs a photon in the presence of an electron donor, free radicals are produced that cause local polymerisation of the acrylamide. A corresponding variation occurs in the local refractive index of the material [15]. This variation is not only attributed to bond conversion in the polymerisation process, but also the secondary effect, whereby a local density modulation occurs as monomers migrate into polymer regions during recording. Evidence exits that there is a counter

diffusion of oligomers from bright to dark regions of the material. This has a negative effect on the overall refractive index modulation.

The photopolymerisation process begins when an erythrosine B molecule (EB) absorbs a photon of light and is promoted to an excited singlet state. It may return to a ground state by radiationless transfer, i.e. fluorescence quenching. Alternatively, it may transfer to an excited triplet state through intersystem crossing and react with the electron donor, triethanolamine (TEA), to produce a dye radical and a triethanolamine free radical.

$$EB + h\nu = {}^{1}EB^{*} \text{ (absorption of light)} \quad (3.1)$$

$${}^{1}EB^{*} = {}^{3}EB^{*} \text{ (intersystem crossing)} \quad (3.2)$$

$${}^{3}EB^{*} + TEA = EB\bullet + TEA\bullet \text{ (dye reduction-electron transfer)} \quad (3.3)$$

By itself, the dye radical is not normally reactive enough to initiate polymerisation. The polymerisation is usually due to the triethanolamine radical reacting with an acrylamide molecule (ACR).

$$TEA\bullet + ACR = TEA - ACR\bullet \text{ (initiation)} \quad (3.4)$$

$$TEA - ACR\bullet + ACR = TEA - (ACR)_2\bullet \text{ (propagation)} \quad (3.5)$$

Finally, two methods of terminating the reaction may occur [9, 16]. These are shown in reactions (3.6) and (3.7). For polymer chains undergoing termination, no new radicals are created, and the process of acrylamide monomer polymerisation ceases. Termination by *combination* occurs when two growing chain ends come into contact, thus allowing the two unpaired carbon electrons to create a chemical bond as they form a pair.

$$\text{TEA - (ACR)}_n\bullet + \text{TEA - (ACR)}_m\bullet = \text{TEA -(ACR)}_{n+m}\text{-TEA}$$

(termination by combination) (3.6)

The second form of termination, known as *disproportionation*, occurs when two chain ends come in contact. The unpaired electron from the first chain end pairs with an electron from the carbon-hydrogen bond. The carbon-hydrogen bond belongs to the carbon atom adjacent to the carbon radical from the second chain end. The unpaired electron from the initial polymer chain takes the hydrogen atom from the carbon-hydrogen bond and so is paired off, thus terminating the polymer chain. The polymer that has given up the hydrogen atom now has two free radicals. It is then possible for the end carbon radical of the chain and neighbouring carbon radical to join their unpaired electrons and to form a double bond, allowing this polymer chain to be terminated.

$$\text{TEA - (ACR)}_n\bullet + \text{TEA - (ACR)}_m\bullet = \text{TEA - (ACR)}_n + \text{m}$$

(termination by disproportionation) (3.7)

3.4 Multiplexing methods

All HDS systems described thus far rely on various multiplexing methods to store large amounts of data in the recording medium. This section takes a look at some of the most commonly used multiplexing methods, which allow more than one hologram to be stored in the same volume of a material. The holograms themselves can be accessed independently. Any particular page of data can be readout by illuminating the stored holograms with the reference wave that was used to store that page. The reference wave is diffracted by the interference patterns in such a manner that only the desired data page is reconstructed. This enables content addressable searching.

3.4.1 Angular multiplexing

With angular multiplexing, the holographic medium is rotated using out-of-plane angular steps between recordings. For reconstruction, the reference beam has to be at the same angular orientation as it was during recording to allow for full reconstruction of the data page. By varying this angle, the reconstruction efficiency of the hologram can be decreased in accordance with the Bragg condition. By utilizing this angular dependence for hologram recording, it is possible to record many holograms at different incident angles in the same volume of material, figure 3.2. Hundreds or even thousands of holograms can be recorded in this manner depending on the available dynamic range of the recording material, thickness, and spatial frequency of recording [17].

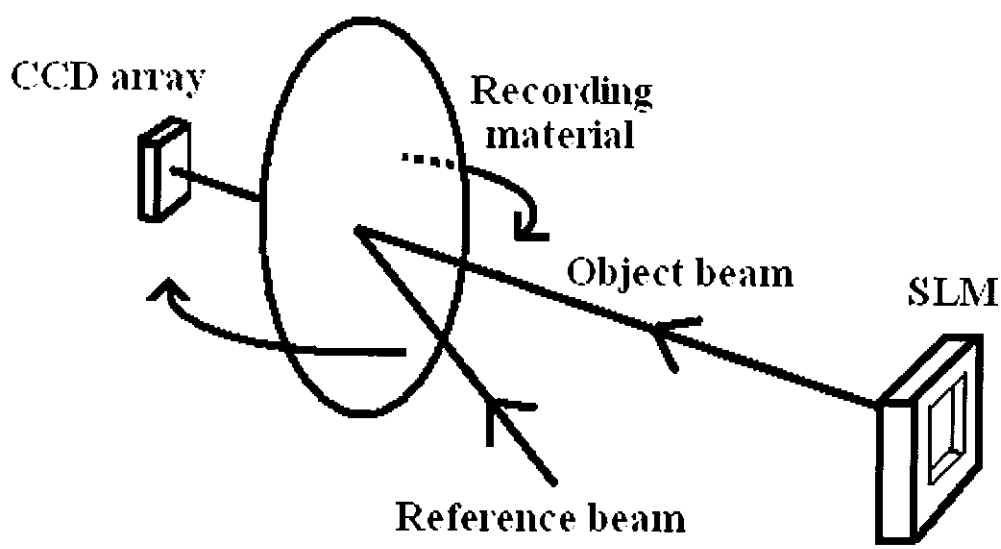

Figure 3.2: An angular multiplexing geometry requires that the recording medium be angularly rotated out of plane with respect to the incident object and reference beams.

3.4.2 Peristrophic multiplexing

Peristrophic multiplexing requires the recording medium be rotated in-plane between hologram recording, as the object and reference beams remain fixed, figure 3.3. Rotating a hologram in this manner achieves two things. Firstly, the reconstructed image is shifted away from the detector and secondly the holograms are Bragg detuned with respect one another [18]. As with all spatial multiplexing techniques, the angle of the reading beam with respect to the hologram has to satisfy the Bragg condition for complete hologram reconstruction. One drawback of implementing peristrophic multiplexing is that the angular selectivity of a recorded hologram is lower than if angularly multiplexed. The selectivity is effectively decreased because, when reconstructed, the holographic image sweeps over the detector array for an extended period as the medium is rotated in-plane, thus broadening the selectivity curve from the viewpoint of the detector. This effect can be minimised by matching and reducing the hologram and detector array areas. Additionally, an aperture can be positioned on the same optical path as the hologram image and detector so that neighbouring holograms will be obscured. [18]

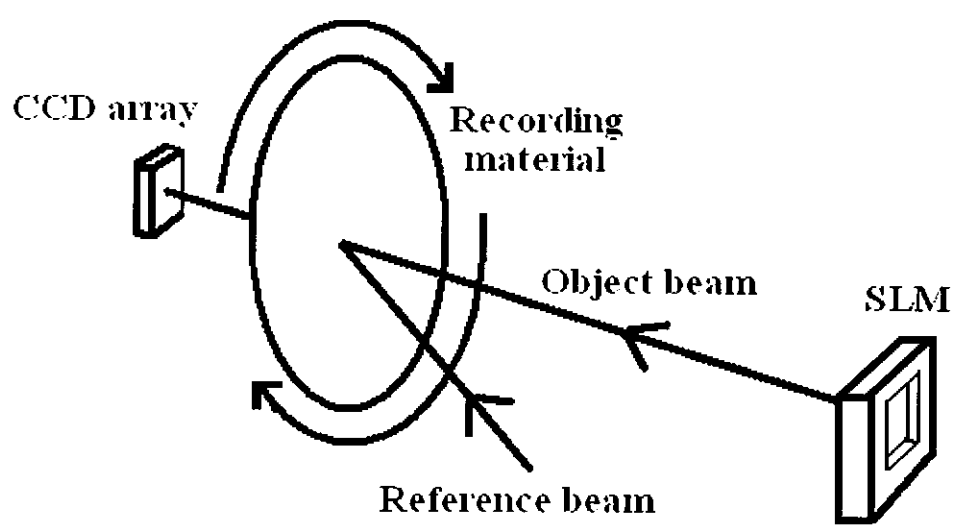

Figure 3.3: Spatial peristrophic multiplexing requires that the holographic recording medium be rotated in-plane between each recording.

3.4.3 Shift multiplexing

The technique of shift multiplexing [19, 20] is implemented by recording a hologram in a recording medium, then repositioning the reference and object beam slightly so that the location of the next hologram recorded is slightly shifted relative to the first. This can be repeated until the entire dynamic range of the material is consumed. To achieve high shift selectivity and reduce crosstalk between holograms, a spherical reference beam wave can be used. Alternatively, a pseudorandom phase mask in the reference beam path generates a speckle pattern that increases the selectivity further [17].

3.4.4 Phase-code multiplexing

As with other multiplexing methods, phase-code multiplexing requires that an object and reference beam be used to record a complex refractive index modulation in a material. A data page can then be encoded as a two-dimensional intensity variation of the signal beam by means of a spatial light modulator. One of the main advantages of implementing phase-code multiplexing in a HDS system is that it does not require moving parts, unlike peristrophic and angular multiplexing [21, 22].

A phase modulator is placed in the reference arm allowing the beam to be divided into n individual reference beams. These beams are each incident upon the holographic medium having an angular separation that obeys the Bragg condition. To achieve angular separation, the beams are focused using a biconvex lens, figure 3.4.

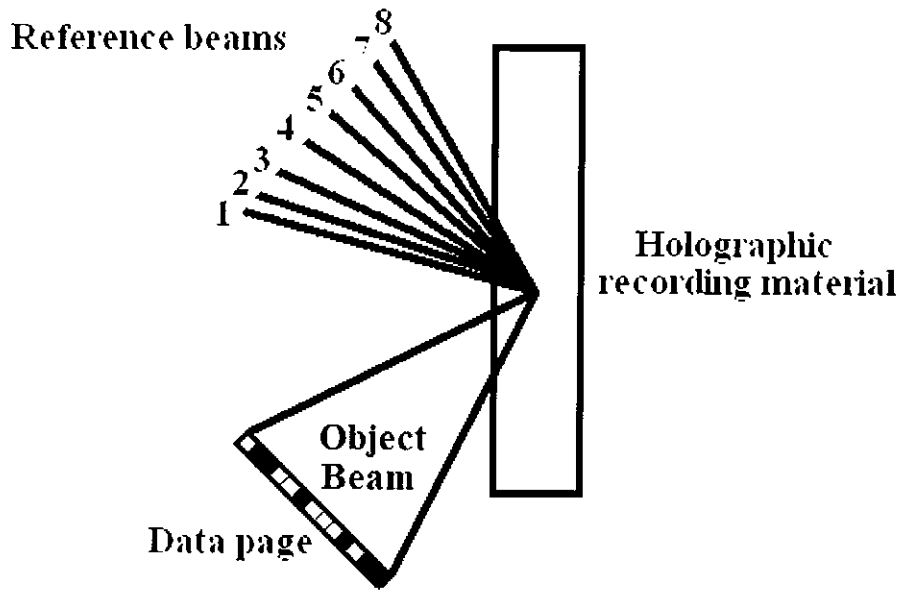

Figure 3.4: Using the above phase-code multiplexing system it would be possible to record eight data pages, as the phase-code would only be eight units in length.

Unlike angularly multiplexed holograms, which are addressed with a single reference beam of appropriate angle, phase-code multiplexing relies on all reference beams being incident on the recording medium simultaneously. Recording and playback of a hologram thus relies on the relative phase shifts such as 0 or π being introduced in each of the incident reference beams.

The pattern of 0 and π phase shifts applied to the set of reference beams is known as the phase-code. To playback any specific hologram without crosstalk, the appropriate phase-code must be used [22]. All the multiplexed holograms are reconstructed simultaneously but since orthogonal phase-codes are used (such as the Walsh Hadamard codes [23]), all non-relevant holograms destructively interfere with one other, allowing only the hologram of interest to be reconstructed. Phase-code multiplexing therefore allows for a high signal-to-noise ratio when compared with other methods of multiplexing. Below is an example of the Walsh Hadamard phase code, figure 3.5.

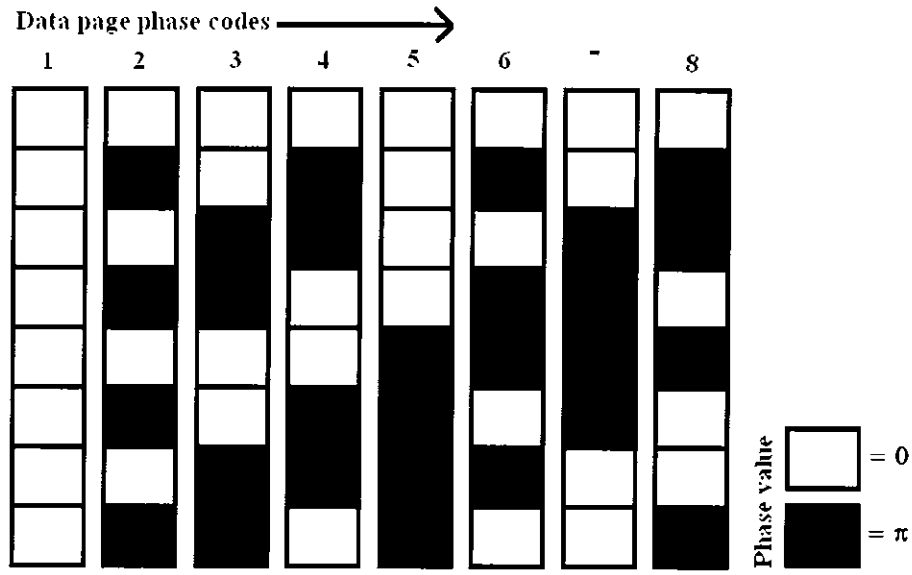

Figure 3.5: Walsh Hadamard phase code used to multiplex eight data pages. The codes are comprised of 0 and π phase shifts.

3.4.5 Wavelength multiplexing

Wavelength multiplexing [24] is normally carried out in conjunction with other multiplexing methods. As the name implies, wavelength multiplexing is based on the principle that holograms are wavelength selective and so exhibit a strong dependence on reference beam wavelength for adequate reconstruction. Therefore, changing the wavelength of the reference beam between recordings allows multiple data pages to be recorded. As of yet, it is not practical to use wavelength multiplexing as the main multiplexing method in current systems as modern lasers have quite a low tuning range.

3.4.6 Polytopic multiplexing

When multiplexing data pages in a volume of material it is desirable that thick photopolymer media (approximately 1 mm) be used as this leads to an increase in dynamic range and Bragg selectivity. However, in the case of angular multiplexing, an

optimal medium thickness exists. Increasing the thickness beyond this point does not produce a corresponding increase in storage capacity [25]. This is due to the surface area of the media limiting how close stacks of multiplexed data pages (may be thought of as *data books*) can be recorded. As the medium becomes thicker, so do the volume and the surface area each book takes up. For adequate playback of any data page, the data books should be separated so crosstalk between neighbouring books is reduced. Separating the books at the surface of the medium has the drawback that interior regions of the material are wasted, as gaps between the books no longer have data recorded in them. This is illustrated in figure 3.6.

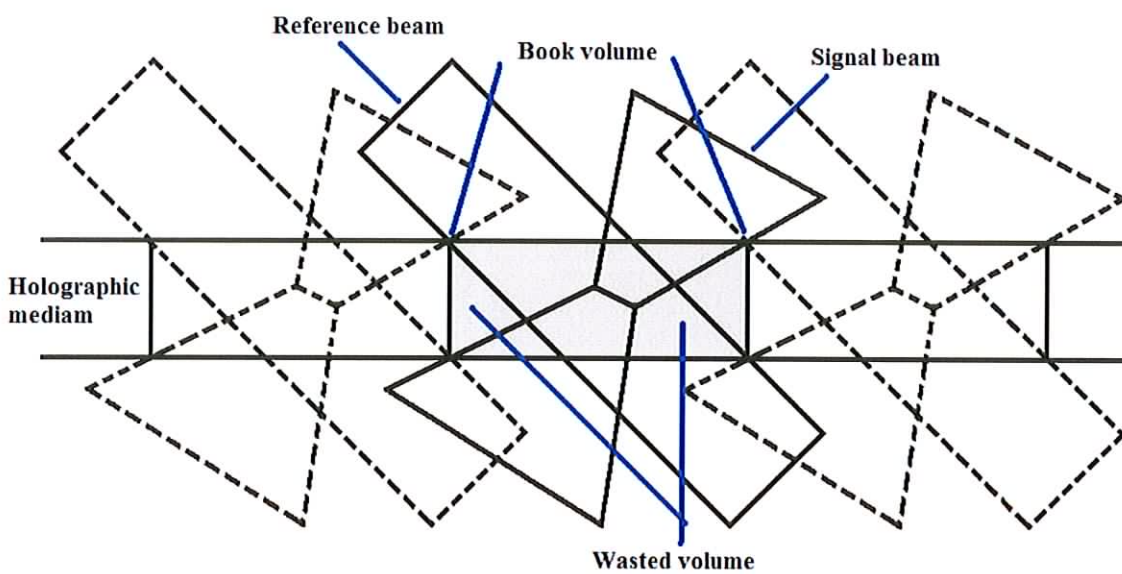

Figure 3.6: Data books that are angularly multiplexed in a holographic medium require that the books be sufficiently shifted with respect one another in such a way that the readout beam only reconstructs the data page of interest. It is due to this geometrical limitation that regions of the medium are wasted.

Using a technique known as polytopic (Greek for *many places*) multiplexing [25], it is possible to bypass the geometric limit of recording and so effectively utilise the full volume of the medium by recording in what otherwise would be wasted regions of the material. Polytopic multiplexing, allows many books to overlap without having to

decease the angular sweep necessary to multiplex a significant number of data pages, figure 3.7. Although the data books overlap in the medium volume, the Fourier planes of each reconstructed book do not. The Fourier planes, containing the Fourier transforms of the data pages, are imaged external to the medium. A Fourier lens is used to focus the signal beam through the layer whereupon it encounters an aperture located on the other side of the medium before being imaged on to a detector array. When reading out a specific page the reference beam simultaneously reconstructs several of the books whilst the aperture placed in the Fourier plane physically blocks data pages of neighbouring books from being imaged on the detector array.

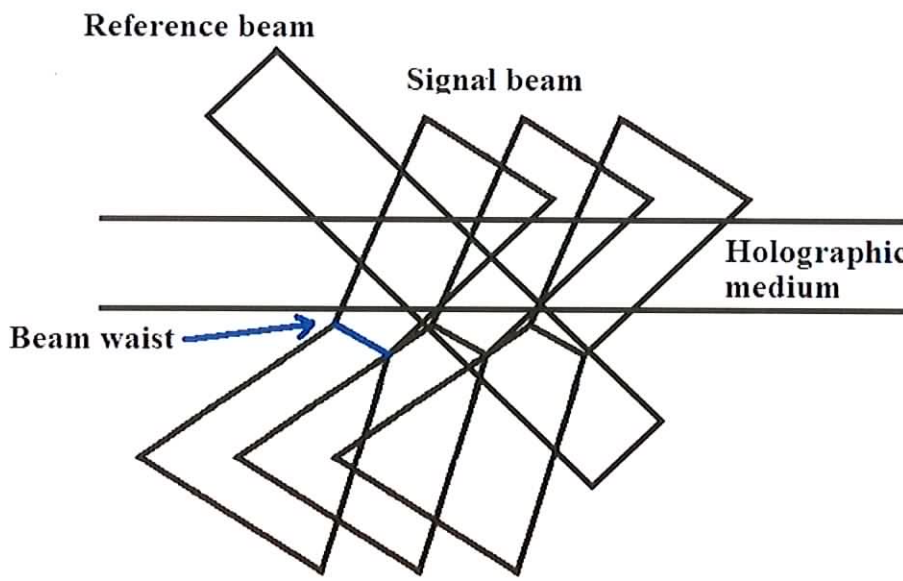

Figure 3.7: With polytopic multiplexing, very little if any volume of the recording medium is wasted, as there is overlap of the data books. It is only required that the Fourier planes of the books be separated from one another. This occurs externally to the recording medium.

Thus, the limiting factor when separating out the overlapping books is to make sure that they are separated by at least the Fourier width of the data beam, as opposed to the maximum width of the beam at the surface of the medium. The aperture size is designed

to produce the best optical SNR performance and density, and as such should be tuned to the bandwidth of the pages being stored [25].

3.5 Current holographic data storage systems and media

Research in the field of HDS is primarily carried out by a number of university groups around the world. A relatively small number of companies have also been active in trying to commercialise HDS systems for industrial and home use. This section looks at the storage media and system technologies that these companies are developing.

Originating out of Bell Laboratories in 2000, InPhase Technologies has carried out significant work in commercialising HDS. The four holographic media known as Tapestry™, which InPhase developed, are all based on a two-chemistry system composed of a low refractive index matrix precursor and a high refractive index monomer [26]. These chemical systems are independently polymerisable allowing the monomer to remain unpolymerised until illuminated. The medium has been sensitised to both green and blue laser light and has demonstrated a storage capacity of 200 GB in a 13 cm diameter coupon disk, with a thickness of 2 mm [27, 28]. A manufacturing process known as Zerowave™ is used to create a layer which has an optical flatness of $> \lambda/4$. This means that the surface of the layer does not vary in height by more than 50 nm over the full diameter. Currently Tapestry™ media are WORM systems and as such are most suitable to archival and entertainment media purposes. Further work to increase the Tapestry™ media storage capacity to the terabyte range is underway.

InPhase's HDS system relies on a combination of angle multiplexing [17] and polytopic multiplexing [25] to achieve high storage capacity. Multiple data pages are stored in the medium in an overlapping formation. These are then accessed by small translations of the medium with respect to the incident signal and reference beams. Data page positional information is impressed on the reference beam in the form of phase information, amplitude information, and the angular differences induced by translation of the medium with respect to the reference beam. In contrast to multiplexing methods that rely on the Bragg condition being fulfilled for optimal data page reconstruction; polytopic multiplexing requires that the reference beam be centred on a particular hologram with an accuracy determined by the correlation function of the reference beam.

Aprilis Inc. is another company making progress in developing a viable HDS system and photopolymer recording medium. It was founded as an independent start-up company in 1999 to commercialise the CROP (cationic ring-opening polymerisation) photopolymer technology developed by Polaroid [29, 30].

The photopolymer consists of an oxirane monomer binder as opposed to the more commonly used vinyl monomer. Consequently, photopolymer shrinkage is reduced as the oxirane monomer relies on cationic ring-opening polymerisation compared with conventional free-radical polymerisation as seen with vinyl monomers. Low material shrinkage is important as it is required for high data page fidelity.

In November 2000, the HDSS consortium successfully demonstrated data transfer rates of 1 Gbit/s using the Aprilis media. Storage capacities up to 200 GB were supported in a disk of 120 mm diameter and dimensionally similar to that of CD format. [17].

Optware, a Japanese based company, has contributed to the realisation of HDS systems. Pioneering a technique known as *collinear holography*, [31] Optware has placed emphasis on backwards compatibility with CD/DVD standards, along with the reduction in optical components and simplification of the optical design of a HDS system. The company has been active in pursuing an international standard for HDS, thus providing a definite technological path, which can be improved upon and optimised in the future. They have developed three WORM storage media that rely on a proprietary photopolymer chemistry that is sensitive to a wavelength of 532 nm. These WORM systems consist of a disk shaped cartridge, which is claimed to have a storage capacity of 200 GB, a credit card sized layer that can store 30 GB, and a 100 GB holographic disk with a diameter of 120 mm [32].

The collinear optical design that is employed for recording and data playback from these media can be seen as an improvement over traditional multiplexing systems because it eliminates the need for separate reference and object beam arms in the setup, figure 3.8. These two beams are aligned on a common coaxial light path by means of a dichroic mirror thus creating a complex interference pattern in the medium. Data pages are shift multiplexed into the disk by rotating the disk with respect to the optical arrangement. As already stated the medium is sensitive to light of wavelength 532 nm while a 650 nm laser is used to readout the data pages without further photopolymerisation of the medium.

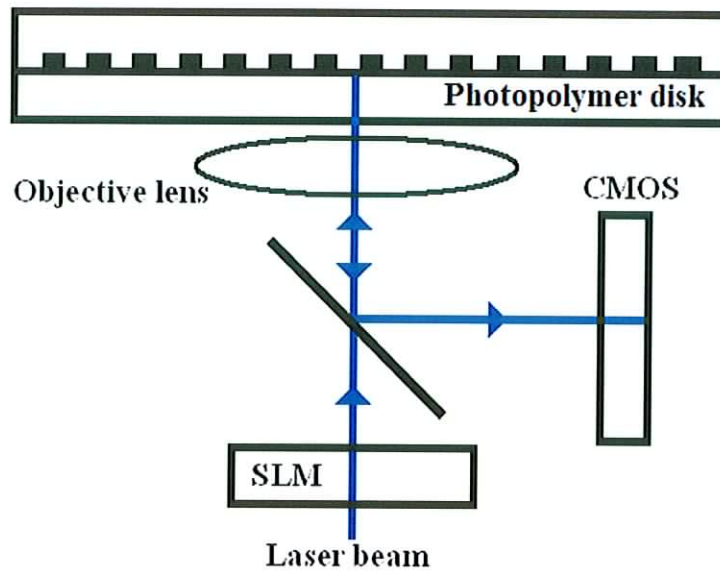

Figure 3.8: The collinear optical design used by Optware reduces the number of components in the system.

3.6 Summary

Holographic data storage systems were first developed in the late 1960s. Although these systems had limited capacities (≈ 0.125 MB), they were instrumental in demonstrating the feasibility of holographically encoding and storing information. By 2000, HDS systems had progressed to the point where densities of 250 bits/μm^{-2} with access times of microseconds and transfer rates of 20 GB/s were being routinely demonstrated. High data densities are achieved by recording the data in the form of 2D bit data pages, which are multiplexed into a volume of material. Maximising the density requires that as many pages as possible are recorded in the same volume, with each data page encoding at least a million bits of data. There are a number of methods of multiplexing data into the material. For this work, both angular and peristrophic multiplexing were employed.

Currently most HDS research is aimed towards developing WORM media (recording data permanently) and erasable WORM media (blocks of data can be rerecorded). The most popular WORM materials being investigated are photopolymers and inorganic photorefractive crystals. Photopolymers have many advantages compared with photorefractive crystals, which include: self-development, being a dry layer, good optical quality, easily mouldable into any shape, inexpensive to produce in bulk, and having high sensitivity and dynamic range. Companies such as InPhase Technologies, Optware, and Aprilis Inc have manufactured photopolymer systems that possess a number of these properties. Work is currently being carried out to characterise the Centre for Industrial and Engineering Optics photopolymer. It is hoped that this work, along with further optimisation of its composition will produce a photopolymer with properties conducive to HDS.

3.7 References

[1] L. K. Anderson, "Holographic optical Memory for Bulk Data Storage", Bell Laboratories Record, Vol. 46, pp. 318-325, Nov. 1968.

[2] R. M. Langdon, "A high capacity holographic memory", The Marconi Review 33, 113-30, 1970.

[3] S. S. Orlov, W. Phillips, E. Bjornson, Y. Takashima, P. Sundaram, L. Hesselink, R. Okas, D. Kwan, R. Snyder, "High-Transfer-Rate High-Capacity Holographic Disk Data-Storage System", Applied Optics, Vol. 43, Issue, 25, 4902-4914, Sept. 2004.

[4] S. Martin, P. Leclere, Y. Renotte, V. Toal, Y. F. Lion, "Characterization of an acrylamide-based dry photopolymer holographic recording material," Optical Engineering, Vol. 33, No. 12, pp 3942-3946, Dec. 1994.

[5] K. Peithmann, A. Wiebrock, K. Buse, "Incremental holographic recording in lithium niobate with active phase locking", Optics Letters, Vol. 23, No. 24, Dec. 1998.

[6] G. W. Burr, E. Mecher, T. Juchem, H. Coufal, C. M. Jefferson, M. Jurich, F. Gallego, K. Meerholz, N. Hampp, J. A. Hoffnagle, R. M. Macfarlane, R. M. Shelby, "Progress in read-write fast-access volume holographic data storage", SPIE Conference on Three- and Four- Dimensional optical Data Storage, 4459-52, July 2001.

[7] C. Neipp, S. Gallego, M. Ortuño, A. Márquez, A. Beléndez, I. Pascual, "Characterization of a PVA/acrylamide photopolymer. Influence of a cross-linking monomer in the final characteristics of the hologram", Optics Communications 224, 27-34, 2003.

[8] G. W. Burr, F. H. Mok, D. Psaltis, "Angle and space multiplexed holographic storage using the 90^0 geometry", Optics Communications, Vol. 117, 49-55, May 1995.

[9] J. R. Lawrence, F. T. O'Neill, J. T. Sheridan, "Photopolymer holographic recording material", Optik (Stuttgart, The International Journal for Light and Electron Optics) 112, 449-463, 2001

[10] F. S. Chen, J. T. LaMacchia, D. B. Fraser, "Holographic storage in lithium niobate", Applied Physics Letters, 13, 7, 223-225, 1968.

[11] H. J. Coufal, D. Psaltis, G. Sincerbox, eds, "Holographic data storage", Springer-Verlag, New York, 2000.

[12] G. W. Burr, "Holographic Storage", Encyclopaedia of Optical Engineering ed., R. B. Johnson, R. G. Driggers, Marcel Dekker, New York, 2002.

[13] C. Gu, Y. Xu, Y. Liu, J.J. Pan, F. Zhou, H. He, "Applications of photorefractive materials in information storage, processing and communication", Optical Materials 23, 219-227, 2003.

[14] J. Ashley, M. -P. Bernal, G. W. Burr, H. Coufal, H. Guenther, J. A. Hoffnagle, C. M. Jefferson, B. Marcus, R. M. Macfarlane, R. M. Shelby, and G. T. Sincerbox "Holographic Data Storage", IBM Journal of Research and Development, Vol. 44, No. 3 May 2000.

[15] P. Hariharan, "Optical Holography, Principles, techniques, and applications" 2^{nd} ed. Cambridge University Press, 1996.

[16] J. M. G. Cowie, "Polymers: Chemistry and Physics of Modern Materials", International Textbook Co., Aylesbury, UK, 1973.

[17] L. Hesselink, S. S. Orlov, M. C. Bashaw, "Holographic Data Storage Systems", Proceedings of the IEEE, Vol. 92, No. 8, 1231-1280, Aug 2004.

[18] K. Curtis, A. Pu, D. Psaltis, "Method for holographic storage using peristrophic multiplexing", Optics Letters, Vol. 19, No. 13, July 1994.

[19] W. -C. Su, Y. -W.Chen, C. -C. -Sun, Y. Ouyang, "Multilayer storage in a shift-multiplexed holographic disk", Optical Engineering, 42(6) 1528-1529, June 2003.

[20] G. J. Steckman, A. Pu, D. Psaltis, "Storage density of shift-multiplexed holographic memory", Applied Optics, Vol. 40, No. 20, July 2001.

[21] C. Denz, G. Pauliat, G. Roosen, T. Tschudi, "Volume hologram multiplexing using a deterministic phase encoded method", Optical Communication, 85, 171, 1991.

[22] K. –O. Müller, C. Denz, T. Rauch, T. Heimann, T. Tschudi, "High capacity holographic data storage based on phase-coded multiplexing", Optical Memory and Neural Networks, Vol. 7, No. 1, 1998.

[23] M. C. Bashaw, J. F. Heanue, A. Aharoni, J. F. Walkup, L. Hesselink, "Cross-talk considerations for angular and phase-encoded multiplexing in volume holography", Journal of the Optical Society of America, B 11, 1820-1836, 1994.

[24] J. J. Eichler, P. Kuemmel, S. Orlic, A. Wappelt, "High-density disk storage by multiplexed microholograms", IEEE Journal of selected topics in Quantum Electronics, Vol. 4, No. 5 Sept. 1998.

[25] K. Anderson, K. Curtis, "Polytopic Multiplexing" Optics Letters, Vol. 29, 12, 1402-1404, June 2004.

[26] L. Dhar, A. Hale, H. E. Katz, M. L. Schilling, M. G. Schones, F. C. Schilling, "Recording media that exhibit high dynamic range for digital holographic data storage", Optics Letters, Vol. 24, No. 7, April 1999.

[27] M. Schnoes, B. Ihas, A. Hill, L. Dhar, D. Michaels, S. Setthachayanon, G. Schomberger, W. L. Wilson, "Holographic Data Storage Media for Practical Systems", http://www.inphasetech.com/technology/whitepapers/pdfs/ElectronicImagingRev14.pdf, 2005.

[28] Tapestry™ Media Specifications, http://www.inphase-tech.com/products/tapestry-media/pdfs/TapestryMediaSpecs.pdf, 2005.

[29] D. A. Waldman, H. -Y. S. Li, E. A. Cetin, "Holographic recording properties in thick films of ULSH-500 photopolymer", SPIE proceedings, Diffraction and Holographic Device Technologies and Applications V, Vol. 3291, 89-103, Jan. 1998.

[30] R. T. Ingwall, D. Waldman, "CROP photopolymers for hologram recording", Holography, 11, 2, 2000.

[31] Optware Technology page, http://www.optware.co.jp/english/index_tech.htm, 2005.

[32] "Ecma International creates TC44 to standardize Holographic Information Storage systems", http://www.optware.co.jp/english/PR_TC44_26_Jan_05.html, 2005.

CHAPTER 4

4. Data page recording

It is quite difficult for every data bit recorded to be faithfully stored in any given digital memory system. This is primarily due to statistical noise effects, which put an upper limit on the number of bits that can be recorded and stored without error. To remedy noise effects, error checking and correcting algorithms are used to eliminate erroneous data bits. The majority of these algorithms are designed with 1D bit-streams in mind and so are optimised for data recorded in this fashion. With HDS, data is stored in the medium as 2D data pages. In this chapter, the inherent advantage of using a 2D approach compared with the traditional method of storing information as a serial bit-stream is discussed. Conditioning methods that allow data to be recorded and retrieved with minimal errors are looked at in section 4.1. In section 4.2.1 and 4.2.2, system and photopolymer noise sources that contribute to overall error rate are discussed. Finally, interpixel and interpage crosstalk are looked at in more detail in section 4.2.3.

4.1 Bit-data page enhancement before and after readout

This section discusses how information recorded in the form of multiplexed data pages can retain a high level of fidelity during writing and readout and at the same time have a correspondingly low error rate. Techniques for achieving this high level of fidelity, such as data page oversampling, local thresholding, and digital image enhancements are looked at in sections 4.1.1 and 4.1.2.

4.1.1 Oversampling

Oversampling is a technique used to increase data page fidelity by reducing the information content of each page. As already shown, data pages consist of binary data, represented by a 2D array of black and white regions corresponding to ones and zeros. The maximum number of bits that a monochrome data page can represent is equal to the number of pixels that make up the spatial light modulator. In the case of the HoloEye LC2002 SLM, this is 480,000 bits since the pixel array has a resolution of 600 x 800 pixels. This is not necessarily the best way to represent the data, as it does not take the limitations of the HDS system into consideration. If the individual pixels of the holographic reconstruction cannot be resolved effectively, this can result in a high bit error rate, as some pixels are mistakenly imaged as being dark instead of bright values and vice versa.

To reduce this problem, a rectangular grid composed of a number of pixels is used to encode a bit value rather than a direct pixel to bit match. Each bit is essentially oversampled thus adding redundancy to the bit value, figure 4.1. The reconstructed image of a single bit is determined by the average intensity of the light of all the pixels assigned to that single bit region. This increases the probability that when imaged on to the CCD array, the pixel grid will be read back as the correct value. For instance, oversampling the SLM so that every 100 pixels represents one bit of data would be equivalent to overlaying a 60 X 80 grid of elements upon the SLM surface, where each rectangular grid is composed of 10 x 10 pixels.

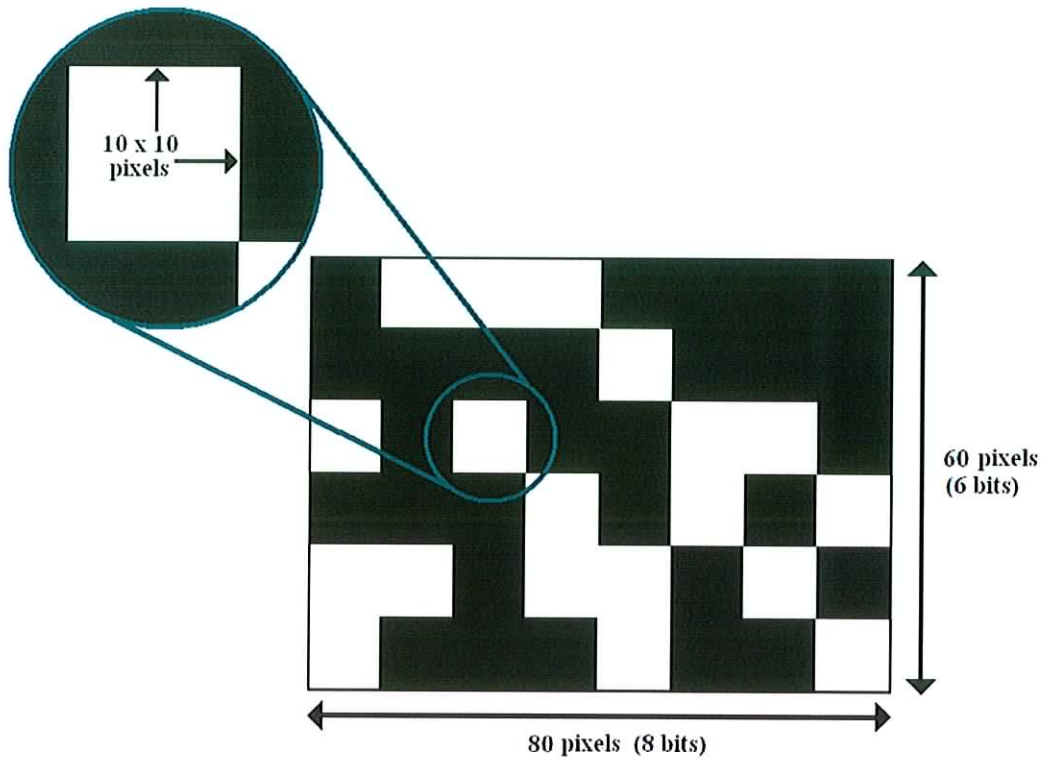

Figure 4.1: Oversampling of data page to decrease the likelihood of bit errors. In the above example, each bit value is comprised of a 10 x 10 array of pixels on the SLM.

4.1.2 Local vs. global thresholding

As previously mentioned, multiple analogue images can be stored within the holographic medium as a direct way of archiving images, section 1.2. However, the majority of research concerning HDS systems has been focused on storing and retrieving 2D binary data pages. Data stored in this digital form is compatible with current computer systems, which rely almost exclusively on an analogue signal being converted to binary information before any processing, transfer or storage of this information is carried out.

To replay any page it is required that the Bragg condition be satisfied for the page in question so that the light diffracted through the medium is encoded with the relevant 2D information. With regard to an ideal HDS system, the bright regions would consist of a

single value of light intensity, while the dark region would have zero intensity. However, in practice this is not the case as imperfections in the recording system and medium result in each region being made up of a distribution of light intensities rather than a single value. Ambiguity may thus arise as to what corresponds to a bright ON bit and a dark OFF bit.

Further ambiguity arises as the laser light used to record the pages may have an inhomogeneous intensity profile in cross section, this profile most commonly being Gaussian (TEM_{00}). For instance, it is quite possible that a bright ON bit near the edge of the detector array may have a lower intensity value than a dark OFF bit located toward the centre of the detector array, this arising from the Gaussian profile of the beam used to replay the data page.

It can be seen from the above example that applying a single *global* threshold to the reconstructed data page image is not a solution since thresholding bit values in one region of the data page will have a negative impact on other regions of the same data page, figure 4.2. There are many ways to improve the HDS system so that global thresholding may be applied successfully. One of the simplest methods is by broadening the laser beam before it has information from the SLM impressed upon it. This has the effect that only the central portion of the Gaussian profile is used and thus the plane wave that encodes the data page will have lower intensity variation across its profile. The homogeneity of the recording beams can further be improved by using an even smaller portion of the laser beam. However, this is at the expense of power consumption, since only a fraction of the laser power is actually being used for the recording process.

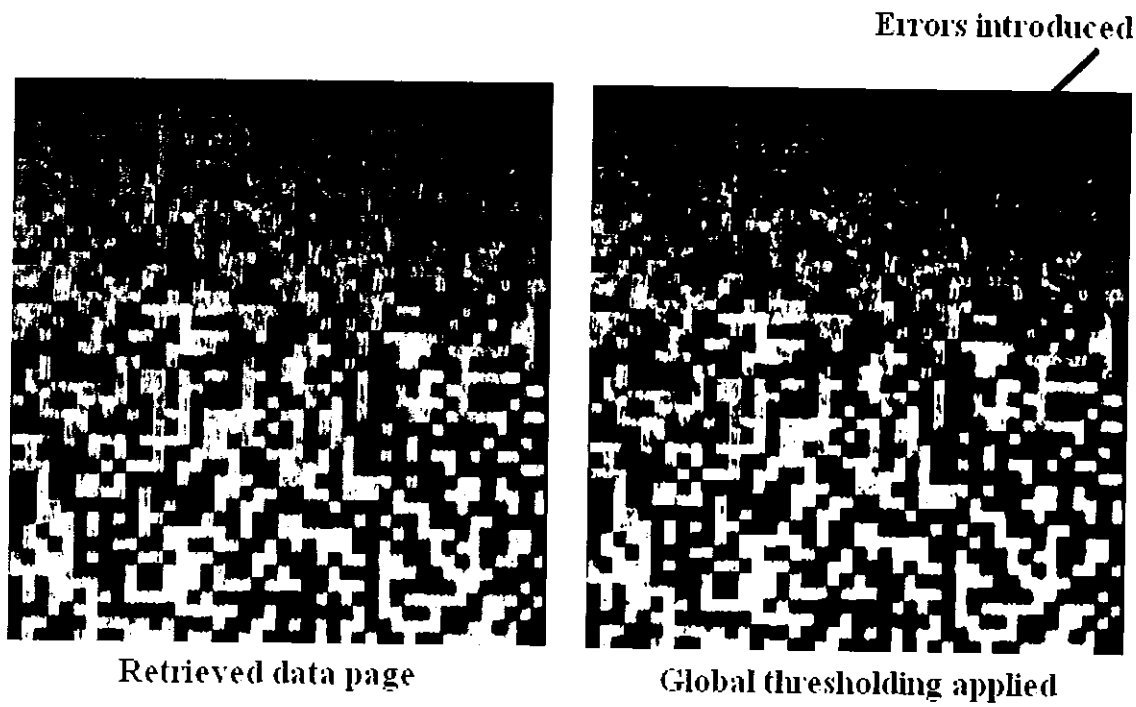

Figure 4.2: Global thresholding can result in errors being introduced when a data page is recorded or played back with an inhomogeneous beam.

Adding an apodizer between the laser beam and SLM is another way to correct for the Gaussian profile. The apodizer consists of a pair of aspheric optical elements, which can redistribute the optical power from an input beam with Gaussian profile to an output beam of uniform intensity [1].

Global thresholding cannot correct other sources of variation that might be experienced in a HDS system. A non-homogeneous medium might lead to regional variations in the dynamic range of the material and so produce data pages with ambiguous bit values that cannot be corrected by simply applying a single threshold value.

Clearly, it is desirable to use numerous local thresholds for each data page as opposed to a global threshold value [2]. One method, which does just that, is known as adaptive thresholding [3]. The reconstructed data page is divided up into relatively small pixel

blocks, for instance groups of 10 x 10 pixels, and a suitable threshold value is determined from the average light intensity over this area. This value can then be added to a correction factor gained from previous threshold values.

A method of adaptive thresholding using parity information can be used to determine the necessary local threshold values. First, the data page is divided up into different regions and the number of ON pixels in each region is calculated and added to the page as parity information. The additional parity information is robustly stored using differential encoding, where an ON-OFF sequence could represent a binary value of zero and an OFF-ON sequence represent a binary value of one [4]. The local threshold for each data block is obtained by calculating the total number of bits within a data block, the number of ON pixels from the parity information, and the contrast ratio between the ON and OFF values.

Modulation coding [5] is another method that can be used to determine local threshold values. Using this method improves the raw-BER at the expense of the code-rate, the ratio of the user bits, n, to the total coding bits, m, where $m > n$. A code-rate of unity implies that the coding method is 100% efficient and so the number of coded data bits is equal to the number of user bits. The constant-weight code can be written as (u, s, w), where u is the number of user bits to be encoded by each modulation code block, s is the size of the data block that is used to encode each user bit, and w is the weight attributed to the data block. For instance, if s were two then there would be two ON bits in the block. The table below, table 4.1, demonstrates the use of a (1,2,1) code. Each data block consists of two bits, with a weight of one that encodes a single user bit.

User data	(1,2,1)-code
0	0 1
1	1 0

Table 4.1: A constant-weight code is shown above, where two bits are used to encode each user bit. The weight of the code is one.

A user bit of 0 is represented by the code OFF-ON and likewise a bit value 1 is represented by ON-OFF. Dividing user data into these uniform code blocks automatically enables the local threshold value to be determined because it is already known that each block will contain one bright intensity value and one dark intensity value. Therefore, determining the code is just a matter of allocating a bit value of 1 to the bright bit and vice versa.

4.2 Sources of data page errors

There is a need to quantify the amount of data that can be sent through a data channel, stored, or read out without any error. In terms of HDS systems and media, this is characterised by the raw-bit error rate (raw-BER). A system with a relatively large raw-BER will exhibit many bit errors for n number of bits readout from the system. If for instance one error occurred for every 1000 read then the raw-BER would be 10^{-3}. This can be decreased to an acceptable level by introducing redundancy into the data, improving the system components and design, or by adding modulation and error correction codes. An acceptable raw-BER expected from present day storage devices is 10^{-12} bits or less, which is one erroneous bit for every million million bits read out from the system [4].

The remainder of this section examines some of the main system noise sources that increase overall raw-BER. Particular attention is paid to the spatial light modulator (SLM) used to encode the data page as well as the CCD array used to detect the encoded page. Noise sources relating to the photopolymer and bit errors that occur due to inter-page and inter-pixel crosstalk are discussed in sections 4.2.2 and 4.2.3 respectively.

4.2.1 Sources of system noise

Unlike most optical systems, HDS is quite intolerant of optical noise as it directly affects system storage capacity. For instance, brightness variations or inhomogeneities across the data page can result in data bits being read incorrectly. This is especially true if a single threshold value (global threshold) is used to separate bright and dark regions into their corresponding binary values, as discussed previously in section 4.1.2.

This kind of brightness variation can be due to inadequately collimated laser beams, inconsistent laser beam profile, or aberrations attributed to the imaging lenses used. These effects tend to be deterministic remaining constant from one recorded data page to the next whilst linearly scaling with increasing signal strength [6].

Spherical aberration (pixels getting uniformly larger) and coma (pixels on the periphery of the data page being elongated) are the main lens aberrations that affect data page readout. It is reasonable to assume that dust or unclean optics can lead to sections of the data page being smeared or cause defects such as concentric ring and other diffraction artefacts.

Unlike conventional holography where it is often important to record one hologram with large diffraction efficiency, data storage relies on the medium's ability to store a large set of data pages, each with low diffraction efficiency. By recording as many holograms as possible, each with the lowest detectable readout signal strength, storage capacity is maximised and effective use is made of the material's dynamic range.

The dynamic range allocated to each hologram has to be judiciously chosen so that the fixed noise floor of the system is less than the readout signal strength of each hologram. An example of systematic noise would be the inherent noise produced in the electron detection process by a CCD array, this noise floor of which remains roughly constant. Therefore, if the number of holograms multiplexed is increased, the amount of light diffracted into each hologram will decrease, resulting in a corresponding decrease in SNR.

To achieve error-free read out of a data page, it can be shown that a system with all other noise sources eliminated still requires a certain diffraction efficiency to overcome the noise floor of the CCD array used to detect the page. As the number of electrons detected for each pixel (this value constitutes the hologram signal strength) approaches the number of noise electrons, an increase in the system raw-BER will be observed [1]. The number of electrons per pixel [7] can be written as,

$$n_{electrons} \propto M/\#^2 . P_{readout} \frac{t_{readout}}{M^2 . N_{pixels}} \qquad (4.1)$$

where $M/\#$ (M-number) characterises the efficiency of the material in the recording geometry used, $P_{readout}$ is the power in the readout beam, $t_{readout}$ is the integration time

of the CCD array, M is the number of multiplexed data pages, and N_{pixels} is the number of pixels per data page.

4.2.2 Photopolymer noise sources

Another source of detector noise that reduces the overall SNR of a system, occurs when the detector pixels are misaligned with respect to the reconstructed data page pixels. This can be due to the relative rotation, focus, tilt, or magnification of the SLM pixels with respect to their corresponding pixels on the detector array. Misalignment can also occur due to dimensional change in the recording material. This is quite often [8] the case when dealing with photopolymers, and in general, any material that undergoes shrinkage effects. For instance, when recording slanted holographic gratings in a material that exhibits shrinkage effects, the holograms will be reconstructed at a slightly different angle to that at which they were recorded. This effectively reduces the diffraction efficiency of the reconstructed hologram, depending on how large the angular deviation is. If shrinkage is deterministic this can be accounted for by adjusting the readout beam angle so that the holograms can be reconstructed with maximum diffraction efficiency.

Photopolymers exhibiting a high degree of light scatter further increase the overall noise of a HDS system. Scattered light from the photopolymer or optical components such as lenses and optical elements for shaping and directing the recording beams may be transmitted to incorrect regions of the detector array and thus contribute to other regions of the data page leading to errors during read out. Light scatter depends [6] on the readout beam power, optical quality of the components, and photopolymer composition.

Reducing the effects of shrinkage and light scatter arising from photopolymer-based media should greatly decrease the BER of potential HDS systems. Optimising photopolymer dynamic range without taking these noise sources into account will ultimately put an upper limit on storage capacity of these types of media.

4.2.3 Crosstalk

Interpixel crosstalk occurs when light from one pixel of the SLM spreads into neighbouring pixels when imaged on to a detector pixel. Diffraction effects and aberrations arising in the optical setup [1] can cause a pixel at the SLM to be blurred over its neighbouring pixels as the image propagates through the system. The limiting aperture used when holographic data pages are recorded in or near to the Fourier plane can further contribute to this blurring effect. The aperture prevents the full Fourier transform of the SLM image being recorded in the storage medium. This is done to reduce unnecessary exposure of the medium. Since the aperture only lets through the central order of the Fourier transform, higher frequency information is discarded. Without these frequency components, it is not possible to maintain the well defined edge features occurring at pixel boundaries of the image. A method known as *deconvolution* can be used to return these frequency components to the imaged data page using a point-spread function to quantify the extent of blurring of the image boundaries [2, 7].

Two important factors that determine whether a pixel will be decoded incorrectly once imaged on to a detector array are inherent system noise and the values of neighbouring pixels. It could be envisioned that eight bright pixels surrounding a single dark pixel could cause the intensity of the central dark pixel to be increased. The combined

contamination from the bright pixels into the dark pixel region could increase the intensity in such a way that it is raised above the threshold value used for distinguishing dark from bright pixels, see figure 4.3 below.

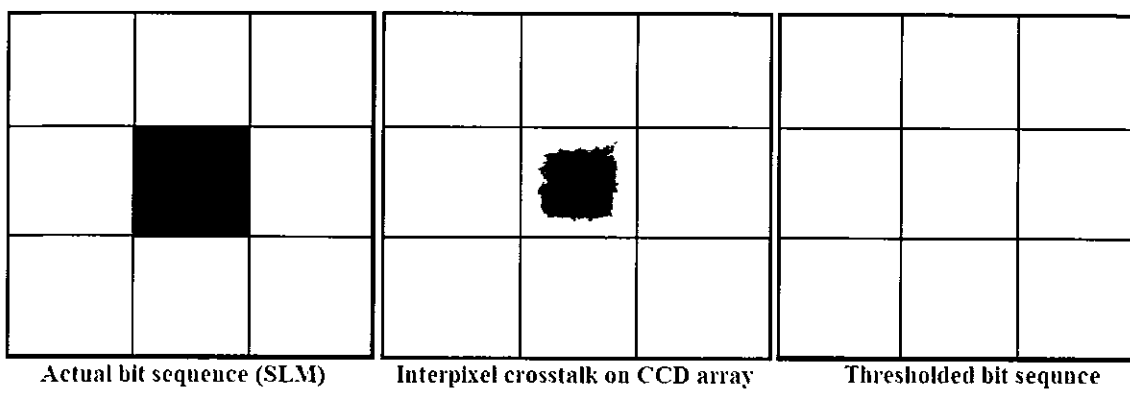

Figure 4.3: Pixel crosstalk from neighbouring pixels may lead to some pixels' intensity values being shifted to a new level causing them to be read out incorrectly.

With regard to volume transmission holograms, as the number of multiplexed holograms increases, the higher the probability that unwanted diffraction from neighbouring holograms will corrupt the signal. This time crosstalk occurs between data pages and so puts a limitation on the possible memory capacity.

Overall, crosstalk has the effect of decreasing the SNR of the system because the intensity difference between the dark and bright pixels is effectively decreased. This type of crosstalk is deterministic as it is expected that, for a given system, diffraction and aberration effects are constant as is the maximum bandwidth available. It should be noted that crosstalk effects scale with the strength of the holograms [2].

In most applications, crosstalk effects occur temporally due to data bits being read as a sequential serial-bit pattern. When data is read from a holographic storage medium, an entire page of information is read at once, so smearing occurs spatially in two

dimensions. Signal processing techniques can be used to reduce crosstalk considerably. Specially designed filters appropriate to the type of crosstalk present can be used to achieve reduction.

4.4 Summary

As with all storage technologies, HDS is prone to system noise causing data to experience bit errors. In terms of HDS, these errors occur spatially across a data page rather than temporally as is the case with 1D serial data. System noise is due to a number of factors such as data page distortions arising from the conditioning optics, non-uniform laser beam profile, and crosstalk between data pages and pixels within a page. Misalignment of the reconstructed data page imaged on the CCD array introduces further bit errors as do data pages with negligible diffraction efficiency with respect to the noise floor of the system. One of the main noise sources is attributable to layer shrinking which is caused by photopolymerisation of the illuminated regions of the material. To reduce the bit error rate, the recorded data needs to be encoded in a manner that reduces its susceptibility to errors. Oversampling as well as modulation and differential coding methods may be used to encode the data in a more robust form before being sent down the optical channel or being stored in the recording medium. As described in chapter 6, oversampled data pages were recorded. The CCD array used to image the data page was mounted on an XYZ stage, which allowed the inconsistent images from each layer to be aligned each time a data page was reconstructed.

4.5 References

[1] J. Ashley, M. -P. Bernal, G. W. Burr, H. Coufal, H. Guenther, J. A. Hoffnagle, C. M. Jefferson, B. Marcus, R. M. Macfarlane, R. M. Shelby, and G. T. Sincerbox "Holographic Data Storage", IBM Journal of Research and Development, Vol. 44, No. 3 May 2000.

[2] G. W. Burr, J. Ashley, B. Marcus, C. M. Jefferson, J. A. Hoffnagle, H. Coufal, "Optimizing the holographic digital data storage channel", SPIE Proceedings, Vol. 3468, pp. 64-75, Advanced Optical Memories and Interfaces to Computer Storage, Nov. 1998.

[3] I. McMichael, W. Christian, D. Pletcher, T. Y. Chang, and J. H. Hong, "Compact holographic demonstrator with rapid access", Applied Optics, 35, 2375–2379 1996.

[4] G. W. Burr, W. Chou, M. A. Neifeld, H. Coufal, J. A. Hoffnagle, C. M. Jefferson, "Experimental evaluation of user capacity in holographic data-storage systems", Applied Optics, Vol. 37, No. 23, August 1998.

[5] G. Berger, K. -O. Müller, C. Denz, I. Földvári, Á. Péter, "Digital data storage in a phase-encoded holographic memory system: data quality and security", In: Advanced Optical Storage, H.J. Coufal, ed., SPIE Proc. 4988, 2003.

[6] G. W. Burr, B. Marcus, "Coding tradeoffs for high-density holographic data storage", Proc. SPIE Vol. 3802, p. 18-29, Advanced Optical Data Storage: Materials, Systems, and Interfaces to Computers, July 1999.

[7] G. W. Burr, "Holographic Storage", Encyclopaedia of Optical Engineering ed., R. B. Johnson, R. G. Driggers, Marcel Dekker, New York, 2002.

[8] G. W. Burr, E. Mecher, T. Juchem, H. Coufal, C. M. Jefferson, M. Jurich, F. Gallego, K. Meerholz, N. Hampp, J. A. Hoffnagle, R. M. Macfarlane, R. M. Shelby, "Progress in read-write fast-access volume holographic data storage", SPIE Conference on Three- and Four- Dimensional optical Data Storage, 4459-52, July 2001.

CHAPTER 5

5. Experimental scheme and control software

A detailed description of the experimental setup used to characterise the photopolymer is given in this chapter. The setup is capable of determining several photopolymer characteristics; these are detailed in section 5.1. In section 5.2, the instrumentation and optical components that make up the test system are described. Control software was written to automate the instrumentation and perform data acquisition from an optical power meter. Finally, a description of the software functionality is given in section 5.3.

5.1 Investigation of photopolymer properties

The test system was used to determine photopolymer characteristics such as dynamic range and dimensional and temporal stability in terms of material shrinkage and diffraction efficiency by observations of variations in angular selectivity curve.

The dynamic range of a holographic recording material refers to the total response of the recording medium when divided up among many holograms multiplexed in the material volume. In terms of holographic data storage it is usually parameterised as M/#, pronounced M-number [1]. In general, the larger the M/#, the greater the number of holograms having a specified diffraction efficiency that can be recorded in a volume. When multiplexing holograms with different diffraction efficiencies, the M/# can be obtained from the maximum value of a cumulative grating strength curve. The

cumulative grating strength is defined as the sum of the square root of the recorded gratings' diffraction efficiencies,

$$M/\# = \sum_{i=1}^{N} \sqrt{\eta_i} \,. \tag{5.1}$$

Where N is the total number of holograms and η_i is the diffraction efficiency of the i^{th} hologram. An alternative way of viewing the M/# is in terms of how the dynamic range scales when different numbers N of equalised holograms are recorded. The square root of the average diffraction efficiency for any one set of equalised holograms is graphed against the reciprocal of the number of holograms recorded in the set. This is repeated for sets containing different numbers of holograms. The slope of a linear fit applied to the data, is equal to the M/#.

$$M/\# = N.\sqrt{\overline{\eta}} \tag{5.2}$$

M/# is directly related to the quantity of data that may be stored in a specific volume of medium, i.e. bit density.

The photopolymer's temporal stability is investigated in terms of shrinkage by measuring the Bragg selectivity curve variation over a certain period. It is important to quantify the level of material shrinkage, as it can decrease the signal-to-noise ratio of a HDS system, see section 4.2.2. By recording slanted gratings using the test system it is possible to determine how much the layer undergoes shrinkage after the photopolymerisation process has taken place, section 6.3. It should be noted that shrinkage measurements are based on how the thickness of the photopolymer changes perpendicularly to the layer plane. Shrinkage parallel to the layer is not quantified, as

this should be mechanically suppressed due to interactions between the photopolymer layer and the glass substrate.

5.2 Main system components

The system, figure 5.1, used to characterise different photopolymer formulations was built from off-the-shelf optical components. These included various lenses, beam splitters, beam expanders, spatial filters, mirrors, an opto-mechanical frame, numerous holders, and mounts. The electronic instruments used were a Newport stage controller (ESP 300), two Newport rotational stages (angular stage M-URM80ACC, peristrophic stage M-URM100ACC), two Unibliz electronic shutters (VMM-T1), a Newport optical power meter (840-C), a PC running Windows 2000, a National Instruments 6013 DAQ card, and a Lambda Ar^{+} laser (Lexel 95) operating at a wavelength of 514 nm was used for recording and readout.

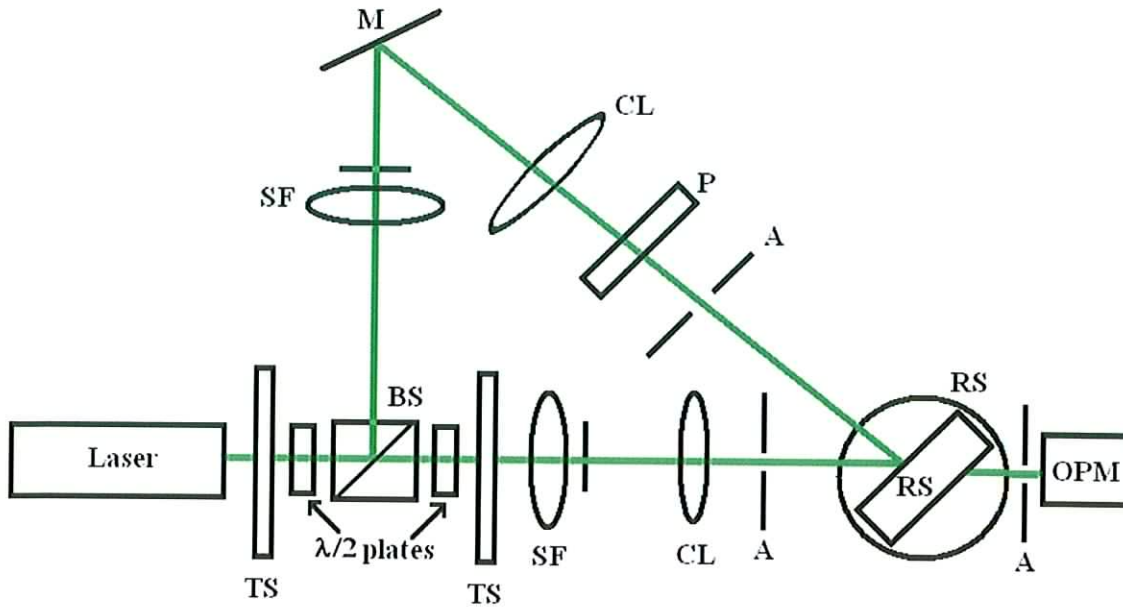

Figure 5.1: Experimental system for characterisation of acrylamide based photopolymer, TS: shutter, SF: spatial filter, CL: collimating lens, BS: beam splitter, P: polariser, RS: rotational stages, PS: photopolymer holder, OPM: optical power meter, M: mirror, A: aperture.

5.3 Control software

The properties of the photopolymer that may be determined using the test system and control software are discussed in section 5.1. The software itself is integral to the overall system design, making the system highly automated, thus minimizing the need for user supervision during experimentation. This reduces the potential for human error and removes a potential heat and vibration source, which could affect the accuracy and repeatability of the experiments.

Experimental conditions are much more repeatable when automated by means of software. Automation greatly reduces the time it takes to characterise a photopolymer sample because there are many individual electrical devices making up the system, all of which have to work correctly numerous times and in a particular sequence. Manually

carrying this out requires a great deal of time as all the devices have to be controlled in turn, and, if operated in the incorrect sequence, an entire set of data may have to be discarded.

Altogether, the computer software controlled two rotational stands, two electronic shutters, and an optical power meter. In addition, it can potentially control a spatial light modulator and a detector array, if these were to be added to the system later. The software was written by the author using LabVIEW 7.0 and designed to be modular and therefore easy for new functionality to be added at a later time. The user interface was designed so that only controls and indicators that related to a particular mode of operation were visible at any time, figure 5.2.

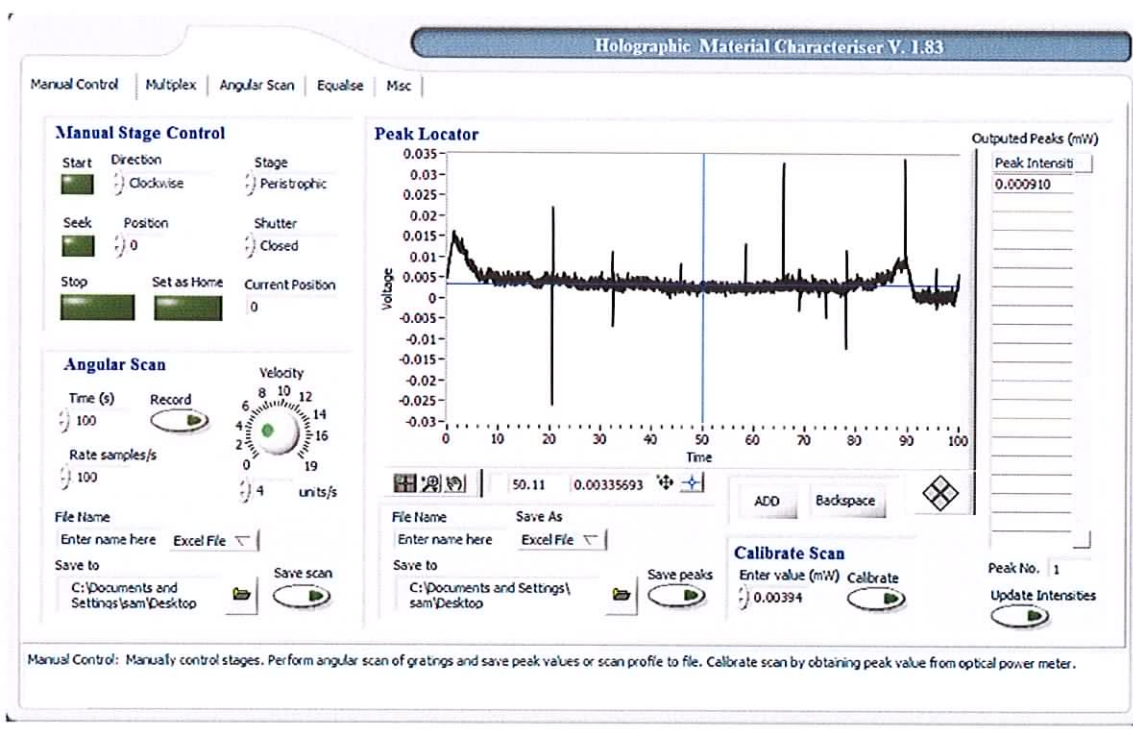

Figure 5.2: Example of one of the control software's interface panels.

This design feature removes unnecessary clutter from the interface making it easier and less distracting for a novice user to conduct experiments. The modules, which form the

basis of the software and their functionality, are described below. The software user interface is based on a tabbed panel layout whereby each module can be accessed by selecting its corresponding tab. A manual describing the operation of the software in more detail can be found in appendix A.

Manual Control – This module enables the user to independently rotate the peristrophic and angular stages to any position. Furthermore, it is possible to rotate a photopolymer layer and at the same time acquire a signal from the optical power meter recording the variation of the diffracted light intensity with angle. Once completed the entire scan data can be calibrated by finding a known peak intensity value using the optical power meter and then using this value to set the relative intensity values of the scan. This data can then be saved to file. Alternatively, the individual grating diffraction peak intensities can be saved in a separate file. If necessary, these peak values can be sent to the *Equalise* module for further equalisation of the multiplexed gratings.

Multiplex – The *Multiplex* module can be used to record a sequence of gratings either angularly or peristrophically or by using a combination of the two methods. Each grating's exposure time can be inputted manually or by sending the newly generated times from the *Equalise* module. Once initiated, the entire multiplexing procedure can be completed without user supervision.

Angular Scan – The *Angular scan* module can be used for experiments where it is necessary to obtain both the diffracted light intensities and corresponding angular values. As with the *Manual Control* module, it is possible to save the scan in its entirety along with the peak intensity values. This module is mainly used for characterising photopolymer layer shrinkage.

Equalise – By providing information to the *Equalise* module regarding previous multiplexing experiments, such as the number of gratings recorded, the peak intensity values, exposure times used for recording, readout beam intensity, and combined recording beam energy, it is possible to generate new exposure times using an iterative scheduling algorithm. Once generated, these times can be sent to the *Multiplex* module to further equalise the strengths of a new set of multiplexed gratings.

Misc – The *Misc* module has two main functions. The first allows the user to model the influence of certain parameters on the Bragg selectivity curve, such as layer thickness, modulation parameter, and/or spatial frequency. The effect of varying these parameters is graphically displayed whilst indicators display the full with half maximum (FWHM) and maximum diffraction efficiency. Secondly, the module enables the user to calculate the appropriate geometry of a right-angled setup needed to record gratings of specified spatial frequency.

5.4 Summary

A test system was built which consisted of an opto-mechanical frame, optical elements for shaping and directing the recording beams, rotational stages, and an optical power meter. Software written in LabVIEW was used to automate the system. The test system made it possible to quickly assess photopolymer characteristics, such as dimensional and temporal stability in terms of material shrinkage, diffraction efficiency, and variations in angular selectivity. The dynamic range for different photopolymers could also be assessed and a value of M/# determined.

5.5 References

[1] F. H. Mok, G. W. Burr, D. Psaltis, "System metric for holographic memory systems", Optics Letters, Vol. 21, No. 12, June 1996.

CHAPTER 6

6. Experimental results

A photopolymer material suitable for HDS applications must exhibit certain key characteristics. In this chapter, several of these characteristics are investigated with regard the CIEO acrylamide-based photopolymer and the experimental data presented. In section 6.2 the photopolymer and layer preparation are discussed and in section 6.3, the problem of material instability in the form of bulk polymerisation induced shrinkage is described. Following this, a description of the scheduling method and algorithm used for equalising the multiplexed gratings is given, section 6.4. In section 6.4.1 the performance of different multiplexing methods in terms of how efficiently overall recording energy and exposure time are conserved is examined. Two definitions of M/# are compared in section 6.5 to determine which is most repeatable and if the values they give are in agreement with each other. Then in section 6.6, a study of the photopolymer's dynamic range is carried out. This relates to the material's ability to store multiple holograms with significant strength in the same volume of material.

Finally, section 6.7 deals with the exposure energies required for recording data pages of sufficiently high quality as well as the time available to record data pages in the same volume of material i.e. recording period.

6.1 Modelling parameters affecting Bragg diffraction

As mentioned in section 2.2, a hologram is considered a volume hologram if the layer thickness is several times greater than the fringe period recorded in the layer. For example, fringe periods measuring approximately half a micron are typically recorded in a photopolymer with a layer thickness of roughly a hundred microns. When light interacts with the recorded fringe pattern, some of the light continues through the medium on the same optical path as the incident beam while a portion of the light is diffracted due to the spatially modulating refractive index.

As discussed in the introduction, the number of holograms that can be multiplexed is highly dependent on the Bragg angular selectivity of the recording geometry and material used. In order to investigate the parameters that influence the Bragg angular selectivity, a transmission phase grating was modelled using the *Misc* panel which is a part of the control software. Certain parameters affecting the Bragg angular selectivity of the photopolymer were investigated, namely, the thickness of the photopolymer layer and the spatial frequency of the holographic grating. Another parameter which affects the angular selectivity is known as the modulation parameter ϕ. This is related to the capability of the material to undergo a refractive index modulation through monomer polymerisation, charge distribution, or other means.

Angular $\Delta\theta$ or wavelength $\Delta\lambda$ deviations can be studied readily, since they influence diffraction efficiency through the parameter χ, which is a measure of the deviation from the Bragg condition [1],

$$\chi = \Delta\theta K d / 2 \tag{6.1}$$

or

$$\chi = \Delta\lambda K^2 d / 8\pi m_0 \cos\theta_0 \tag{6.2}$$

where d is the layer thickness, K is the grating vector (resultant vector of the incident and diffracted beams), and $\Delta\theta$, is the angular deviation from the angle satisfying the Bragg condition θ_0. Curves showing the normalised diffraction efficiency of a lossless transmission phase grating as a function of the parameter χ are plotted in figure 6.1 for three values of the modulation parameter ϕ.

$$\phi = \frac{\pi\, n\, d}{\lambda \cos\theta} \tag{6.3}$$

The modulation parameter ϕ depends upon λ the wavelength of the laser, d the thickness of the layer, and n the refractive index variation. As the angle of incidence of the incident beam deviates from the value required to satisfy the Bragg condition, the diffraction efficiency becomes,

$$\eta = \frac{\sin^2\sqrt{(\phi^2 + \chi^2)}}{(1 - \chi^2/\phi^2)} \tag{6.4}$$

The plots, figure 6.1-6.3, below were calculated by means of the *Misc* panel in the control software.

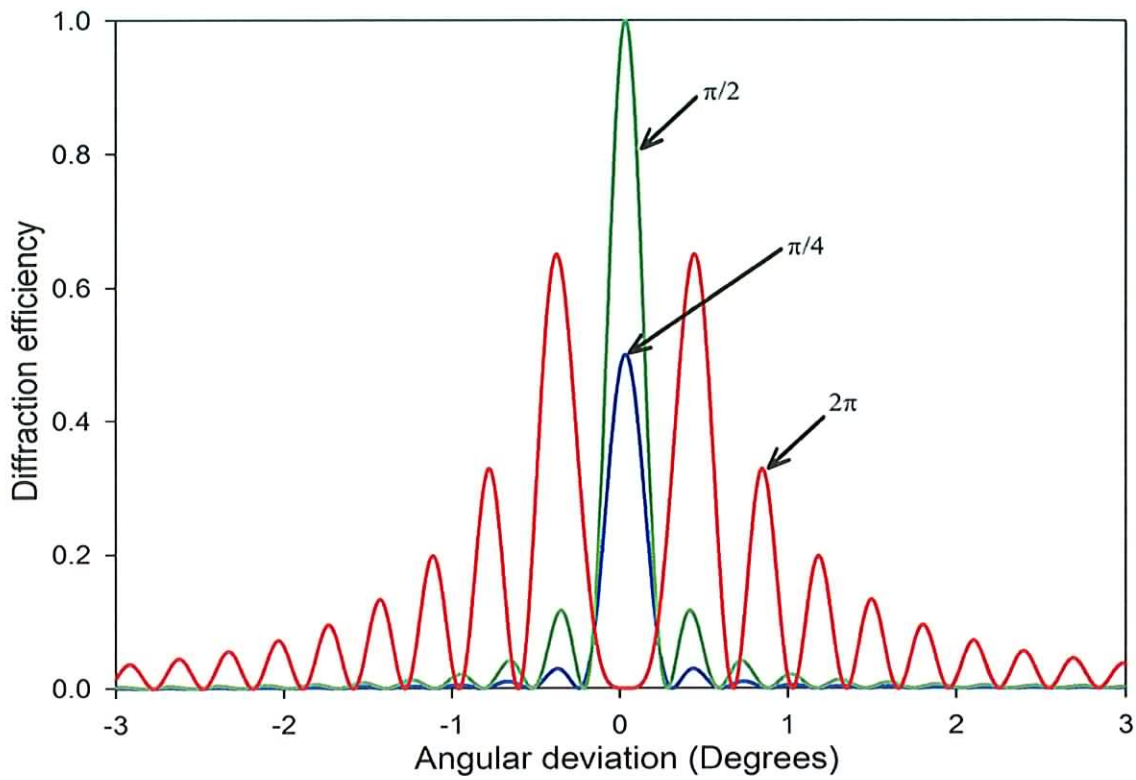

Figure 6.1: Model of the dependence of the diffraction efficiency on the deviation from the Bragg angle for different modulation parameters, ϕ.

When the modulation parameter ϕ, increases from $\pi/4$ to 2π the diffraction peak becomes "over-modulated", figure 6.1. With a modulation parameter of $\pi/4$, the diffraction efficiency is 0.5. When this is increased to $\pi/2$ the efficiency rises to 1.0. If the modulation parameter is increased beyond $\pi/2$, light energy is diffracted mostly in the second and subsequent diffraction lobes. In the context of multiplexing, this is a problem because data pages will experience considerable interpage crosstalk from neighbouring data pages. The values for the thickness and spatial frequency were 200 μm and 1000 lines/mm respectively.

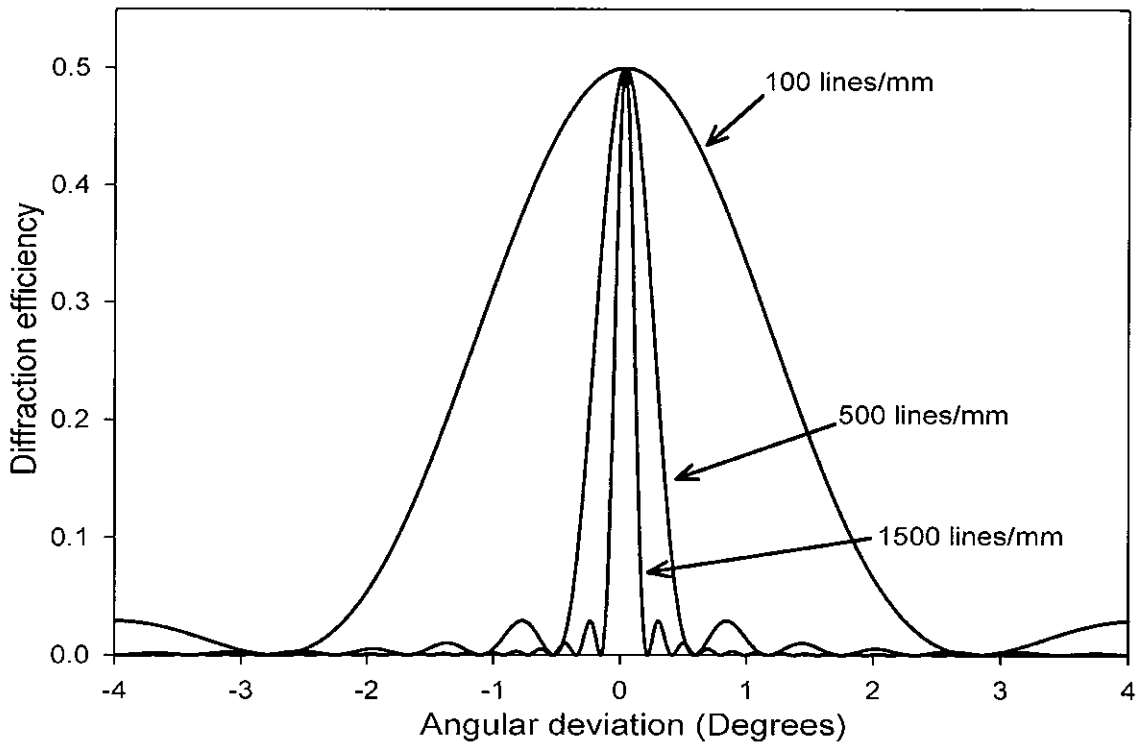

Figure 6.2: Model of the dependence of the diffraction efficiency on the deviation from the Bragg angle for different spatial frequencies.

In figure 6.2, the dependence of the diffraction efficiency on the deviation from the Bragg angle for a number of different spatial frequencies is shown. As the spatial frequency increases from 100 to 1500 lines/mm, the FWHM of the curve decreases. In terms of HDS, the FWHM should be relatively low so that many data pages can be recorded with only a small angle separating them from one another. The values for the thickness and modulation parameter were 200 μm and $\pi/4$ respectively.

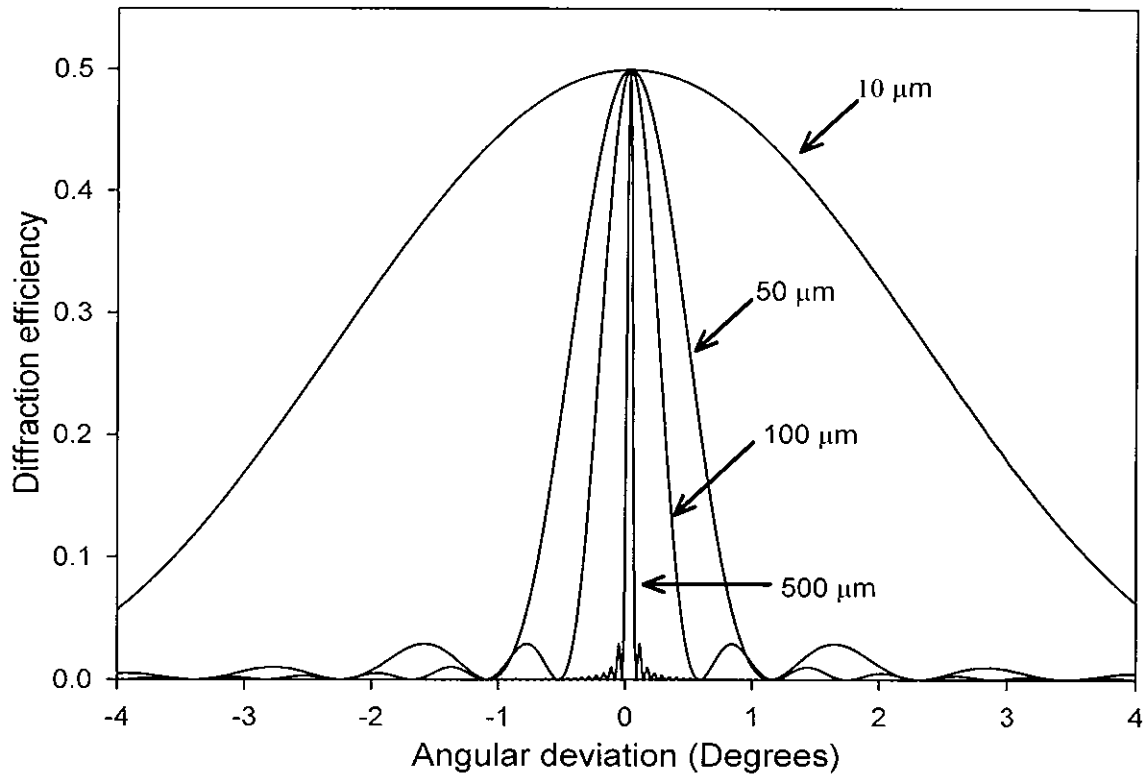

Figure 6.3: Model of the dependence of the diffraction efficiency on the deviation from the Bragg angle for different thicknesses of holographic material.

As the thickness of the recording medium increases from 10 μm to 500 μm, the FWHM decreases from 4.96^0 to 0.1^0, see figure 6.3. Thus, the angular selectivity becomes greater. With regard HDS, thick photopolymer layers are desirable as angular selectively is increased considerably, allowing more data pages to be stored in the same volume of recording media. The spatial frequency was held constant at 1000 line/mm while the modulation parameter was set at $\pi/4$.

6.2 Preparation of standard composition photopolymer layers

Firstly, the polyvinyl alcohol (PVA) solution was prepared. 10 ± 10^{-4} grams of PVA was measured with a piezoelectric scale and then placed onto a glass plate. The electronic scale is draft isolated and has a spirit level incorporated into the design to

enable horizontal adjustment by means of x and y alignment knobs. Once the PVA was measured out, 100 ± 0.5 ml of distilled water was added to a beaker and slowly heated up to temperatures not exceeding the water boiling temperature. The PVA was then slowly added to the beaker of distilled water and stirred vigorously using an electronic stirring plate until completely dissolved. Once dissolved, the solution was left to gradually cool to room temperature.

The dye solution was prepared by weighing out 0.11 ± 10^{-4} grams of Erythrosine B and adding it to 100 ± 0.5 ml of distilled water, resulting in a stock solution having a concentration of 0.11% w/w. The solution was kept in an ultrasonic bath at room temperature until all the dye was dissolved. Since Erythrosine B is photosensitive to white light, all dye preparation is carried out in a low red lit "dark-room".

The photopolymer was prepared by measuring 17.5 ml of the PVA solution into a glass beaker. To this 0.6 ± 10^{-4} grams of acrylamide (monomer), 0.2 ± 10^{-4} grams of N, N'-methylenebisacrylamide (cross-linking monomer), 4 ml of the Erythrosine B dye solution (sensitizer) and 2 ml of triethanolamine (electron donor) were added. This was made up to 25 ml by adding a few drops of distilled water.

Photopolymer layer preparation:

Gravity settling was used to coat the photopolymer layer onto glass substrates. This produced relatively thick layers having good optical quality and optical flatness. To obtain different layer thicknesses different amounts of photopolymer solution were dripped onto glass slides (5 x 5 cm) using a 2 ml plastic syringe. The solution was then evenly spread over the entire slide area with the back of a spatula. Finally, the solution

was left to gravity settle for 24 to 36 hours in complete darkness. Once dry it could then be used for hologram recording.

6.2.1 Investigation of zeolite nanoparticle-doped photopolymer solutions

It was demonstrated by Suzuki et al. [2,4] and Tomita et al. [3,5] that doping photopolymer solutions with specific inorganic nanoparticles such as TiO_2 and SiO_2, can lead to an overall increase in dynamic range while at the same time suppressing shrinkage. Both characteristics have the effect of increasing storage densities of a photopolymer-based HDS medium.

As mentioned above, incorporating non-reactive nanoparticles, having different refractive indices, to that of the photopolymer composition has been shown to increase dynamic range. This may be attributable to the nanoparticle components being spatially redistributed in the photopolymer and hence producing an increase in the refractive index modulation when a hologram is recorded in the photopolymer volume [5].

Zeolite nanoparticles were incorporated into the photopolymer (standard composition) to determine which dopant suppressed shrinkage the most, section 6.3.1. Zeolite A, zeolite Y, zeolite aluminium beta, and Si-MFI zeolite were chosen for comparison. Once the dopant exhibiting the least amount of shrinkage was identified, its M/# was compared with that of the standard composition to determine whether an improvement in dynamic range in the regime of multiple recording had also occurred, section 6.6.1.

6.3 Photopolymer shrinkage

Photopolymer layer shrinkage during or after recording of a slanted grating, may result in a reduction in the diffraction efficiency of the reconstructed grating or worse, no diffraction at the expected reconstruction angle. This is true of most free-radical based photopolymer systems. During the process of photopolymerisation the polymer volume decreases. This is believed to be due to double bonds being converted to single bonds.

Shrinkage tends to occur in a direction perpendicular to the layer plane because the glass substrate on which it is deposited mechanically restrains the layer in the in-plane direction. When a slanted grating is recorded in the layer the slant angle will change as the layer thickness shrinks. This leads to a corresponding change in the fringe period and reconstruction angle, figure 6.4. To reconstruct the grating with maximum diffraction efficiency, it is required that the reference beam angle be changed with respect to the grating.

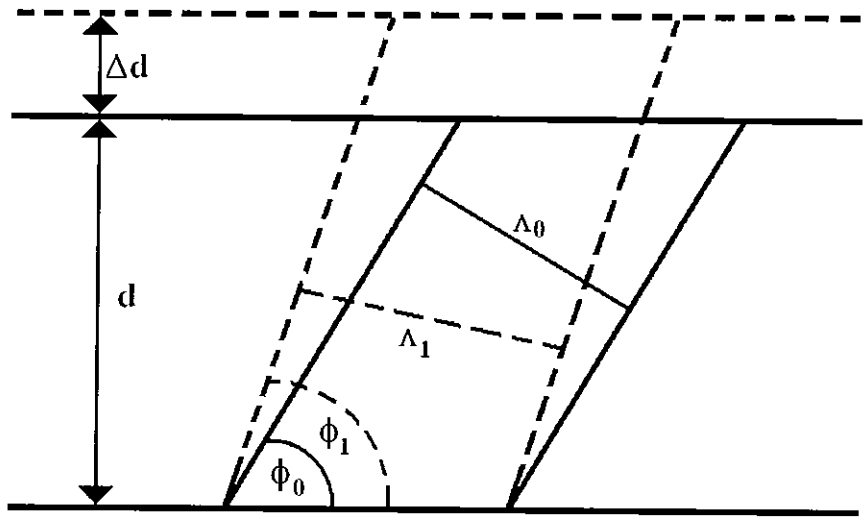

Figure 6.4: Shrinkage occurring in the direction perpendicular to the layer plane will cause a change in the reconstruction angle of a slanted grating recorded in the layer. This is due to a change in the orientation of the recorded fringe planes with respect the normal to the layer plane.

To determine the shrinkage of a photopolymer layer (standard sample), a single slanted holographic grating of 1 cm diameter was recorded. The layer was approximately 120 μm thick and was recorded with a slant angle of 20°. This is taken to be the angle between the photopolymer layer normal and the bisector of the recording beams. The grating spatial frequency was 1500 lines/mm and the exposure energy density used to record the grating was 23 mJ/cm^2. This exposure energy was delivered to the photopolymer layer by means of an Ar^+ 514 nm wavelength laser. After recording, the grating was probed with the same wavelength beam using an intensity of 59 $\mu W/cm^2$. To protect the layer from the environment, it was sandwiched between two glass plates and sealed before recording. The layer was then probed using the reference beam and an angular scan was made of the diffracted light intensity.

As stated previously, the occurrence of photopolymer layer shrinkage results in a change in the fringe spatial period [6]. It is therefore necessary to alter the readout beam angle for maximum diffraction efficiency. The fractional change in material thinckness,

Δd, can be obtained [7] by knowing the initial slant angle of the grating ϕ_0 and the final slant angle ϕ_1.

$$\Delta d = d \left[\frac{\tan \phi_1}{\tan \phi_0} - 1 \right] \qquad (6.5)$$

From equation 6.5, the percentage shrinkage was calculated to be 1% after the first day. This increased to 2 % after 37 days, figure 6.5.

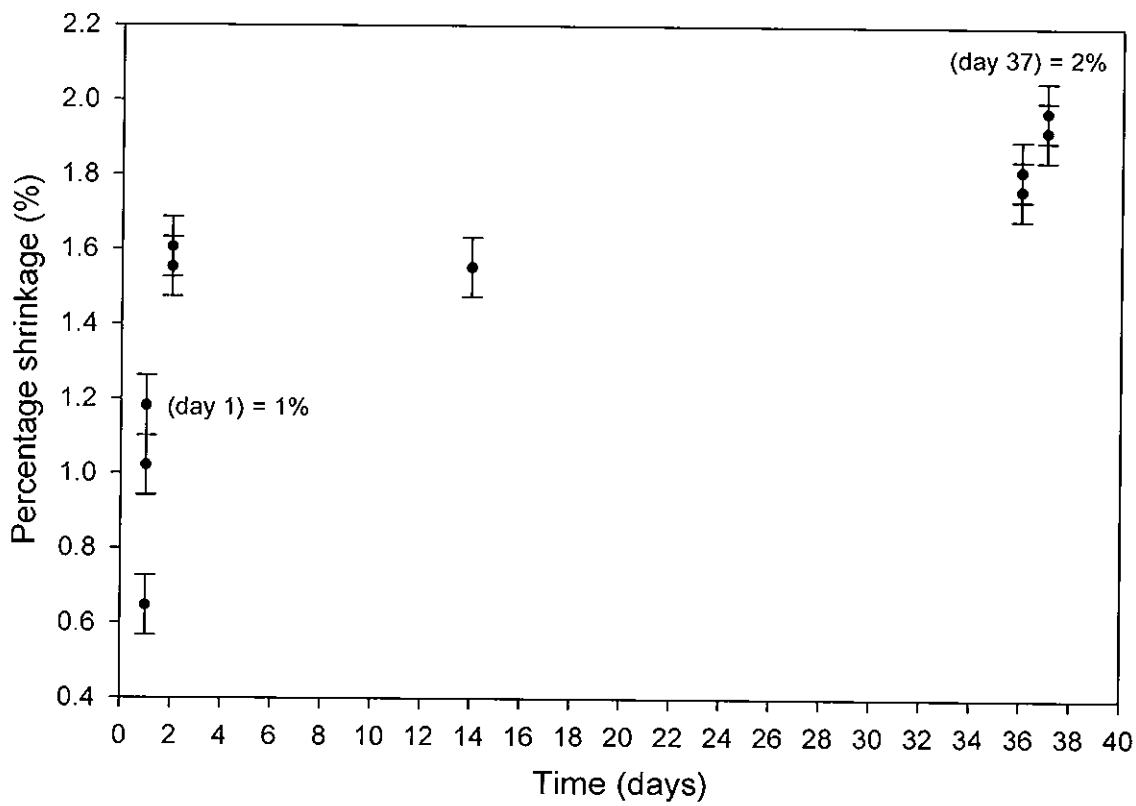

Figure 6.5: Study of the percentage shrinkage change of a slanted grating. The investigation was carried out over a period of 37 days.

It was seen that during the 37 day period, the replay angle of the slanted grating had shifted from the angle at which it was recorded. From the graph, it is clear that the photopolymer layer could have continued shrinking beyond the 37 day investigation. The maximum percentage shrinkage reached could not be obtained, as it was necessary

to use the test system to characterise other photopolymer samples. It can be seen in figure 6.6 that there was no significant change in the shape of the Bragg selectivity curve over this period of investigation, however the maximum diffraction efficiency varied by 11% between the initial and the final angular scan.

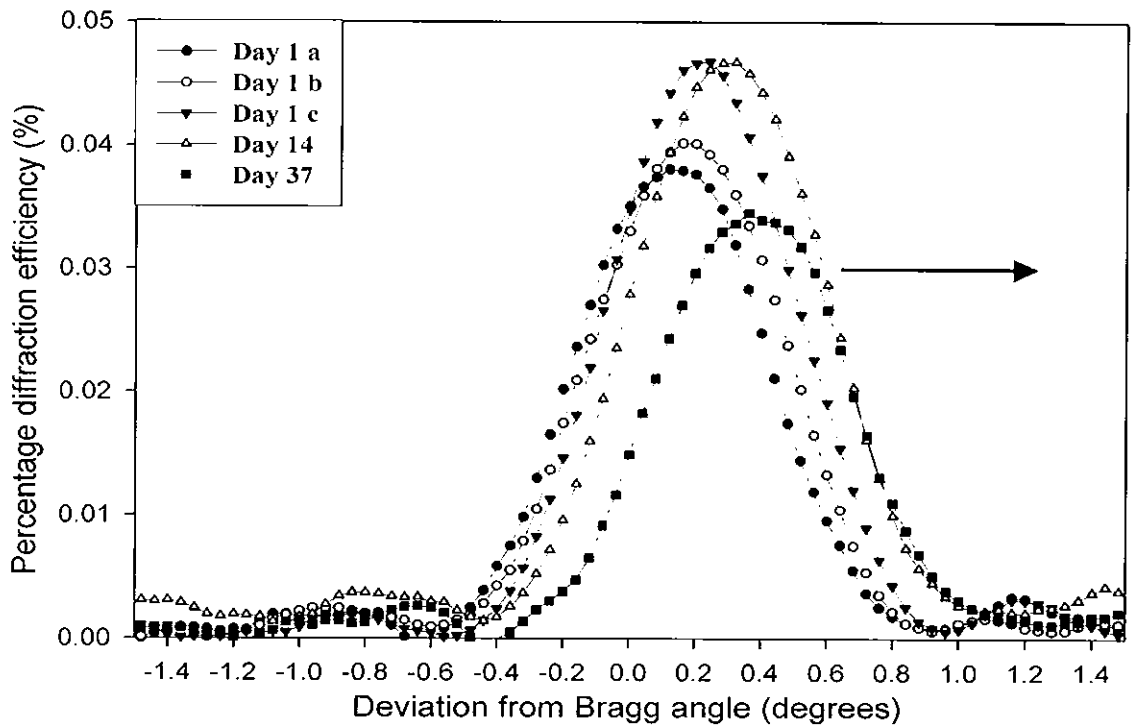

Figure 6.6: This graph shows the variation in the Bragg replay angle of the slanted grating during the period of investigation. The arrow indicates the direction of shrinkage.

6.3.1 Comparison of various zeolite nanoparticle dopants

Photopolymer layers doped with various zeolite nanoparticle components were investigated to determine whether the presence of these nanoparticles suppressed layer shrinkage. Zeolite nanoparticles were investigated, each having different channel diameter in their molecular structure. To determine whether zeolites contributed to suppressing layer shrinkage, the results were compared with the percentage shrinkage of

an undoped sample prepared using the standard composition. The percentage shrinkage was measured directly after the slanted grating was recorded in the layer; this was repeated for all experiments. Each grating was recorded with a slant angle of 6 degrees from the bisector of the incident beams and a spatial frequency of 1320 lines/mm. A pre-exposure of 0.5 seconds was used and each grating was recorded with an exposure time of 20 seconds using 6 mW/cm^{-2} exposure intensity. The percentage relative humidity was noted before each grating was recorded.

Nanoparticle dopant	**Layer thickness (μm)**	**Mean relative humidity (%)**	**Mean shrinkage (%)**
Standard Composition	223 ± 17	46.0 ± 0.05	2.19 ± 0.11
Si-MFI zeolite	91 ± 7	47.2 ± 0.05	1.67 ± 0.08
Zeolite A	110 ± 9	46.8 ± 0.05	1.65 ± 0.08
Zeolite Y	112 ± 9	46.9 ± 0.05	1.25 ± 0.06
Zeolite Al-Beta	83 ± 7	46.8 ± 0.05	2.16 ± 0.11

Table 6.1: Shrinkage results for various zeolite doped photopolymer layers compared with standard composition samples containing 10% and 20% PVA. The shrinkage was measured directly after the slanted gratings were recorded in the layers.

In table 6.1, it is seen that all the doped photopolymer layers still exhibit some degree of shrinkage. However, layers doped with Si-MFI zeolite, zeolite A, and zeolite Y nanoparticles show a marked reduction compared with that of the undoped photopolymer (standard composition). The greatest reduction being observed in zeolite Y, which showed a 57% improvement in shrinkage suppression directly after recording, compared with the standard composition. Presently, the exact mechanism for shrinkage

suppression due to incorporation of zeolite nanoparticles into the photopolymer solution is not known. Investigating the influence of the zeolite nanoparticle's morphology and size are believed to aid in understanding this mechanism.

6.4 Equalisation of multiplexed gratings

Since the photopolymer is a saturable material, the material's dynamic range is unequally shared among equal exposure energy gratings multiplexed in the photopolymer layer. As a result, each additional grating multiplexed in the layer has reduced capability for modulating the photopolymer's refractive index. This is not an ideal situation for holographic data storage considering that all data pages should have the same SNR with each data page having a diffraction peak as strong as its neighbour. With this in mind, it becomes clear that a large series of weaker but equalised data pages is most desirable.

The diffraction efficiency of multiplexed gratings scale as $1/N^2$, where N is the number of gratings multiplexed [8]. Therefore, as the number of gratings stored in the photopolymer increases, appropriate exposure scheduling becomes ever more important, figure 6.7. To improve the uniformity of the multiplexed gratings, it is necessary to progressively increase the exposure times used for recording in such a way as to compensate for the reduced dynamic range that may exist by the time a particular grating is recorded. A grating that, without scheduling, would have a large diffraction efficiency is therefore recorded using a shorter exposure time and a grating that would otherwise have a low diffraction efficiency is exposed for longer. In this way the diffraction efficiencies can be equalized for a large number of gratings. To achieve this, an iterative exposure scheduling method was used [9], enabling the dynamic range to be equally shared between all the recorded gratings.

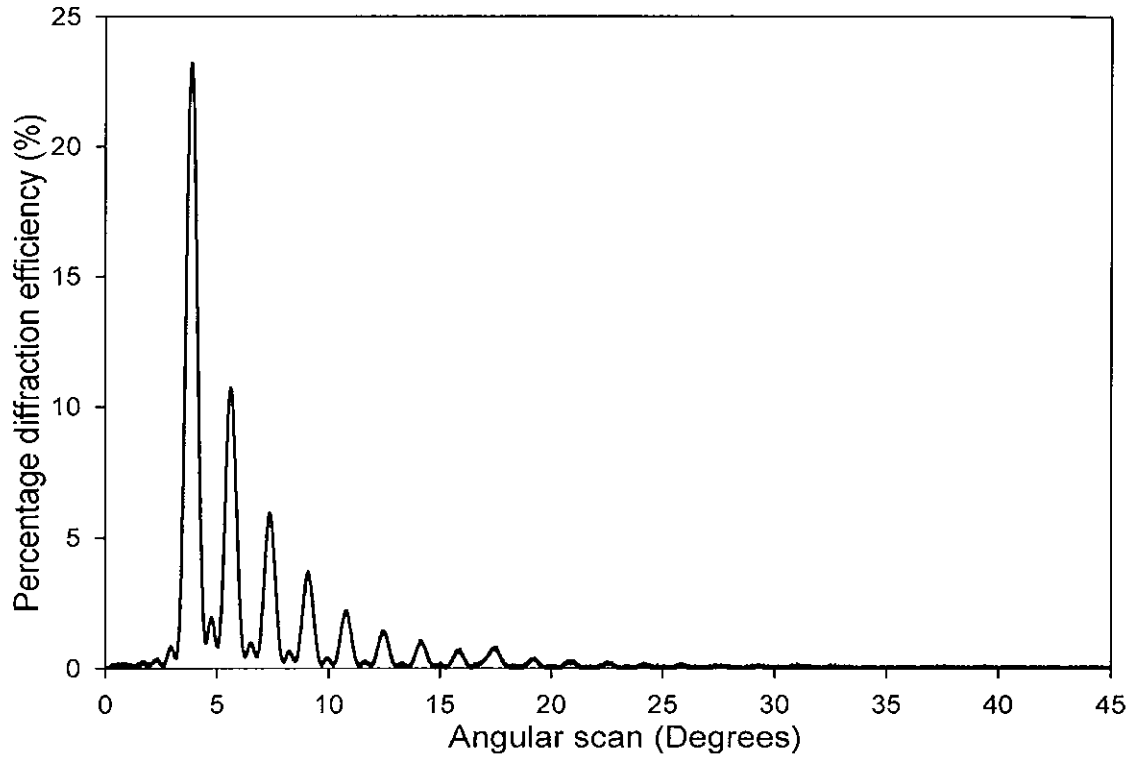

Figure 6.7: When a number of gratings are multiplexed in the same volume of material with equal exposure energy, in this case 30 gratings, a $1/N^2$ scaling of the diffraction efficiency is observed.

To equalise the diffraction efficiencies of individually multiplexed gratings it is necessary to adjust the exposure energy at which the grating in question is recorded. This was acomplished by keeping the laser intensity constant and adjusting the exposure time as required. It can be assumed that increasing the exposure times sequentially with grating number will aid in equalising the multiplexed gratings. A formalised algorithm was used to do just that; this is decribed in more detail in the following paragraphs.

Firstly, a plot of diffraction efficiency η against exposure energy for gratings recorded with equal exposure energy was obtained. To determine the scaling nature of the gratings, a second plot of cumulative grating strength was made, figure 6.8.

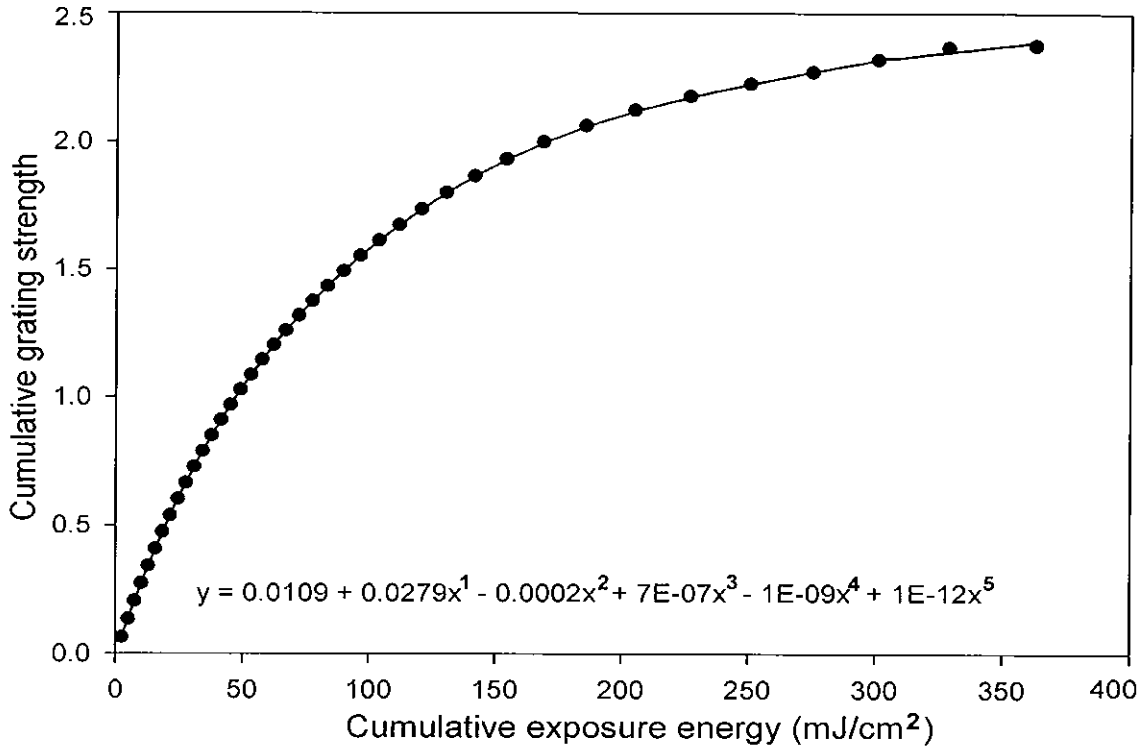

Figure 6.8: Cumulative grating strength as a function of exposure energy.

$$A = a_0 + a_1 E + a_2 E^2 + a_3 E^3 + \ldots + a_6 E^6 \qquad (6.6)$$

A is the cumulative grating strength and E is the total exposure energy. By differentiating the polynomial, the grating strength growth rate as a function of cumulative exposure energy is obtained. Fourth-, fifth-, and sixth-order polynomials were found to have sufficient degrees of freedom to fit the data,

$$\frac{dA}{dE} = a_1 + 2a_2 E + 3a_3 E^2 + \ldots + 6a_6 E^5 \qquad (6.7)$$

Obtaining equal strength gratings is a matter of dividing the available dynamic range equally among the number of gratings to be multiplexed. Thus, the desired exposure schedule becomes,

$$\frac{A_{Sat}}{N} = \left.\frac{dA}{dE}\right|_{E=\Sigma_{i=1}^{n-1}E_i} \times E_n \qquad (6.8)$$

where N is the number of gratings to be recorded, A_{Sat} is the saturation grating strength, E_i is the amount of energy the photopolymer received to record the i^{th} grating, and E_n is the amount of energy required to record the n^{th} grating. Each grating is then allocated $1/N$ of the photopolymer's dynamic range.

From the energy equation $E = I.t$, where I is the combined intensity of the two beams and t is the exposure time, the exposure schedule in terms of time becomes,

$$t_n = \frac{A_{Sat}}{N \times I\left[a_1 + 2a_2\left(\sum_{i=1}^{n-1} Ei\right)^1 + 3a_3\left(\sum_{i=1}^{n-1} Ei\right)^2 + \ldots + 6a_6\left(\sum_{i=1}^{n-1} Ei\right)^5\right]} \qquad (6.9)$$

where t_n is the exposure time of the n^{th} grating and I is the total incident intensity. The a terms are the coefficients obtained from the polynomial fit, which was applied to the cumulative grating strength curve.

The actual algorithm, eqn. 6.6-6.9, was implemented in the *Equalise* module, figure 6.9. The module enabled new exposure times to be determined relatively quickly that could then be sent to the *Multiplex* module for further equalisation.

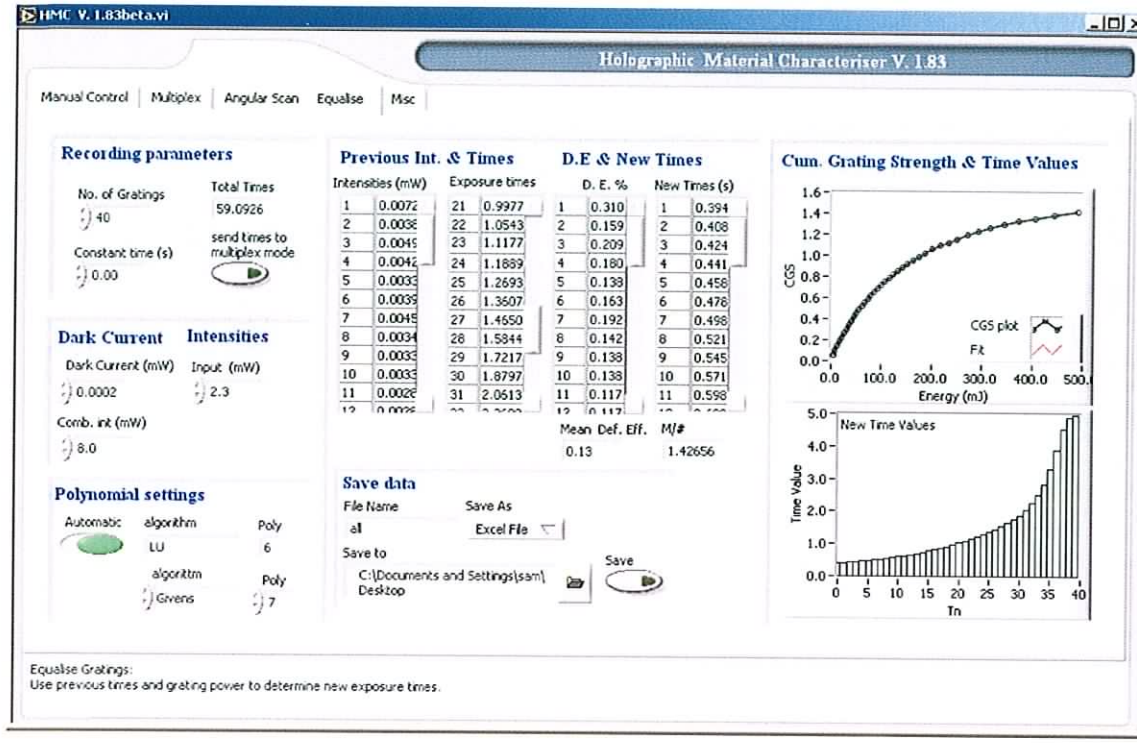

Figure 6.9: Example of the control software used to calculate new exposure times.

By recording a new set of gratings using the exposure times generated from eqn. 6.9, the diffraction efficiencies of the newly recorded gratings are more uniform, figure 6.10. Increasing the uniformity further is simply a matter of repeating the exposure scheduling method outlined above as many times as required. This is at the expense of the overall diffraction efficiency, which was observed to decrease after a number of iterations. See section 6.4.1 for a discussion of this exposure energy reduction with iteration.

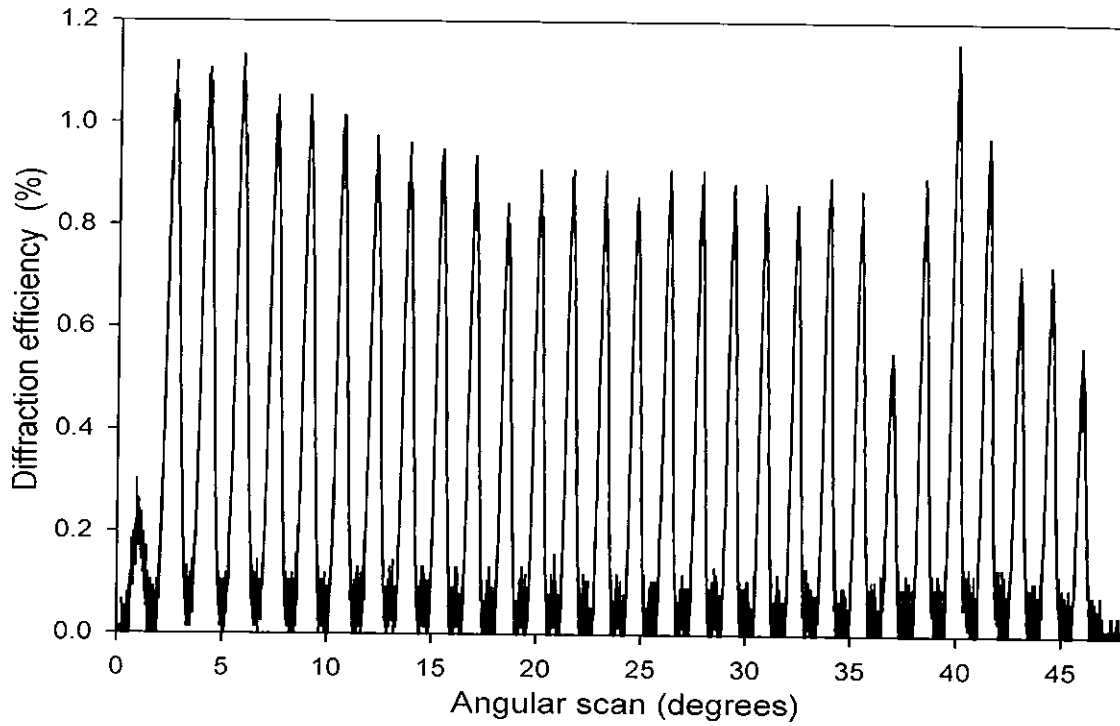

Figure 6.10: Graph of 30 gratings, which have been equalised using the iterative scheduling method.

Once each set of gratings was recorded with approximately uniform diffraction efficiency, the new exposure times were used to repeat the experiment for several series of photopolymer layers, each having a thickness ≈ 160 μm. The combined data from these experiments was used to determine the M/#, section 6.6.

6.4.1 Reduction in exposure energy with iteration of scheduling method

Applying the scheduling method proposed by Pu et al. [9], to a set of peristrophically or angularly multiplexed gratings results in an increase in the uniformity of the gratings with iteration. However, it has been observed that the cumulative exposure time needed to record all gratings decreases with further iteration. Since the exposure intensity is held constant, this implies that there is a reduction in exposure energy. To quantify this, a set of 40 gratings was peristrophically multiplexed to determine whether a reduction

in exposure energy leads to a corresponding reduction in M/#. The gratings were recorded in a variation of the standard photopolymer composition. It differed in that it consisted of a 20 % w/w PVA binder and half the usual dye concentration. The layer thickness was approximately 198.5 ± 10 μm.

Initially, 40 gratings were recorded with a constant exposure time of 2 seconds. A combined exposure intensity of 6 mW/cm^{-2} was used for initial recording and all subsequent scheduling iterations. A pre-exposure of 0.5 seconds was used to sensitise the material and so overcome the inhibition period for each iteration. The inhibition period is the time it takes for the concentration of an inhibitor molecule (oxygen in this case), to fall below a critical value whereby the polymerisation process can begin [10]

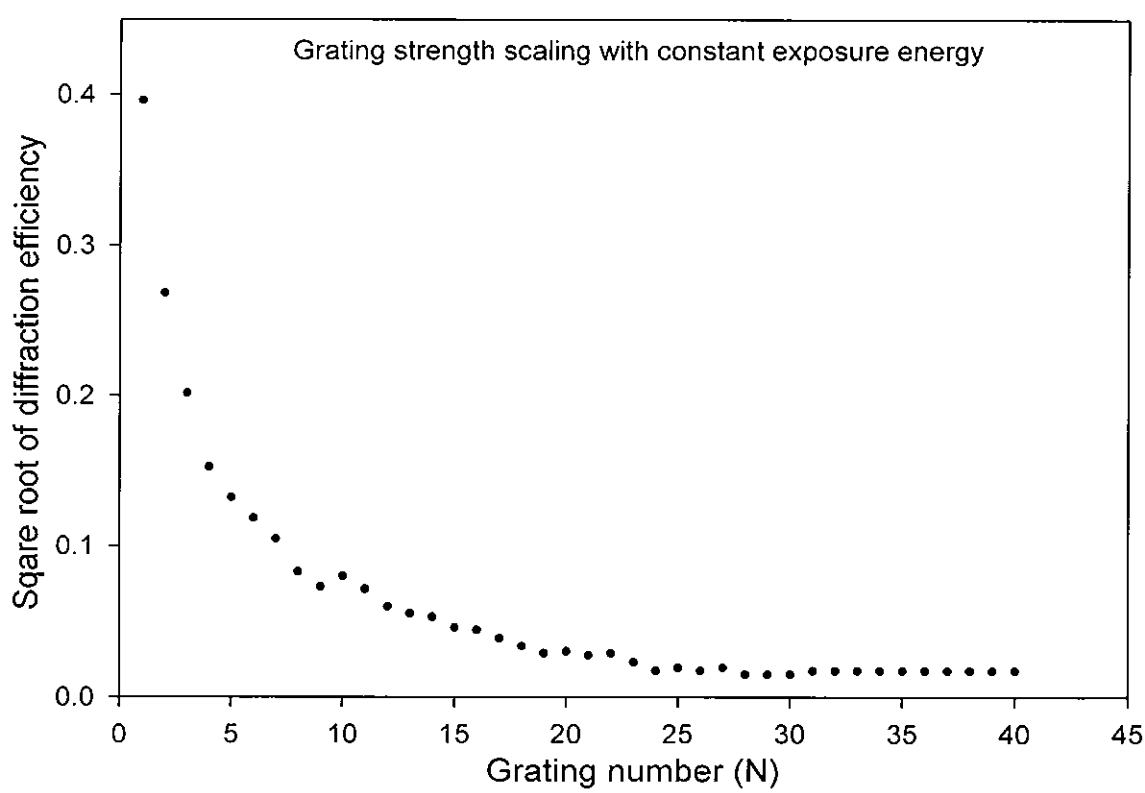

Figure 6.11: Scaling of grating strengths when gratings are recorded with constant exposure energies.

Using constant 2 second exposure times resulted in the typical $1/N^2$ scaling of the grating strengths due to unequal consumption of the dynamic range, figure 6.11. After performing six iterations of the exposure scheduling method, the grating strengths were partially equalised as seen in figure 6.12

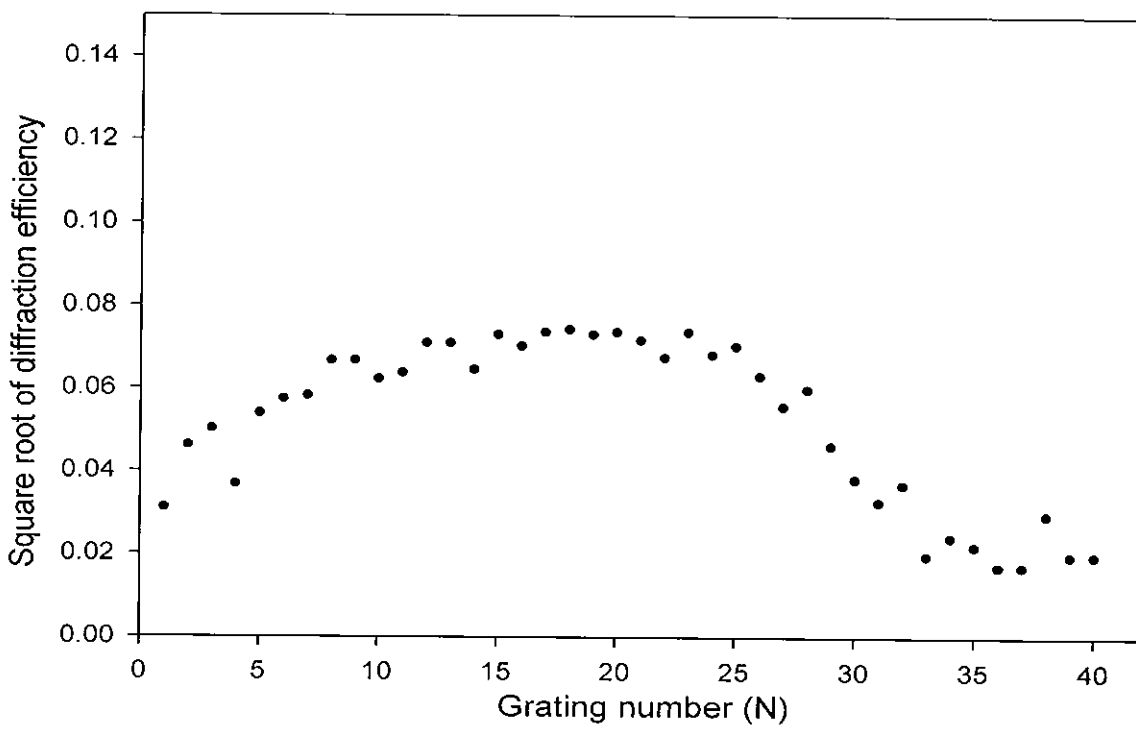

Figure 6.12: After six iterations of the exposure scheduling method, 40 gratings were partially equalised.

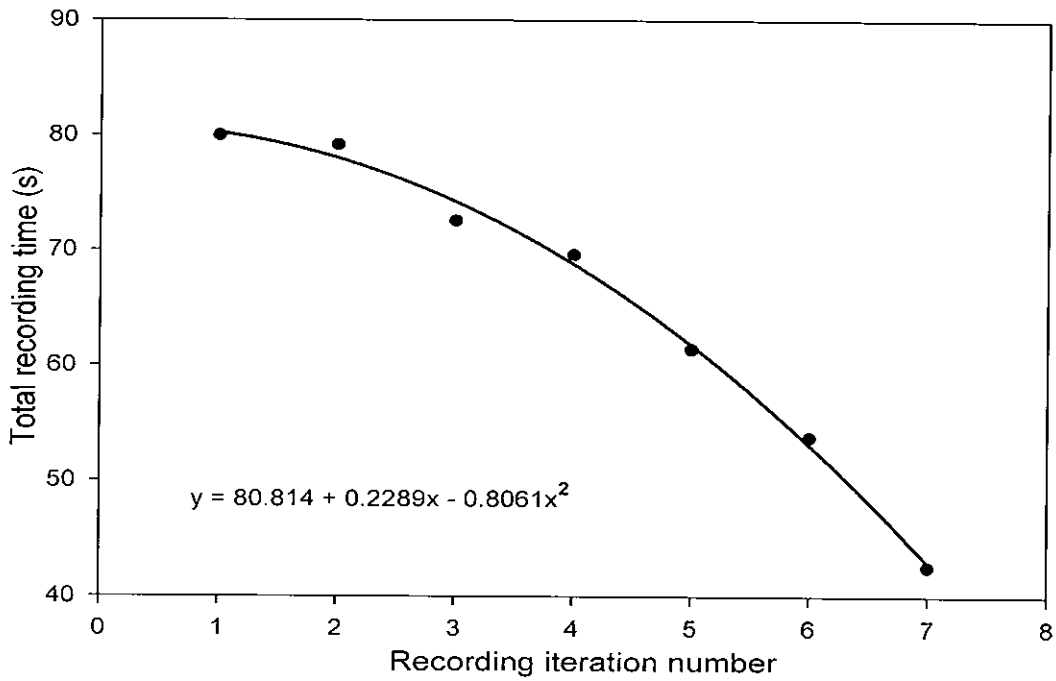

Figure 6.13: With each iteration of the scheduling method there is a drop off in total exposure time required to record 40 gratings.

It was observed that the total exposure times used to record the 40 multiplexed gratings decreased with each iteration of the exposure scheduling process, decaying in a quadratic fashion, figure 6.13. It should be noted that the drop-off may be influenced by the fact that the least square method used to calculate the best polynomial fit applied to the cumulative grating strength curve can vary. Using different fits for the cumulative grating strength curve can directly influence the exposure times that are computed by the scheduling algorithm. The least square methods that may be used are as follows: single value decomposition (SVD), givens, givens2, householder, LU decomposition, and Cholesky [11]. The software can automatically determine the best fit or the user can manually chose which least square method and polynomial order to use.

The software automates the fitting process by evaluating every least square method up to a polynomial order of seven in a brute force manner. The evaluation process is based upon which fit produces the lowest mean squared error. However, this can yield erroneous times so a fit of the cumulative grating strength curve is displayed on the *Equalise* panel. It is then at the user's discretion to decide which fit appears best by manually adjusting both parameters.

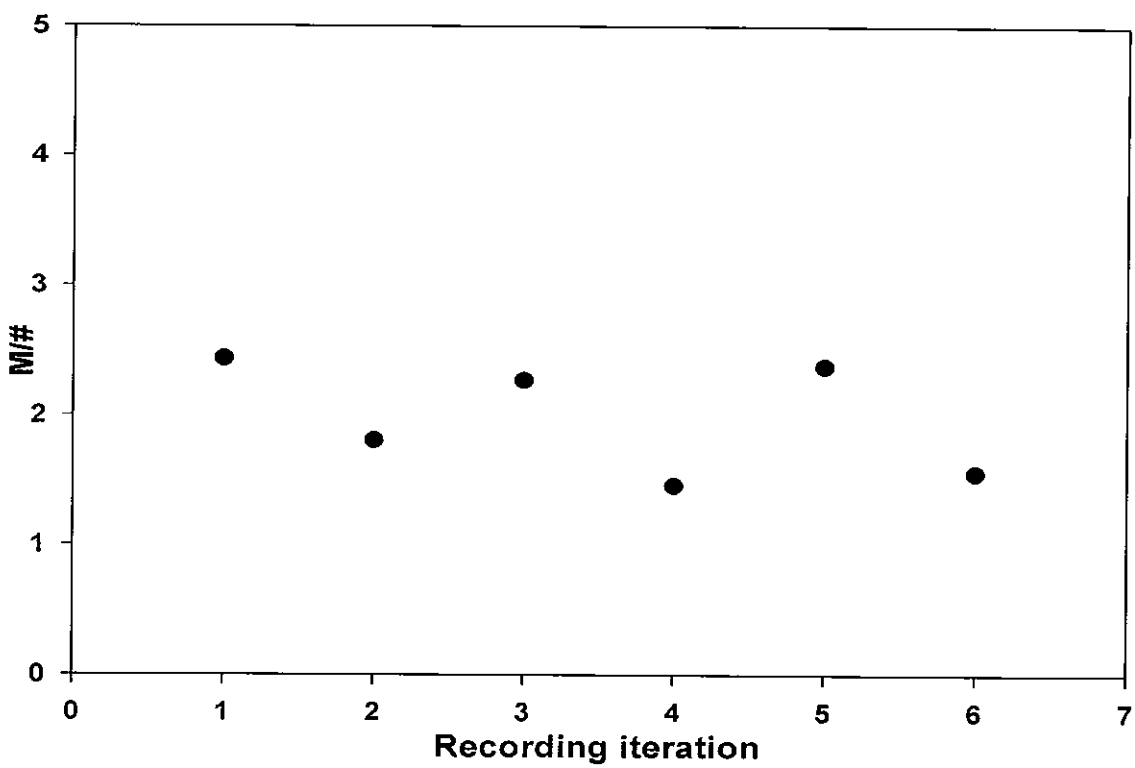

Figure 6.14: A variation in the measured M/# of 40 peristrophically multiplexed gratings was observed with each iteration of the scheduling method. The M/# fluctuated from 1.5 – 2.5.

In figure 6.14 it is seen that the M/# appears to vary with each additional iteration of the scheduling method. The range of M/#s can be attributed to the layers having slightly different thicknesses, different levels of optical scattering, and the generated exposure times not utilising the photopolymer's dynamic range effectively.

The M/# remained within the range 1.5 – 2.5 for six iterations of the exposure scheduling method. Iterating the scheduling method beyond this point resulted in decreasing exposure times that drastically reduced the M/# value and indicated that only a portion of the dynamic range was being used. Further work needs to be carried out to ascertain exactly what causes the exposure energy to be reduced between iterations. More importantly, the reason why the exposure energy can be reduced without adversely affecting the dynamic range needs to be qualified. As of yet it is unclear what allows the material's dynamic range to be utilized more efficiently; this study should help elucidate this.

6.5 Comparison of M/# definitions

As discussed in section 5.1, M/# is a parameter used to quantify dynamic range when discussing HDS media. Two methods for calculating M/# were presented, the first is based on the total response of the medium when divided among multiple holograms recorded in the same volume, and can be calculated from,

$$M/\# = \sum_{i=1}^{N} \sqrt{\eta_i} \qquad (6.10)$$

where N is the total number of holograms and η_i is the diffraction efficiency of the i^{th} hologram. The second method of calculating M/# is based on how the total dynamic range response scales as different sets of multiplexed holograms are recorded. This is obtained from the following equation,

$$M/\# = N.\sqrt{\eta} \qquad (6.11)$$

where N is the total number of holograms recorded in each set of multiplexed holograms. By recording several of these sets and then plotting $\sqrt{\eta}$ against the reciprocal number of holograms for each set, the slope of a linear fit applied to the data will yield the M/#.

By progressively equalising a set of multiplexed gratings it was possible to determine whether the M/#, eqn. 6.10, changed with each iteration of the exposure scheduling method. A change in M/# from one iteration to the next needs to be quantified as there may be a diminishing return in the number of iterative cycles of the scheduling method before a reasonable value of M/# is arrived at. When an optimal number of iterations was arrived at, an experiment was carried out to study the results from these two methods (eqn. 6.10 and 6.11) of determining M/#.

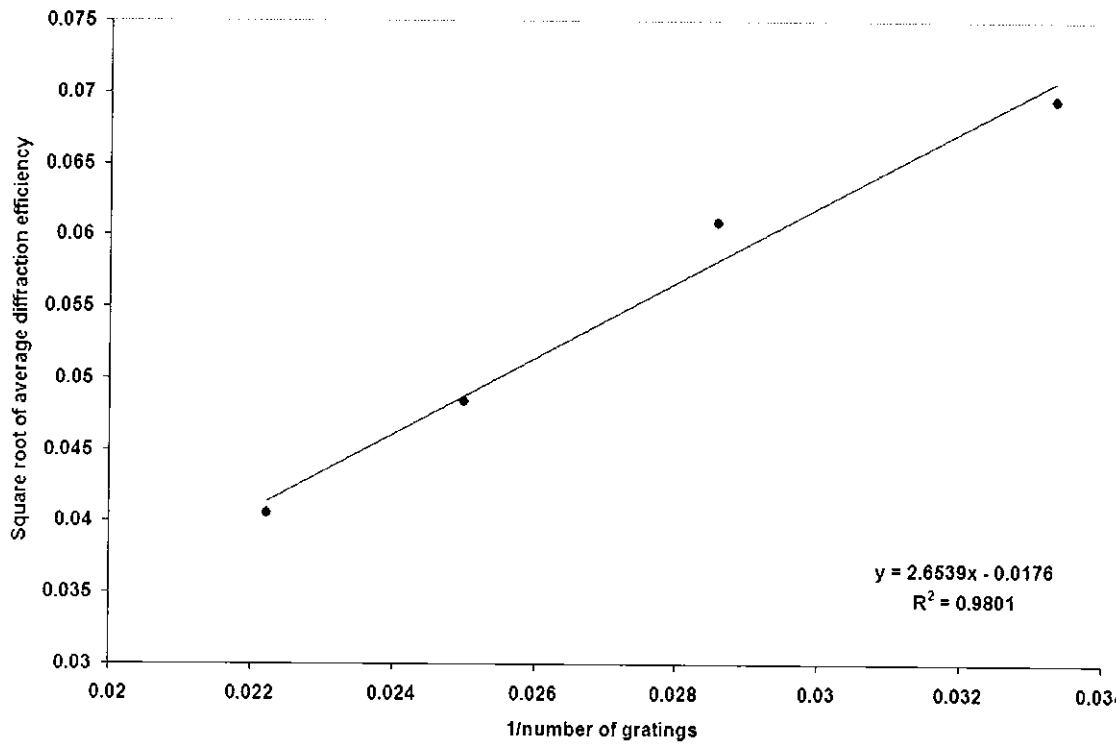

Figure 6.15: 30-45 peristrophically multiplexed gratings yielded an M/# of 2.65 in layers approximately 220 μm thick. The equation used to determine this value is $M/\# = N.\sqrt{\eta}$ where N is the number of gratings multiplexed and η is the diffraction efficiency.

From multiplexing sets of 30, 35, 40, and 45 gratings it was found that the scaling M/# was 2.65 in layers approximately 220 μm thick, figure 6.15. The M/# obtained from the maximum cumulative grating strength was found to have a mean value of 1.89. Since there is quite a large difference between the two values this would indicate that the method for determining M/# should always be stated. Even though the scaling M/# is useful in predicting what the average diffraction efficiency for n number of multiplexed holograms will be, it is quite time consuming as multiple sets of equalised gratings need to be recorded. In general, it is very straightforward to determine the maximum cumulative grating strength M/# and so should be used for comparative studies of different photopolymer compositions where time constraints may be an issue.

6.6 Dynamic range study

The test system, figure 5.1, was used to determine the photopolymer's M/# by recording holographic gratings with low diffraction efficiency. The M/# varies depending on experimental conditions, such as the thickness and absorption of the material, recording geometry, and the ratio of reference to signal beam intensity [9]. Once the M/# is known for a particular setup, it is possible to predict the overall diffraction efficiency for any number of multiplexed gratings. In general materials with large values of M/# are more suitable for use as HDS media.

The M/# is calculated from the graph of the square of the diffraction efficiency against the reciprocal of the number of gratings recorded in the same volume, figure 6.16.

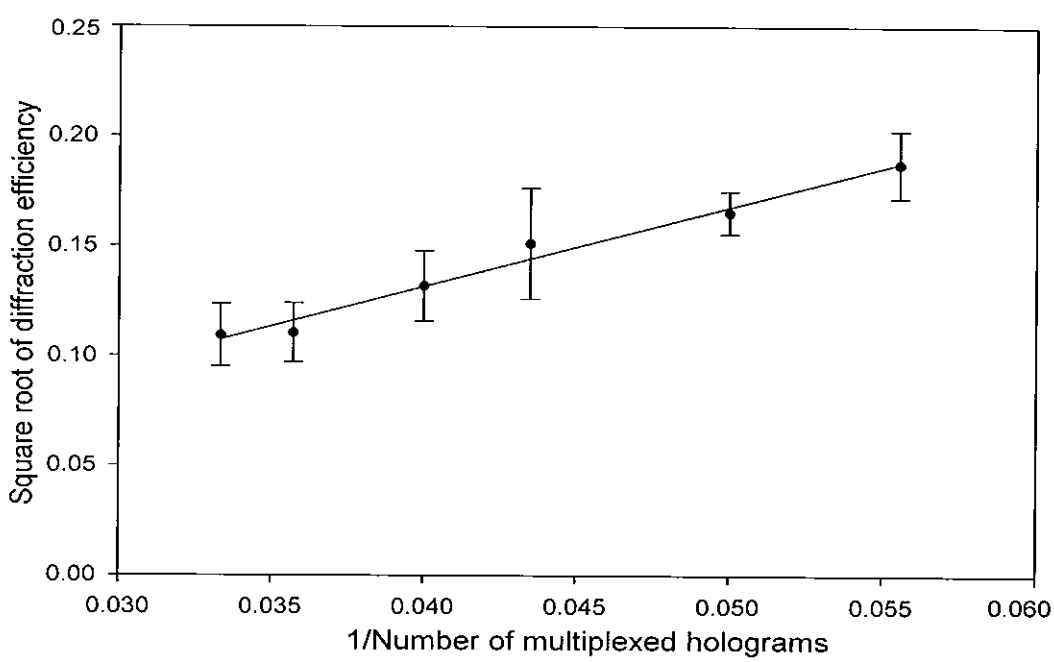

Figure 6.16: Dependence of the square root of average diffraction efficiency on number of equalized gratings. The M/# can be determined from this dependency.

To determine the material's (standard sample) M/# for layers ≈ 160 μm thick, series of 18 to 30 gratings were angularly multiplexed in a photopolymer layer. As more gratings are multiplexed in the volume, the smaller the angle between the photopolymer layer and the bisector of the recording beams becomes. It is for this reason that only 30 gratings were recorded, as more than this would result in high Fresnel reflection losses. To overcome the inhibition period, a pre-exposure of 480 $\mu J/cm^2$ was used before the multiplexed gratings were recorded. This energy was delivered to the material by means of the reference beam. Using angular multiplexing it was found that the M/# for the standard composition was 3.6.

6.6.1 Comparison of zeolite Y and standard composition

From the results obtained in section 6.3.1 it was determined that photopolymer layers doped with zeolite Y nanoparticles suppressed shrinkage by as much as 57 %, compared with the undoped standard composition. It has been observed that the presence of nanoparticles in a photopolymer system can increase the material's dynamic range [2-4]. This is due to the nanoparticles being spatially redistributed in the photopolymer, which in turn causes an increase in the refractive index modulation when regions of the photopolymer are illuminated. To verify if an increase in the refractive index modulation did occur in the recording regime of a large set of low diffraction efficiency gratings, the M/# for the zeolite Y doped layers was determined.

Forty gratings were peristrophically multiplexed into standard composition samples doped with zeolite Y and undoped standard composition samples. A combined exposure intensity of $6mW/cm^{-2}$ was used to record each grating for 2 seconds. The scheduling algorithm was then used to calculate new times and so equalise the gratings. This was

repeated three times, and by the third iteration the M/# of the equalised gratings was determined. For each iteration, a pre-exposure of 0.5 seconds was used to sensitise the material and so overcome the inhibition.

Nanoparticle dopant	Layer thickness	M/#
Standard composition	223 ± 18	1.89 ± 0.09
Zeolite Y	176 ± 14	1.74 ± 0.09

Table 6.2: M/# dependence on zeolite Y dopant added to the standard photopolymer composition.

It was observed that the zeolite Y doped sample had less dynamic range than the undoped sample. The fact that the M/# of the zeolite Y doped layer was 8% less than that of the standard composition layer does not necessarily contradict the findings of Suzuki et al. and Tomita et al. [2-4], as the zeolite Y layer was 21% thinner than the standard composition layer.

6.6.2 Effect of post-exposure

A set of 40 equalised gratings was peristrophically multiplexed into a photopolymer layer (standard composition) with a layer thickness of 198.5 ± 10 μm. The formulation differed from the standard photopolymer composition in that a 20% PVA binder and half the usual dye concentration was used. The layer was then post-exposed with the reference beam by rotating the layer through the same angular range as used during recording, this was repeated a number of times. During each post-exposure the grating strengths were recorded and the M/# was determined.

The 40 gratings were recorded with a combined beam intensity of 6 mW/cm^{-2} and a pre-exposure of 0.5 seconds. The exposure time for each grating was constant for the first recording, this being 2 seconds per grating. After three iterations of the exposure scheduling method, an M/# of 1.97 was arrived at. To determine if subsequent illumination of the recorded gratings brought about an increase in the individual gratings diffraction efficiencies and therefore M/#, the multiplexed gratings were peristrophically rotated ten times while being illuminated by the reference beam. Each post-exposure lasted approximately 162 seconds and the reference beam intensity was set to $0.91 mW/cm^{-2}$.

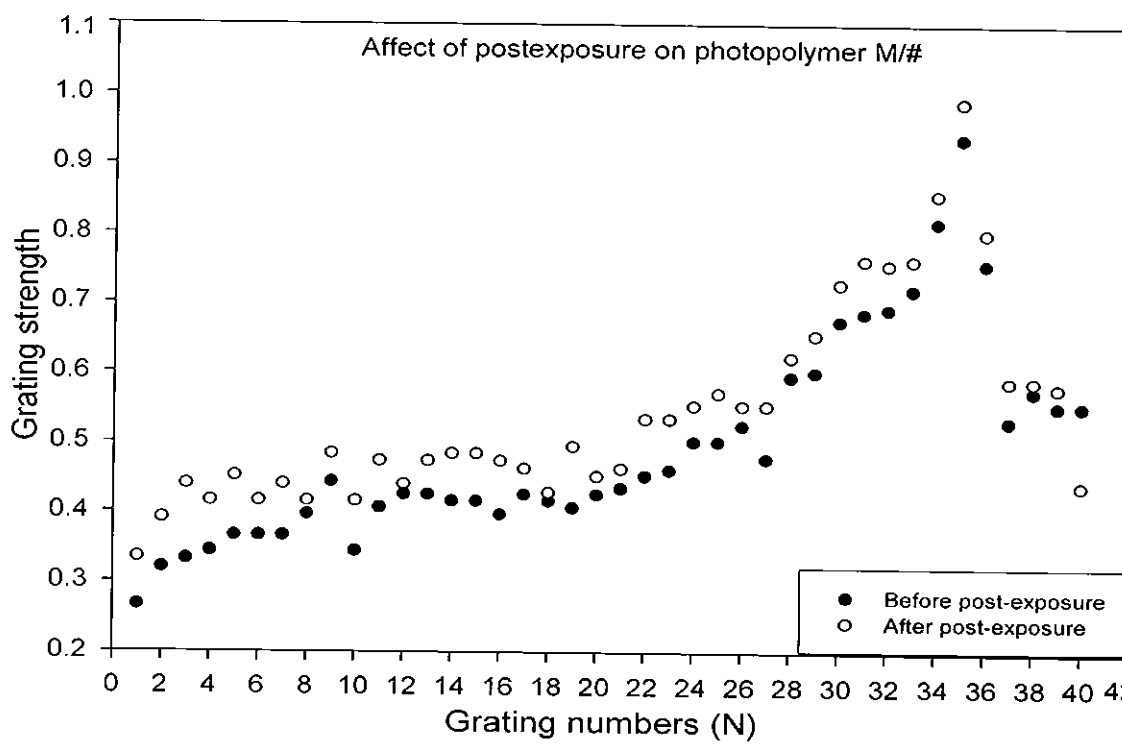

Figure 6.17: Post-exposing a set of 40 multiplexed gratings resulted in a slight increase in grating strength of the individual gratings and thus an increase in M/#.

After post-exposure of the photopolymer layer it was observed that the material's M/# increased to 2.05 with post-exposure, implying that not all of the dynamic range was consumed during the recording of the gratings, figure 6.17. Consequently, further polymerisation of the monomer was possible leading to the dynamic range being more effectively utilised [9].

6.7 Data page recording

A phase-code multiplexing system built at the Wilhelms-Universität Muenster [12-14] was used to characterise the photopolymer (standard composition) in terms of the material's ability to store bit-data pages, figure 6.18.

A 488 nm diode laser was used for recording and replaying the data pages. Positioned immediately after the laser were a $\lambda/2$ plate (HWP (1)), and a polarising beam splitter. These were used so that the object and reference beam intensity ratio could be adjusted. A beam expander and mirror configuration was used in each arm of the system to increase the width of the Gaussian profile of the laser beam. The central portions of the beams were reflected orthogonally towards each other so they could interfere. With this arrangement, the homogeneity of the beams passing through the phase-code modulator and the SLM (HoloEye LC2002) was increased significantly. This is essential for recording and playback of data pages with low BER, as is seen in section 4.1.2.

The expanded beam in the signal arm was collimated before entering the SLM. A polariser was placed between the collimating lens and the SLM to ensure the incident beam was vertically polarised. A second polariser was positioned after the SLM, which only allowed horizontally polarised light to pass through. The light was then vertically

polarised by rotating it through 90^0 by means of a $\lambda/2$ plate, HWP (3) and a converging lens was placed in front of HWP (3) so that the SLM could be imaged on to the CCD array. A 4 x 4 mm square iris was placed in the beam path to allow only the central order of the Fourier image to pass through to the photopolymer layer. A second converging lens was placed in the reference arm to focus the reference beam onto the photopolymer.

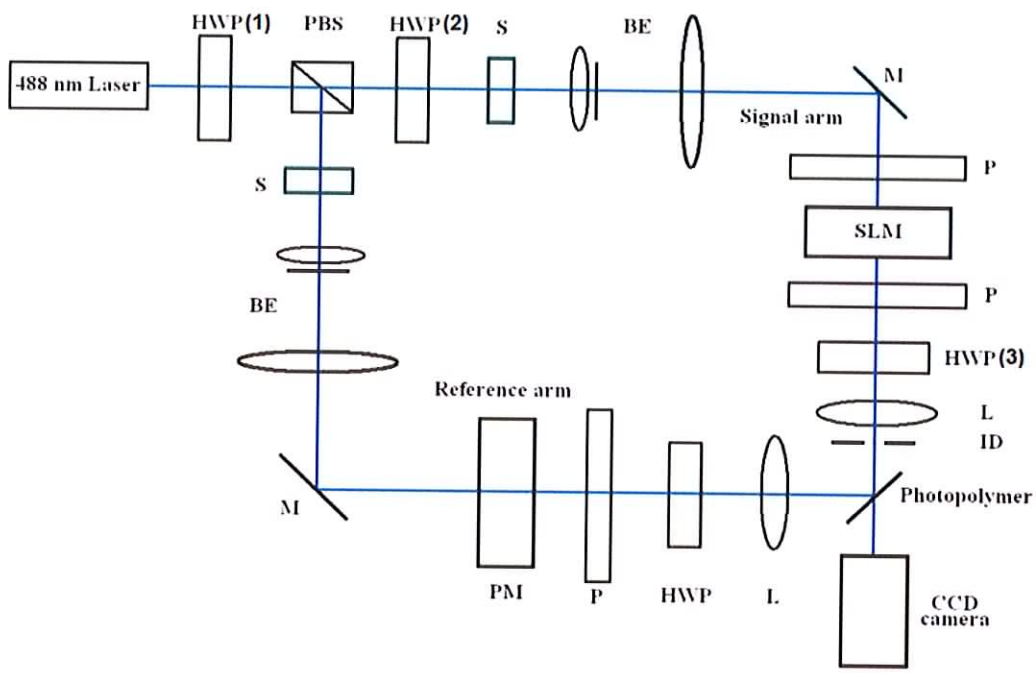

Figure 6.18: Experimental setup used for recording data pages (HWP = $\lambda/2$ plate, PBS = polarising beam splitter, S = electronic shutters, BE = beam expanders, M = mirrors, SLM = spatial light modulator, L = lens, ID = iris diaphragm, P = polarisers, PM = phase modulator).

The photopolymer layer was placed perpendicular to the surface of the bench. It was adjusted so it made angles of 35° to the signal beam and 55° to the reference arm. These angles were chosen as opposed to a 45° angle between each beam, because interference fringes from the glass slide were being observed. As these were of comparable size to the imaged data page bits, it was necessary to remove them by using asymmetrical

angles of incidence. The area of overlap on the photopolymer between the incident beams occurred approximately 2 mm in front of the Fourier plane of the lens to prevent damage to the photopolymer layer by subjecting it to too much light energy. A homogeneous region of the reference beam was overlapped with the signal beam, thus minimising the effect of an uneven beam profile. The signal and reference arm intensities were equalised by rotating the first half wave plate, HWP (1).

The data page was recorded in the photopolymer layer as a modulation of the material's refractive index resulting from the complex interference pattern produced by the object and reference beam. A standard (800 x 600 pixel) VGA image digitally addressed the SLM to produce the data page. A random two-dimensional array of bright and dark squares corresponding to the binary numbers 1 and 0 comprised the data page, the amplitude ratio between the two values being 1000:1. The same data page was used for all experiments thus maintaining consistency between experiments. Each bit that went to make up the data page was oversampled so that every block of 10 x 10 pixels on the SLM corresponded to a single data bit. Therefore, the final image consisted of 80 horizontal bits by 60 vertical bits. When imaged onto the photopolymer, the page measured 1 mm by 0.75 mm with each bit measuring 12.5 μm square. Computer controlled shutters determined the duration of recording.

Once recorded, the data page was reconstructed by means of the reference beam and finally imaged on to a CCD array. An XYZ linear stage was used to mount the camera. This allowed the reconstructed image to be aligned and focused on the CCD array. This was critical, as each photopolymer layer tends to have slightly different optical properties. Thus, the reconstructed data page would not necessarily be aligned to the CCD array for different experiments.

For the majority of experiments, a combination of neutral density filters was used to attenuate the readout beam by 74%. This was done to reduce the possibility of further polymerisation of the layer. When determining the photopolymer's recording period, section 6.7.2, only 0.6 % of the reference beam intensity was used to playback the recorded holographic data page each time it was monitored. This was done to reduce the effect of post-polymerisation of the recorded data page over the course of the investigation. A consequence of attenuating the readout beam was that the integration time of the CCD array had to be increased to allow weakly reconstructed data pages to be adequately imaged.

6.7.1 Optimisation of recorded data pages

A series of data pages was recorded with exposure energy densities ranging from 4 mJ/cm^2 to 12 mJ/cm^2. For each exposure energy density, a number of different combinations of exposure time and intensity were used to record the pages. Data pages of consistently high quality were observed when recorded with intensity 2.8 mW/cm^2 for 2.8 seconds. These pages were observed to have high bit contrast with well-defined edges and good image resolution. It is assumed that the volume of photopolymer that stores the data could be reduced even further whilst still maintaining faithful reconstruction of the data. This can only be confirmed once a quantitative study is carried out to examine how the raw-BER increases as data page size decreases.

Figure 6.19(a) shows the data page imaged on to the SLM. The same page was used for examining the recording period of the photopolymer, section 6.7.2. An analogue image, figure 6.19(b), was also imaged on the SLM and then holographically recorded using the optimal exposure time and intensity, to test the material's response to an image

containing a large number of spatial frequencies. It can be seen that both reconstructions of the recorded holograms exhibit good resolution, figures 6.19(c-d).

Figure 6.19 (a)

Figure 6.19 (b)

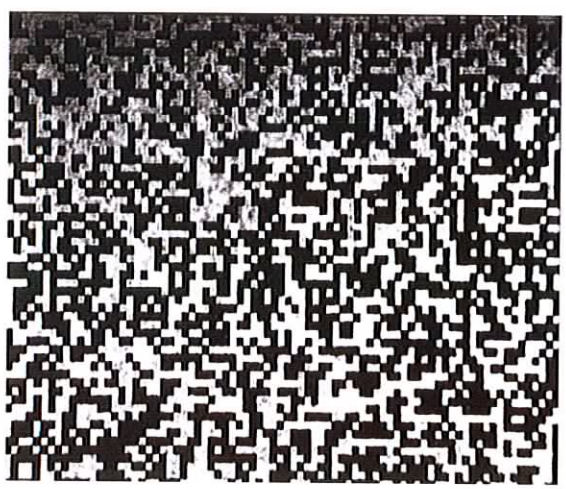

Figure 6.19 (c)

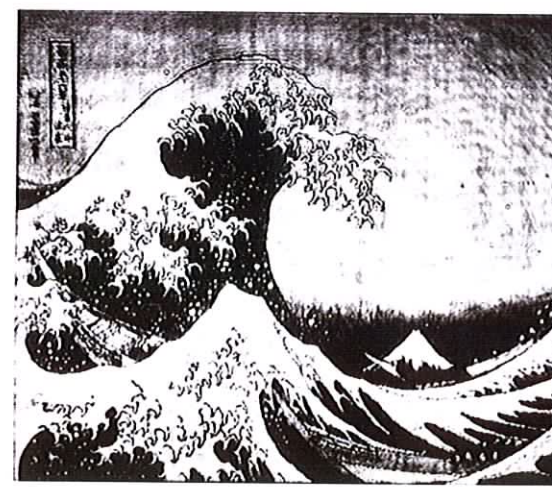

Figure 6.19 (d)

Figure 6.19: Data page (a) and analogue image (b) as they appeared on the SLM. The reconstructed holographic images which were produced with a combined beam exposure energy density of 8 mJ/cm^2 (c) & (d).

6.7.2 Determination of recording period

Another important HDS media parameter is the time period available for data page recording with low BER after initial photopolymerisation has begun. All holographically multiplexed data should be recorded during this period. The photopolymer can finally be "bleached" to inhibit further photopolymerisation by halting the creation of free radicals.

It is seen in figure 6.20(d) that after 1 hour there is significant degradation of the data page in terms of a decrease in diffraction efficiency in certain regions of the image. The well defined borders between individual bits are also seen to smear with time.

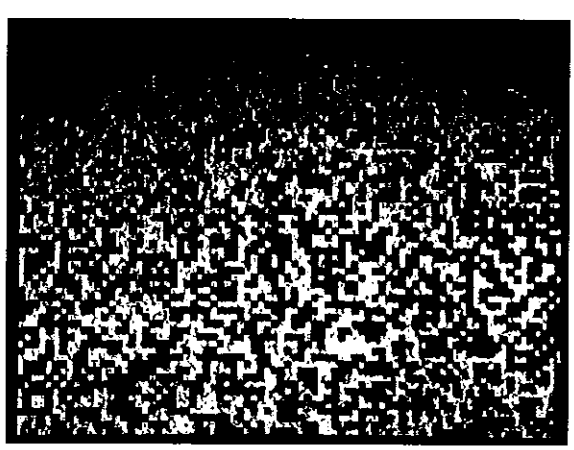

Figure 6.20 (a) 20 seconds

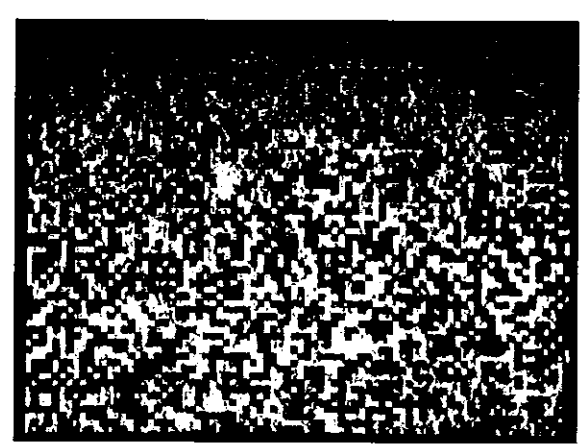

Figure 6.20 (b) 10 minutes

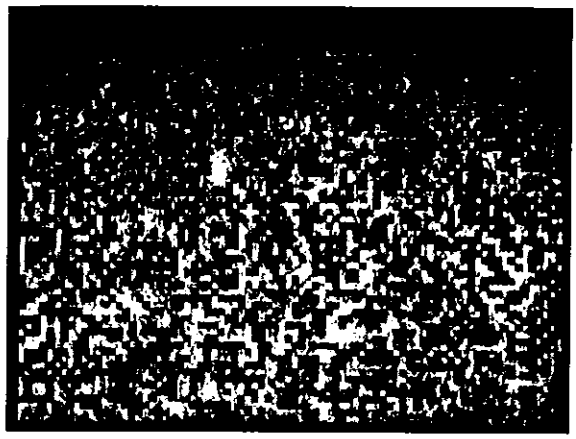

Figure 6.20 (c) 30 minutes

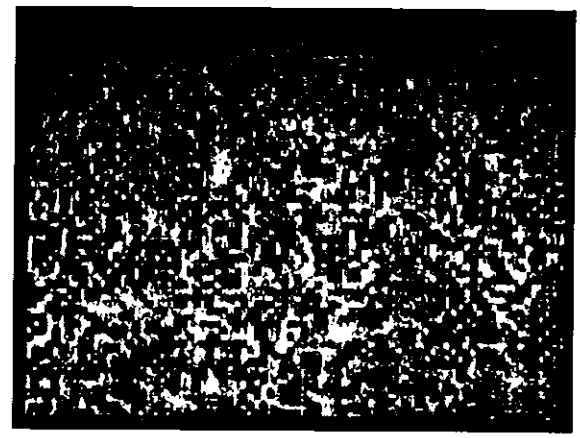

Figure 6.20 (d) 1 hour

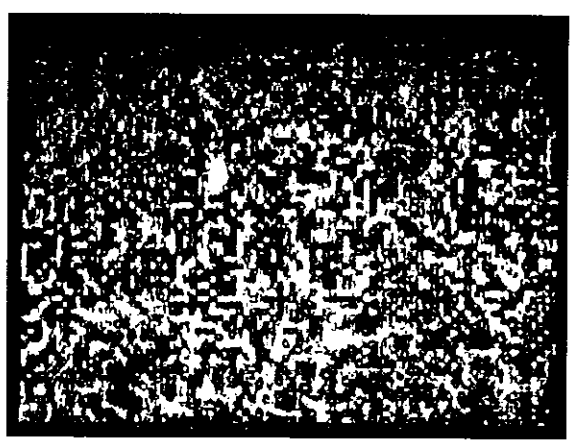

Figure 6.20 (e) 4 hours

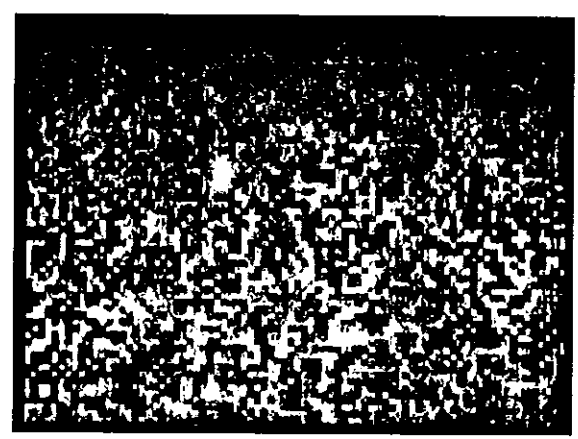

Figure 6.20 (f) 8 hours

Figure 6.20: Images (a) to (f) show a reconstructed holographic data page at different times over a period of 8 hours after initial recording. A degradation of image quality is observed.

The observed change in the recorded data page is attributed to the diffusion of material between exposed and unexposed regions of the photopolymer. It is known that two different diffusion processes take place during and after holographic recording in the photopolymer system. The first process occurs when the monomer molecule diffuses from dark to bright fringe areas of the photopolymer, resulting in a positive contribution to the final refractive index modulation. The second process involves diffusion of

terminated or unterminated short polymer chains from bright to dark fringe regions [15]. This has a negative contribution to the final diffraction efficiency.

6.8 Summary

Parameters affecting the angular selectively and diffraction efficiency of transmission phase holograms were modelled. These include the thickness of the layer, spatial frequency of recording, and refractive index modulation parameter.

The test system, which was purposely built for this work, was used to characterise the shrinkage of a standard composition photopolymer layer monitored over the course of 37 days. A number of zeolite nanoparticles were incorporated into the composition to determine whether their presence assisted in suppressing shrinkage immediately after recordings.

Following this, a study of the photopolymer's dynamic range was made. This entailed recording a number of equalised gratings in the same volume of material to determine the material's M/#. The gratings were equalised by means of an iterative exposure scheduling method.

During the course of this work two definitions of M/# were used. It was found that the scaling M/#, does not necessary agree with the M/# values determined from the maximum value of the cumulative grating strength curve. An experiment was also carried out to determine whether post-exposing a set of peristrophically multiplexed gratings would result in further polymerisation of the acrylamide.

A phase-code multiplexing system built at the Wilhelms-Universität Muenster was used to characterise the photopolymer (standard composition) in terms of the material's ability to store bit-data pages. The recording period (time available for data page recording with low BER after initial photopolymerisation has begun) was also determined.

6.9 References

[1] P. Hariharan, "Optical Holography, Principles, techniques, and applications" 2nd ed. Cambridge University Press, 1996.

[2] N. Suzuki, Y. Tomita, T. Kojima,"Holographic recording in TiO2 nanoparticle-dispersed methacrylate photopolymer films", Applied Physics Letters, **81,** 4121, 2002.

[3] Y. Tomita and H. Nishibiraki, Improvement of holographic recording sensitivities in the green in SiO2 nanoparticle-dispersed methacrylate photopolymers doped with pyrromethene dyes", **83**, (3), 410-412, 2003.

[4] N. Suzuki, Y. Tomita, "Silica-nanoparticle-dispersed methacrylate photopolymers with net diffraction efficiency near 100%", Applied Optics, **43** (10), 2125-2129, 2004.

[5] Y. Tomita, N. Suzuki, K. Chikama, "Holographic manipulation of nanoparticle distribution morphology in nanoparticle-dispersed photopolymers", Optics letters, Vol. 30, No. 8, 839-841, April 2005.

[6] P. Trochtchanovitch, N. Kostrov, E. Goulanian, A. F. Zerrouk, E. Pen, V. Shelkovnikov, "Method of characterization of effective shrinkage in reflection holograms", Optical Engineering, Vol. 43, No. 5, 1160-1168, May 2004.

[7] F. T. O'Neill, J. R. Lawrence, J. T. Sheridan, "Thickness variation of self-processing acrylamide-based photopolymer and reflection holography" Optical Engineering, 40(4) 533-539, April 2001.

[8] R F. H. Mok, G. W. Burr, D. Psaltis, "System metric for holographic memory systems", Optics Letters, Vol. 21, No. 12, June 1996.

[9] A. Pu, K. Curtis, D. Psaltis, "Exposure schedule for multiplexing holograms in photopolymer films", Optical Engineering, 35 (10): 2824-2829 Oct 1996.

[10] T. V. Galstian, S. Harbour, A. V. Galstyan, R. S. Hakobyan, Electronic-Liquid Crystal Communications, 2004, http://www.e-lc.org/Documents/T._V_Galstian_2004_05_05_11_13_17.pdf

[11] National Instruments developers of LabVIEW, http://zone.ni.com/reference/en-XX/help/lv/71/gmath/General_Polynomial_Fit/, 2005.

[12] C. Denz, G. Pauliat, G. Roosen, T. Tschudi, "Volume hologram multiplexing using a deterministic phase encoding method", Optics Communications, Vol. 85, no. 2.3 171-176, Sept. 1991.

[13] C. Denz, K. -O Müller, F. Visinka, T. Tschudi, "A Demonstration Platform for Phase-Coded Multiplexing" Published in "Holographic Data Storage", H. Coufal, D. Psaltis, G. Sincerbox (Eds.), Springer, S. 419-428, 2000.

[14] G. Berger, K. -O. Müller, C. Denz, I. Földvári, Á. Péter, "Digital data storage in a phase-encoded holographic memory system: data quality and security", Proc. SPIE, Vol. 4988, 104-111, 2003.

[15] J. R. Lawrence, F. T. O'Neill, J. T. Sheridan, "Photopolymer holographic recording material", Optik (Stuttgart, The International Journal for Light and Electron Optics) 112, 449-463, 2001.

CHAPTER 7

7. Future work

During the course of the project, it became evident that a number of improvements could be made to the test system. These improvements would facilitate further research and development of a photopolymer with properties suitable for use in HDS applications. Modifications to the test system that allow more accurate measurements and characterisation of additional photopolymer properties are discussed in section 7.1 Finally, the steps needed to optimise the photopolymer chemistry specifically for holographic data storage are examined in section 7.2.

7.1 System improvements

Described below are a number of ways that the current test system may be improved to allow additional photopolymer properties to be quantified.

It would be advantageous to have the capability to rapidly characterise the M/# for different photopolymer compositions. This requires an equalisation process that is more efficient and less time consuming than the exposure scheduling method that is currently employed. A study could be conducted to determine whether an alternative method of equalisation such as incremental recording would be more effective for equalizing the diffraction efficiency of multiplexed gratings. Additionally, a study should be carried out to determine whether constant exposure times and varying exposure intensities

could increase the dynamic range. This is important as it is preferable to record data pages with relatively short and equal durations rather than progressively longer recording times.

Replacing the current AR^+ laser with a diode laser would allow for a much more compact system design. For example, the Sapphire 488 diode laser produced by Coherent Inc. is 12.5 x 7 cm in dimension and could be incorporated into the test system architecture quite easily. This has the benefit that the laser intensity could be controlled by the software, which would further increase automation of the experiments. One way of adjusting the intensity of the current AR^+ laser is by incorporating a graded neutral density filter into the path of the laser beam and then rotating the filter by means of a stepper motor to the desired optical density. By tapping off a small portion of the laser light using a $\lambda/2$ wave plate in conjunction with a polarising beam splitter the intensity in the larger beam can be determined. This is done by monitoring the intensity of the weaker beam with a calibrated photodiode, which can be interfaced to the PC.

At present recording and monitoring holographic gratings of single spatial frequency, is the main method of characterising the photopolymer. To better approximate material behaviour when data pages are stored, SLM and CCD arrays may be incorporated into the current test system. This would allow the raw-bit error rate of the recorded data pages to be quantified for various photopolymer formulations, thus facilitating the study of page longevity and recording period.

7.2 Photopolymer optimisation

Further optimisation of the photopolymer's dynamic range and shrinkage is needed to make the material better suited to HDS applications. Work has already been carried out to improve these characteristics. For instance, reducing shrinkage and increasing dynamic range are being tackled by incorporating various nanoparticle dopants into the photopolymer chemistry. Additionally, a number of different binder polymers are being studied to determine whether they produce a more rigid matrix that does not suffer dimensional instability. So far there has been some success in this direction but to produce a viable photopolymer for HDS, shrinkage needs to be less than 0.1% while the M/# should be at least in double figures.

Initial characterisation of thicker photopolymer layers ($\approx$ 800 micrometers) has been carried out. The thicker layers were observed to have increased angular selectivity with reduced shrinkage. Further work needs to be carried out in determining appropriate recording parameters, reducing scattering and optical density before the dynamic range can be determined.

A requirement of any commercial HDS medium is that it can be stored prior to information being recorded in the medium for a reasonable amount of time, i.e. it has an adequately long shelf life. Additionally, it is important that the medium longevity is sufficiently long that data recorded in the medium may be faithfully retrieved for several years after initial recording. This length of time is normally dictated by consumer demands. Both shelf life and data longevity need to be quantified and optimised once a suitable photopolymer candidate is found.

Finally, an appropriate method of protecting the layers from the environment needs to be developed. This will entail finding a suitable method of encapsulating the layer between glass slides. This should make the layers less susceptible to the environment and help improve shelf life and longevity after recording. Initially an epoxy resin that is index matched with the layer and glass, and does not adversely affect the layer could be investigated.

CHAPTER 8

8. Conclusion

The work conducted for this thesis represents the initial characterisation of an acrylamide-based photopolymer system developed in the Centre for Industrial and Engineering Optics for HDS applications.

A test system, which has the ability to characterise parameters relating to the photopolymers suitability for HDS, namely dynamic range (M/#) and temporal stability in terms of shrinkage was built. The test system has the capability of multiplexing sets of equalised holographic gratings using either angular or peristrophic multiplexing, a combination of the two, or recording single slanted and unslanted gratings.

The photopolymer's (standard composition) temporal stability was studied over a 37 day period. It was observed that the layer shank by as much as 2% ± 0.1% after the 37 day period, which is quite large compared with shrinkage values quoted for InPhase Technology's 523530 and 323530 photopolymers, these being 0.1% and 0.5% respectively [1].

To reduce the standard photopolymer shrinkage, zeolite nanoparticle components were incorporated into the photopolymer composition. It was found that zeolite doped photopolymers are characterised by less shrinkage when compared with non-doped samples. Zeolite A, zeolite Y, zeolite aluminium beta, and Si-MFI zeolite were the

nanoparticle candidates chosen for this experiment. It was observed that incorporation of Zeolite Y type nanoparticles leads to lowest shrinkage in the photopolymer. At present, the exact mechanism by which nanoparticles suppress the shrinkage is unknown. Further studies of the characteristics of photopolymers doped with different size and structure of the zeolite dopants will be necessary in order to answer this question.

The dependence of dynamic range upon photopolymer layers doped with different zeolite nanoparticles was quantified. The photopolymer doped with zeolite Y was investigated in terms of M/# to determine whether an increase in dynamic range had resulted when gratings were recorded peristrophically in the doped layer. It was found that zeolite Y doped layers shrank by 1.25% ± 0.06% and had an M/# of 1.74 for layers 176 ± 14 μm thick. This compares favourably with the standard composition which has a shrinkage of 2.19% ± 0.1% and a M/# of 1.89 for layers 223 ± 18 μm thick. Even though there is an improvement in the level of shrinkage with only slight reduction in the M/#, both properties need to be significantly improved to be competitive with that of commercially developed photopolymer systems.

It was found that the exposure scheduling method described in section 6.4, results in a reduction in overall exposure energy from one iteration to the next. The cumulative exposure time decreased in a quadratic manner without a marked reduction in M/# for the first 6 iterations. Iterating beyond this point affects the M/# adversely. It was found that the M/# defined by the equation $M/\# = N.\sqrt{\eta}$, i.e. the scaling M/#, does not always agree with the M/# values determined from the maximum value of the cumulative grating strength curve, this M/# being defined by the equation

$M/\# = \sum_{i=1}^{N} \sqrt{\eta_i}$. Using both definitions of M/#, values of 2.65 and 1.89 for layers approximately 220 μm thick, were obtained respectively when recording in peristrophic mode. It was found that the second method of determining M/# is quite repeatable and can be obtained relatively quickly. For this reason it may be useful when large selections of samples need to be compared and using the scaling M/# would be prohibitive.

Finally, the photopolymer's ability to record and store bit wise data pages was evaluated. The optimal exposure intensity and exposure time needed to record a single holographic data page having good quality was determined to be 2.8 mW/cm^2 for 2.8 seconds. It was found that exposure energy densities ranging from 6 – 12 mJ/cm^2 can be used to record good quality data pages.

The period for which all holographically multiplexed data should be recorded before being bleached was studied. It was observed that 1 hour after recording there was significant degradation of the data page in terms of a decrease in diffraction efficiency in certain regions of the image and smearing of the well-defined borders between individual bits. The observed change in the recorded hologram was attributed to the diffusion of material between exposed and unexposed regions of the photopolymer.

Outlook:

It is clear that further research needs to be conducted to better understand the recording processes within the material. In particular, a detailed study should be conducted into the effect various dopants and binders have on the photopolymer composition and how they aid in suppressing shrinkage. This will allow the material's attributes to be specifically tailored for its use as a HDS medium.

At present the test system is capable of quantifying dynamic range and shrinkage. These are important material characteristics but alone do not guarantee a viable HDS media. Augmenting the test system and control software so that other HDS material properties may be characterised is essential for this photopolymer to be commercially competitive. Properties that need to be investigated in the future include shelf life, longevity, scatter, and raw BER of recorded data pages.

8.1 References

[1] M. Schnoes, B. Ihas, A. Hil, L. Dhar, D. Michaels, S. Setthachayanon, G. Schomberger and W. L. Wilson, "Holographic Data Storage Media for Practical Systems", www.inphase-technologies.com/technology/whitepapers, 2005.

APPENDICES

A. System operation manual

The test system consists of software written using LabVIEW 7.0, optical elements for shaping and directing the recording beams and electronic instrumentation. In this appendix, the software operation is described. Since the software is designed to be modular, each module is described in turn with its associated interface panel. The LabVIEW code for each control module is given separate attention in appendix B. To access a module interface panel the user clicks on the desired module tab located in the top left corner of the software display.

Manual control mode:

The top left section labelled *Manual Stage Control* of the *manual control* panel, figure A.1, is used to adjust the two rotational stages. First, the stage to be rotated is selected by choosing either *Peristrophic* or *Angular* in the list box. After being selected, the software monitors the position of the chosen stage at all times; the position is displayed in the *Current Position* indicator.

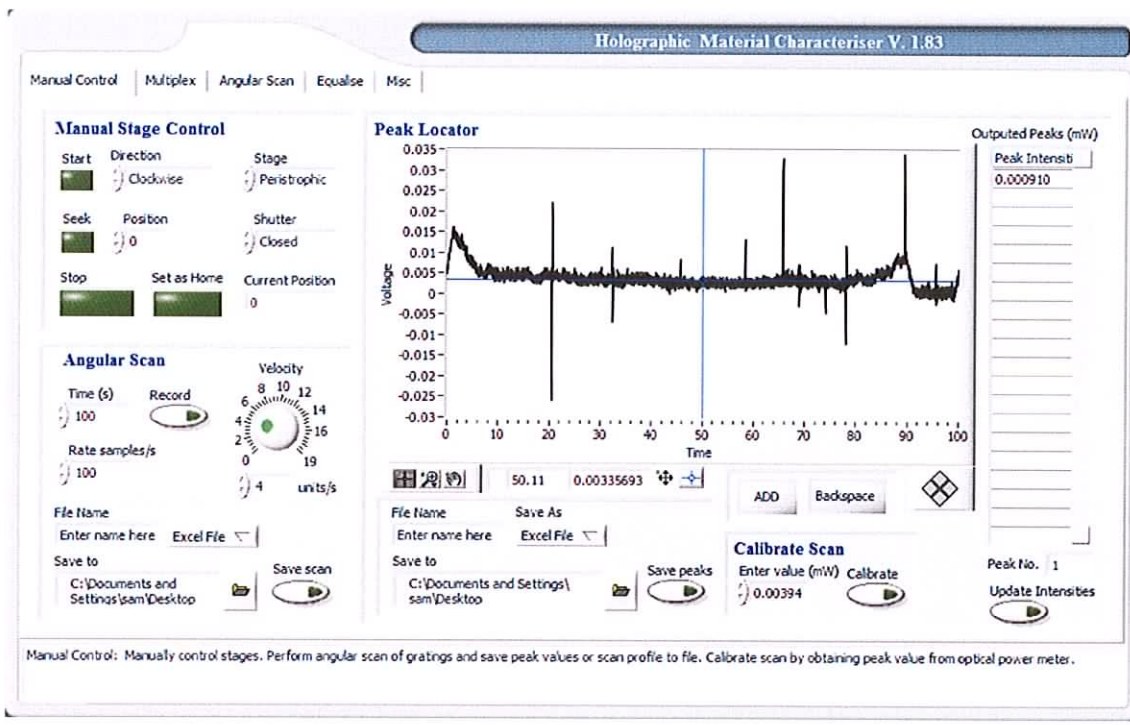

Figure A.1: The *manual control* panel was used for positioning the two rotational stages and can be used for angularly scanning a photopolymer layer while performing data acquisition from an optical power meter.

There are two ways of rotating the stages. The first requires that the user select a clockwise or anticlockwise direction and then press *Start*. The stage will then rotate in the chosen direction until it reaches the hardware limit of its rotation, or until the user presses *Stop*. The second way of rotating a stage requires that the user input the angle to which the stage should be positioned into the *Position* text box; this value may be

positive or negative and is in degrees. Once this value has been entered, pressing the *Seek* button will start the rotational stage rotating until it reaches this new position. Once the desired position has been reached, it is possible to set the position as a reference zero so that all further rotational operations will be with respect to that stage position. Zeroing a new position is achieved by pressing the *Set as Home* button.

Beneath the *Manual Stage Control* is the *Angular Scan* section; this is used to quickly scan the light diffracted from the photopolymer as it is rotated. The rotational sweep of this scan is determined by the velocity of the rotational stage. The velocity is adjusted using the *Velocity dial* and the length of the scan in seconds, this being entered in the *Time (s)* text box. The number of samples that need to be obtained every second is entered in the *Rate samples/s* text box.

To perform the angular scan, the user first selects whether the stage is to rotate peristrophically or angularly, and in what direction it is to rotate. When these values are inputted the user then selects *open* on the *Shutter* control to allow the reference beam to illuminate the photopolymer sample. The user then presses *Record* to start the scan. During the scan, the rest of the software becomes locked and will not respond to inputted user commands. The reason for this is that the data acquisition VI, which LabVIEW uses to control the PCI DAQ card, runs in a while-loop and will only continue once the scan time has elapsed. If it is necessary to stop the scan, this is possible by pressing the *Abort Execution* button located on the top right hand corner of the LabVIEW Front Panel window. It should be noted that the rotational stage would continue to rotate as the rotational controller is now executing the command and not the software. Therefore, the program needs to be run once so that a terminate rotation command can be sent to the stage by pressing the *Stop* button.

Once the scan has been performed, the graph in the *Peak Locator* section will display the scan results. It is possible to save the entire scan by inputting a file name and path in the *Angular Scan* section. The scan data can either be saved as a text or Excel file by clicking on the drop down menu next to the *File Name* text box and then pressing *Save Scan*.

Usually, when multiplexing a number of gratings, the peak intensity information is all that is required from a scan. This can be obtained by first calibrating the scan data so that the y-axis values represent light intensity in milliwatts and not millivolts. To calibrate the scan, it is first necessary to rotate the stage to a well defined peak of suitably high diffraction efficiency. The shutter is then opened so that the intensity of the diffracted light can be obtained directly from the optical power meter. The blue crosshair on the graph is then moved to the centre of the peak in question. The peak value from the optical power meter is entered into the *Calibrate Scan* section and then the *Calibrate* button is pressed.

To start collecting peak data, the blue crosshair is moved to the top of the peak furthest to the left and then the *ADD* button is pressed to obtain its intensity value. The crosshair can then be dragged to the maximum of each peak in turn to obtain the remaining intensity values. As the peak intensities are added, the corresponding value is added to the *Outputted Peaks* array on the right side of the panel. These intensity values can then be sent to the *Equalise* panel to generate new exposure times by pressing the *Update Intensities* button below the intensity array. To delete an incorrect intensity value, the *Backspace* button can be pressed until the erroneous intensity value has been removed. If a peak proved difficult to locate, either because its intensity is relatively low compared to that of its neighbours, or due to being buried in detector noise, it is possible

to zoom in on the peak using the graph viewing tools directly below the graph on the left hand side. It is possible to move the region of the graph by selecting the hand tool and then dragging the graph to the desired position, figure A.2.

Figure A.2: The centre zoom button and hand symbols can be used to manipulate the graph and show areas of interest on the graph in more detail.

It is possible to save the peak information by using the save text boxes located at the bottom of the *Peak Locator* section. The Block Diagram code for this module is shown in appendix B, figure B.7.

Multiplex gratings mode:

The *Multiplex* mode, figure A.3, allows a user to multiplex a set of gratings angularly, peristrophically, or with a combination of the two methods. Before any gratings can be multiplexed it is required that the starting positions of the rotational stages be zeroed; a button is provided for this purpose. An example of how a user would perform a multiplexing experiment is described below.

If for instance a user would like to angularly multiplex 20 gratings with an angular separation of 4 degrees, they would first select *Angular* in the *Main Method* text box, to indicate to the software which kind of multiplexing method to use. The value 20 would then be entered into the *No. of Gratings* text box and the angle 4 would be entered into the *Angular Separation* text box. The amount of time that each grating is to be recorded is entered sequentially into the *Exposure Times* array. The section at the bottom left

hand side of the panel provides text boxes to enter a pre-exposure time and delay between the pre-exposure and the main multiplexing sequence if these are required. Once the user has input the recoding parameters, they can press *Start* to begin the multiplexing recording.

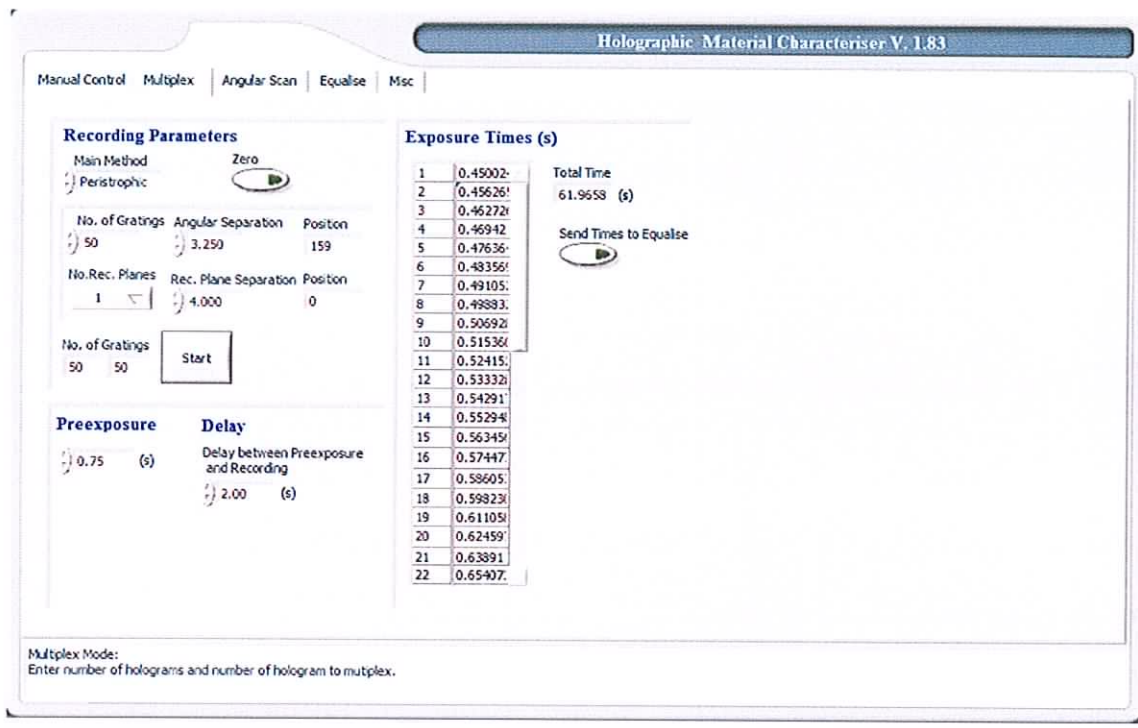

Figure A.3: The *Multiplex* is used to automatically multiplex gratings into a photopolymer layer. Peristrophic, angular, or a combination of the two multiplexing methods can be used.

To record a set of gratings using both multiplexing methods, the number of peristrophic planes needs to be inputted. This is done by selecting a value from the drop down menu labelled *No. Rec. Planes*. Its default value is 1, which means that the same plane is used for all angularly recorded gratings. If this value is set higher than 1, the number of gratings entered in the *No. of Gratings* text box will be recorded angularly in that number of peristrophic planes. For example, if 20 was entered in the *No. of Gratings*, 4 in *No. Rec. Planes*, 2 in *Angular Separation*, and 1.5 in the *Rec. Plane Separation* text

boxes, then 20 gratings would be angularly multiplexed with an angular separation of 2 degrees in four peristrophic planes, which are angularly separated by 1.5 degrees; therefore, 80 gratings would be recorded in total. The code for this module is presented in figure B.8.

Angular scan mode:

The *Angular Scan* mode, figure A.4, allows a user to scan through a specified angular range. The scan can either be peristrophic or angular, this being set in the *Stage* text box. The scan range is set by entering the start and finish angles in *Start Position* and *Finishing Position* respectively, with the angular step increment being entered in the *Interval* text box. Before the scan is initiated by pressing the *Scan* button, it is essential that both shutter controllers be set to normally-closed. It is not necessary to open the reference shutter as this is done by the software when each intensity value is acquired.

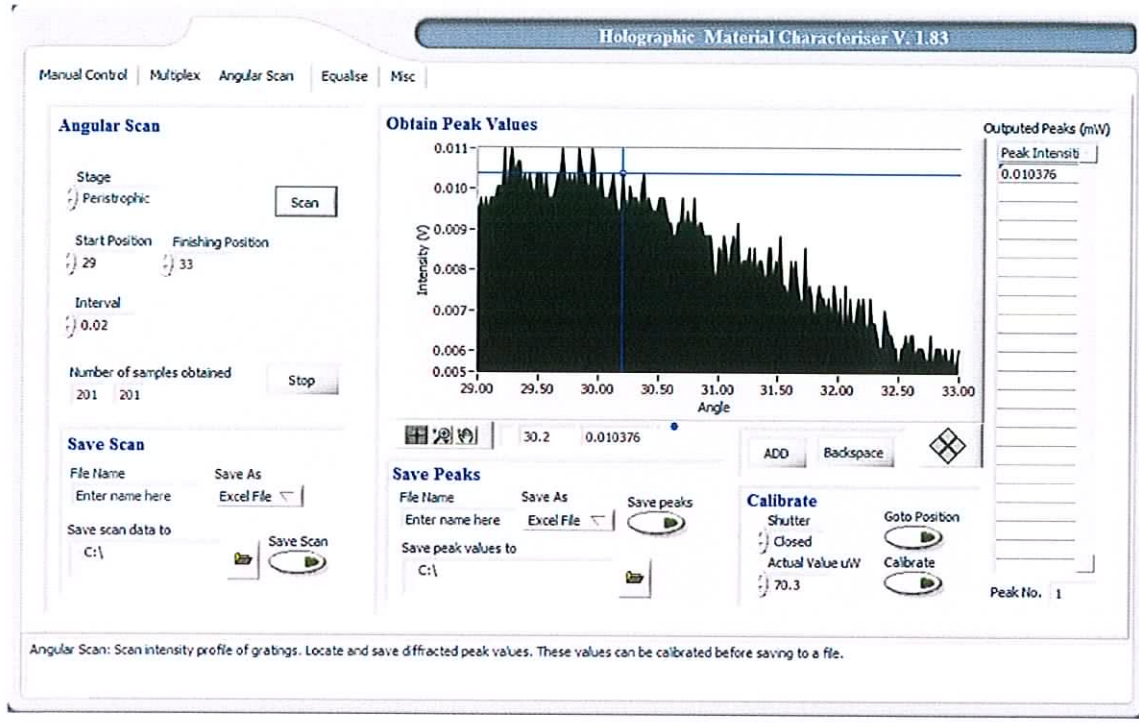

Figure A.4: Using the *Angular Scan* panel enables a specific range of angles to be scanned and intensity information to be obtained by means of data acquisition.

As with the *Manual Control* mode, the raw scan can be calibrated by positioning the stage so the peak intensity of a relatively high diffraction efficiency peak can be obtained. To achieve this, the blue crosshair is first centred over the peak. The *Goto Position* button is then pressed so that the stage rotates to this new position. To obtain the peak intensity value, the reference beam shutter is opened by selecting *Open* from the *Shutter* menu and the value is read from the optical power meter. The intensity value is then entered into the *Actual Value* text box and the *Calibrate* button is pressed.

The raw scan data can be saved to file by filling in the desired name, file path location, and file type into the *Save Scan* section. The peak information can be obtained and saved in the same manner as outlined in the *Manual Control* section. The *Angular Scan* LabVIEW code can be found in figure B.9.

Equalise gratings mode:

As discussed in sections 5.1 and 6.6, multiplexing N number of gratings in the same volume of photopolymer with equal exposure energy results in a huge variation in grating strengths because the strengths scale as $1/N^2$. It is therefore necessary to equalise the strengths for accurate determination of M/#. One method of equalisation is to adjust the individual exposure energies of each grating in such a way that each grating equally shares the overall dynamic range of the material and so that all gratings have equal diffraction efficiencies.

By adjusting the exposure energy density for each grating, it was possible to equalise an entire set of multiplexed gratings. This was achieved by keeping the exposure intensity constant whilst varying the exposure time. The exposure times were calculated by means of an iterative exposure algorithm, described in section 6.6. The *Equalise* mode, figure A.5, allows these exposure times to be generated by entering intensity values for previous gratings recorded in the same material. Firstly, the number of gratings multiplexed in the previous iteration is entered in the *No. of Gratings* text box in the *Recording Parameters* section. If the gratings are to be recorded for the same length of time, this is entered into *Constant Time*. If not, this text box should be supplied with a zero value to inform the software that variable exposure times are to be read in from the *Intensities* array. The dark current, combined exposure intensity, and the reference beam intensity value from the previous multiplexing experiment should be entered into the *Dark Current*, *Comb. Int*, and *Input* text boxes respectively; the intensity should always be entered in milliwatts/cm^{-2}.

The *Intensities* array should be filled in with the diffracted intensity of each grating peak from the previous experiment. This can be done manually, or alternatively, can be supplied with the located peak values that were inputted in the *Manual Control* panel. It should be noted that this should be carried out directly after obtaining the peaks in the *Manual Control* panel by pressing *Update Intensities,* otherwise these values will be deleted from the panel when *Save Peaks* is pressed or when a different panel is chosen. Next to the "Intensity" array is another array text box labelled *Exposure Times*. The time used to record each grating should be entered in this array. This can be done manually or by returning to the *Multiplex* panel and clicking *Send Times to Equalise* if they are the corresponding recording times.

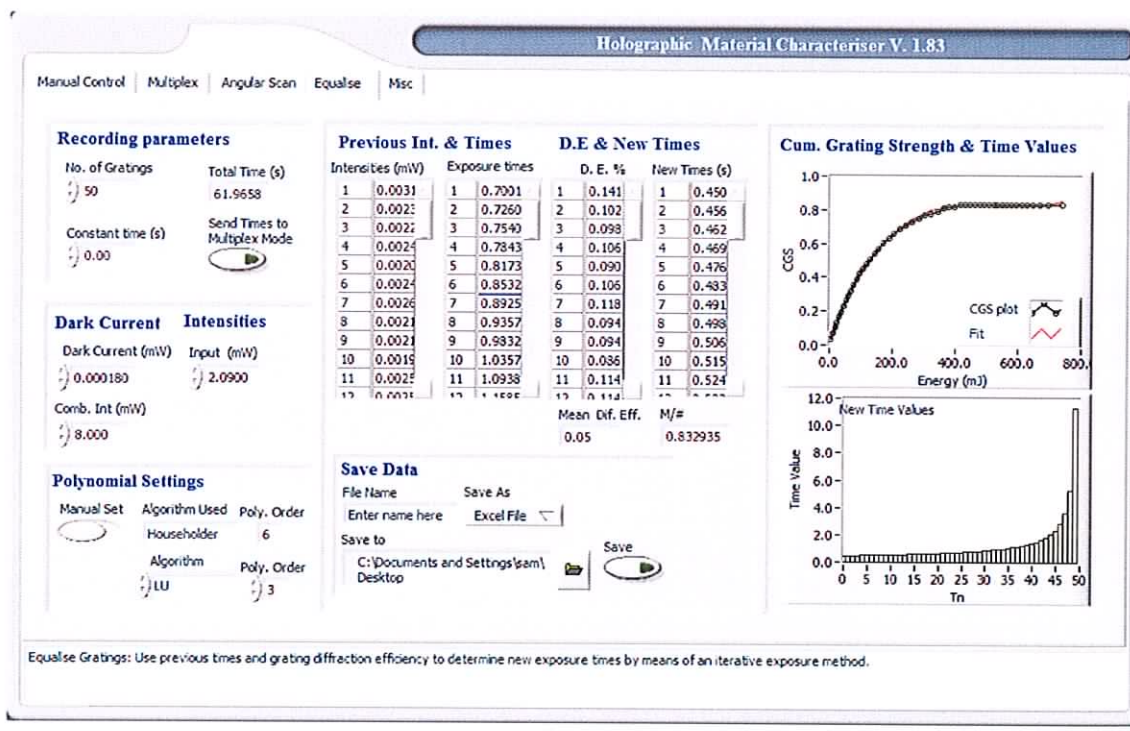

Figure A.5: The *Equalise* panel is used to generate a set of exposure times by means of an exposure scheduling algorithm. The new times can then be used to equalise the strengths of the multiplexed gratings.

To calculate the exposure times it is necessary to apply a polynomial fit to the cumulative grating strength curve, which is graphed in the top right corner of the panel. Six fitting algorithms can be selected to improve the overall fit of the curve, these being, single value decomposition (SVD), Givens, Givens2, Householder, LU decomposition, and Cholesky. The polynomial order can be varied, but it is recommended that it remain lower than or equal to the number of grating intensities minus one, i.e. N-1, otherwise an erroneous fit will be generated. As new information is supplied to the *Equalise* panel, the software updates the fit and exposure times automatically. The software also has the capability of testing all fitting algorithms for seven polynomial orders and determining which algorithm and order yield the lowest mean squared error, these then being applied to generate the new exposure times. This however, does not always result in the best fit as the polynomial VI proves to be unstable with certain settings regardless of whether they have the lowest mean squared error. To work around this, it is possible to set the *Poly. Order* and *Algorithm Used* manually, this being done by switching the slide button in the *Polynomial Settings* section to *Manual Set* and then adjusting these parameters directly. A graph located in the lower right corner of the panel can be used to qualitatively assess the new exposure times.

In addition to generating new exposure times, the panel displays the diffraction efficiency of each grating and the mean diffraction efficiency. The M/# value displayed by the panel is calculated using the formula,

$$M/\# = \sum_{i=1}^{N} \sqrt{\eta_i}$$

where the square root of the diffraction efficiency η for each grating is summed.

Finally, the newly generated exposure times can be sent to the *Multiplex* panel for further equalisation by pressing the *Send Times to Multiplex Mode* button. If required, it is possible to save the data from this scheduling iteration by providing a file path and name in the lower *Save Data* section at the bottom of the panel and pressing *Save*. This file will contain the grating exposure intensities, times used to record each grating, and the individual diffraction efficiencies and new exposure times generated. In addition, the file contains the information for plotting the cumulative grating strength curve. All these data are tabulated in columns in either Excel or text format. The code written to equalise the gratings can be seen in figure B.10.

Mode for modelling Bragg condition and calculating optical setup parameters:

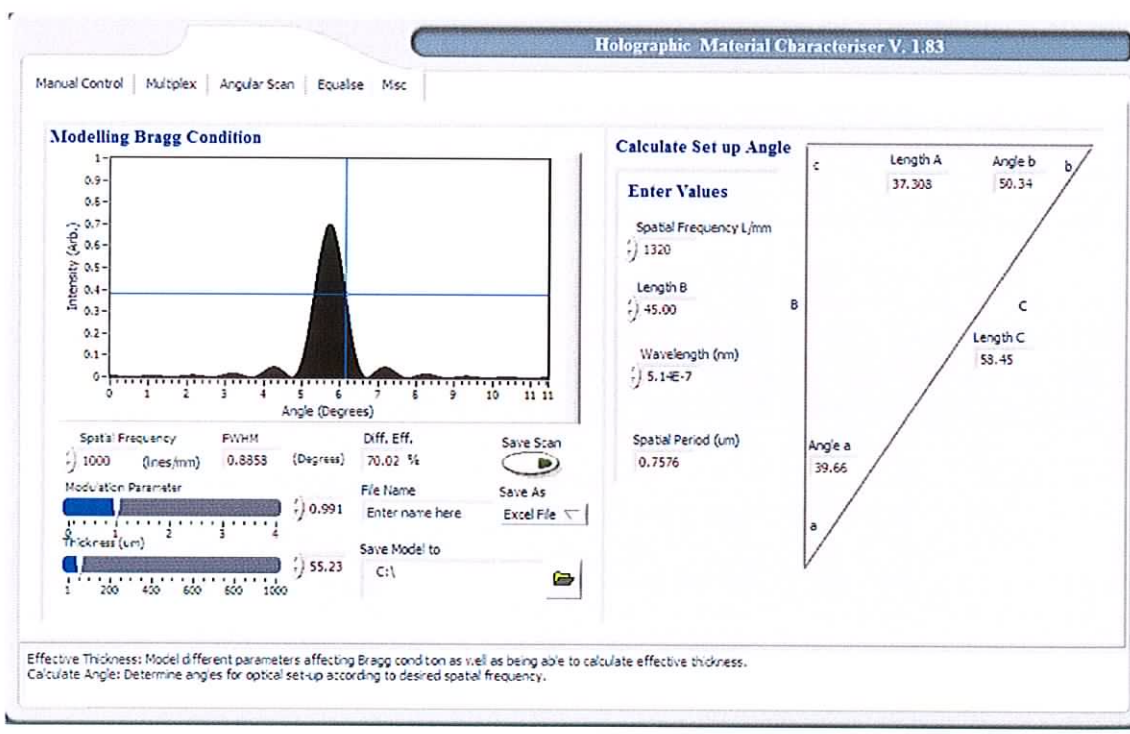

Figure A.6: The diffraction efficiency dependency on deviation from the Bragg angle for a number of parameters can be modelled using the *Misc* mode. The angles and sides of a right-angled triangle, forming the recording setup, can be calculated using this mode.

The *Misc* mode, figure A.6, has two distinct functions. The first one is modelling the Bragg curve of a transmission phase grating in terms of diffraction efficiency drop off vs. angle when certain parameters are varied. Secondly, it can be used to quickly calculate the necessary lengths and angles of a holographic recording setup based on a right-angled triangle configuration.

The *Modelling Bragg Condition* section of the panel allows the user to observe what happens to a transmission phase grating when the layer thickness, modulation parameter, and spatial frequency are adjusted. The full-width half-maxima value and percentage diffraction efficiency are displayed in the text boxes labelled *FWHM* and *Diff. Eff.* respectively. A graph showing the resultant change in absolute diffraction efficiency vs. angle is displayed as well. The equation used to model these parameters takes the form

$$\eta = \frac{\sin^2 \sqrt{(\phi^2 + \chi^2)}}{(1 - \chi^2 / \phi^2)},$$

and is described in more detail in section 6.1. The dependency models may be saved as text or Excel files by clicking on the drop down menu next to the *File Name* text box and then pressing *Save Scan.*

The *Calculate Setup Angle* section of the panel allows the user to quickly adjust the system so that different spatial frequency gratings can be recorded. The desired spatial frequency, the length of the long arm of the triangle, and the laser wavelength are entered into *Spatial Frequency L/mm*, *Length B*, and *Wavelength*, respectively. Once entered, the spatial period that will result from the inputted parameters and the lengths

of each side and the angles of the triangle are displayed. The block diagram code for the *Misc* mode is seen in figure B.11.

B. Block diagrams of photopolymer characterisation software

Appendix A is essentially a manual describing how to effectively operate each module of the control software used for photopolymer characterisation. Each of the modules was written using LabVIEW and so has a corresponding block diagram where the diagrammatical code is represented and compiled at runtime. Images of each of the module's block diagrams are presented below. The control software is contained on a CD accompanying this thesis.

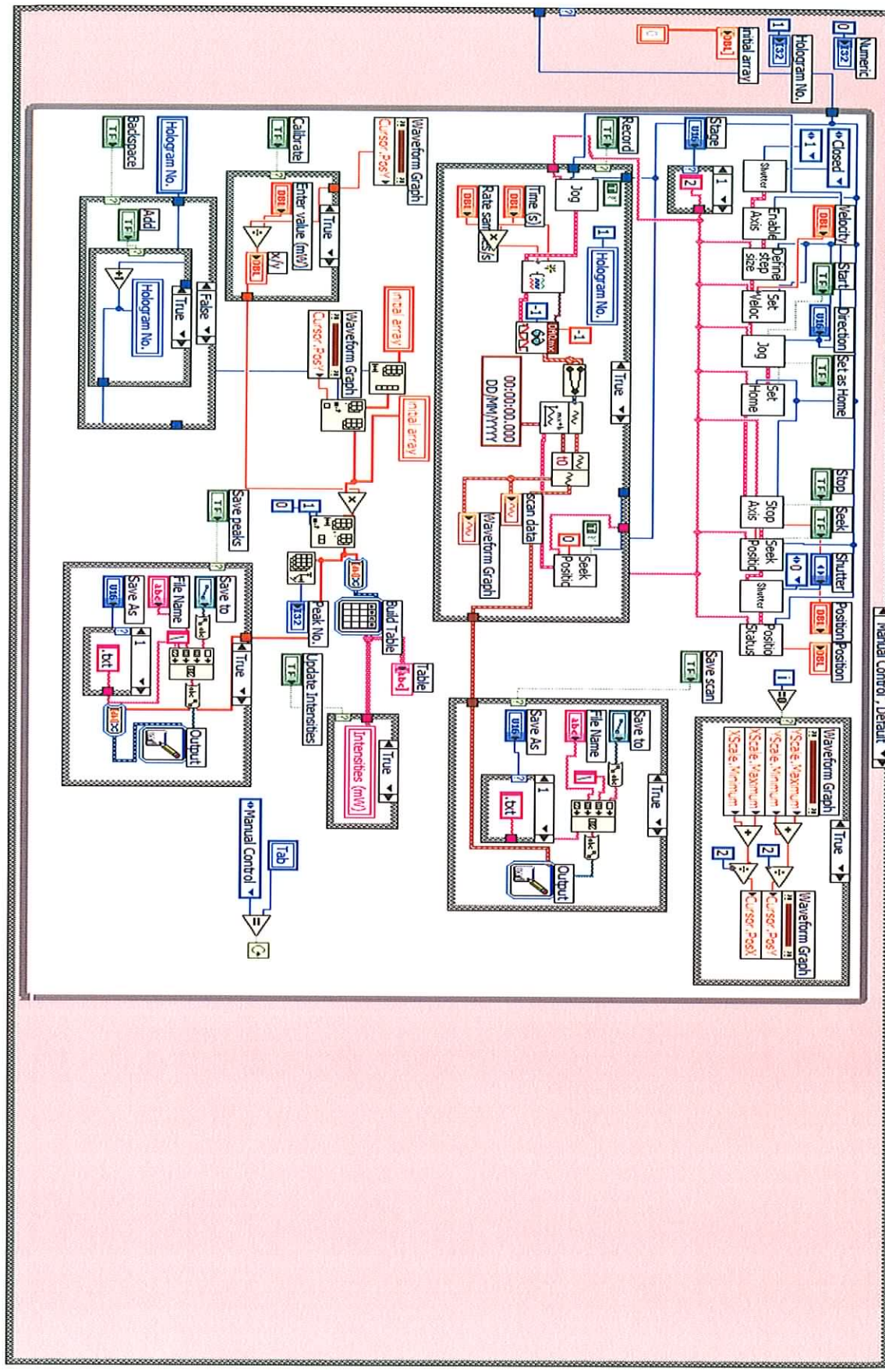

Figure B.7: Block diagram for *Manual Control* mode.

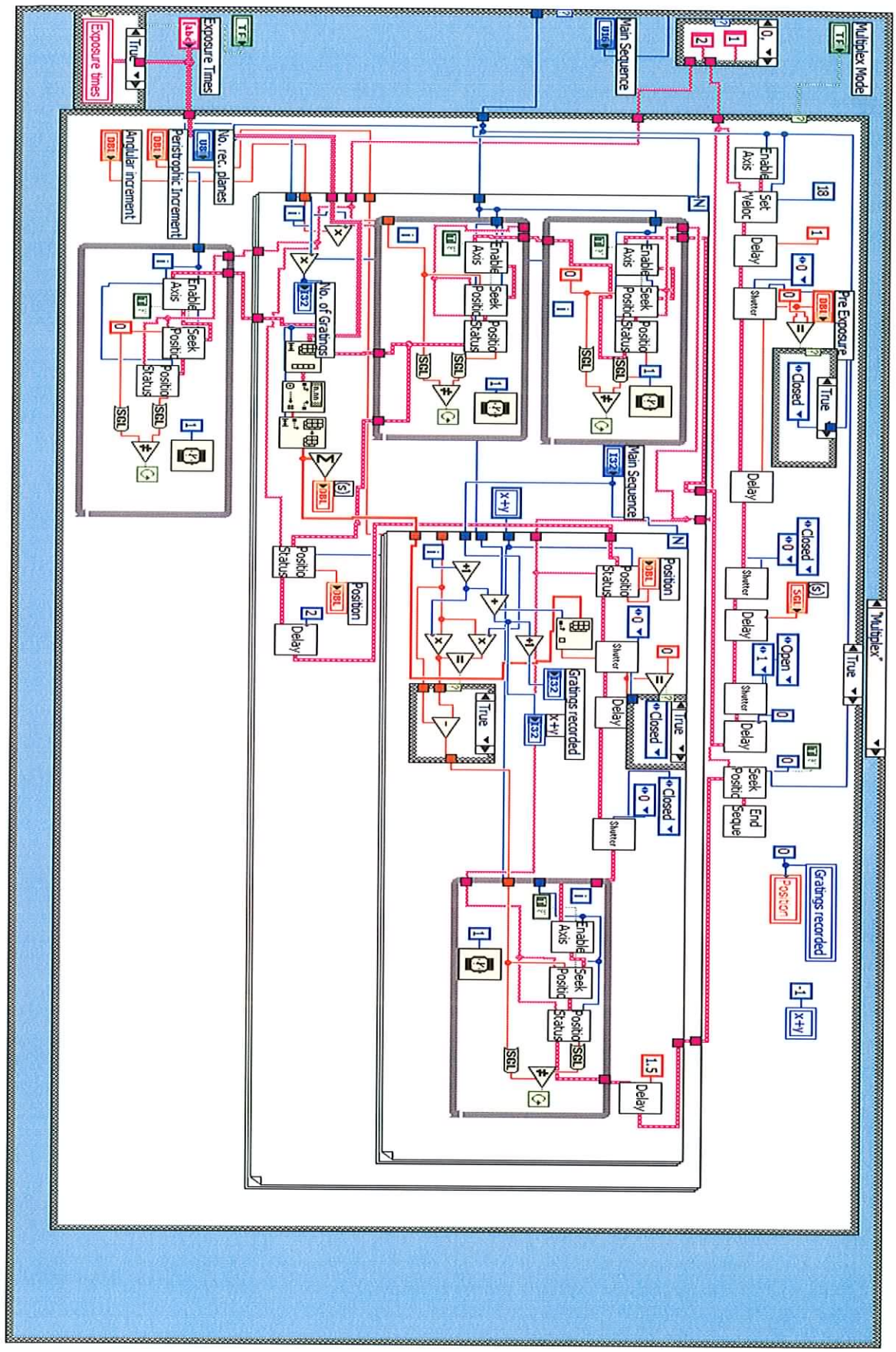

Figure B.8: Block diagram for *Multiplex* mode.

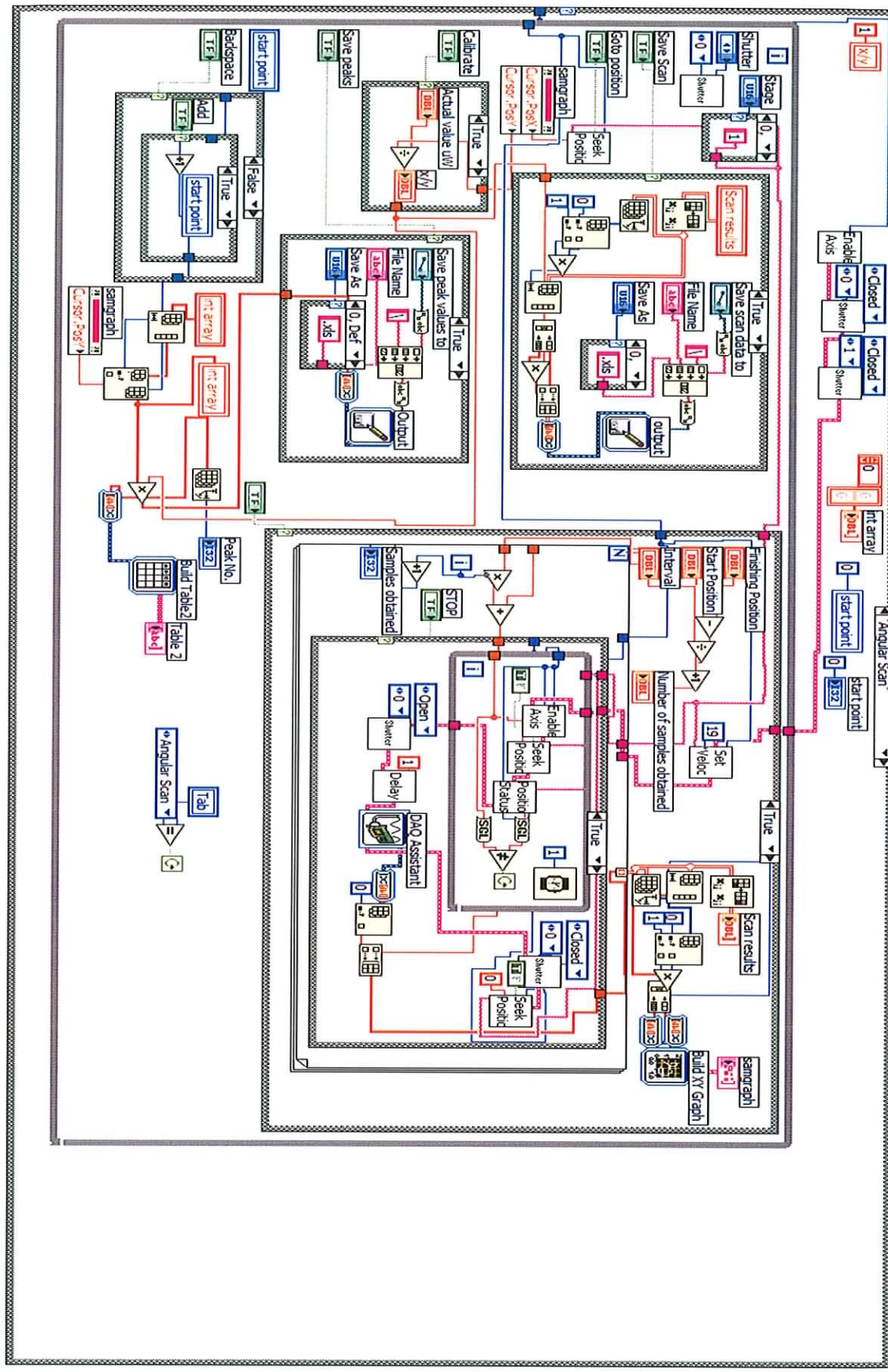

Figure B.9: Block diagram for *Angular Scan* mode.

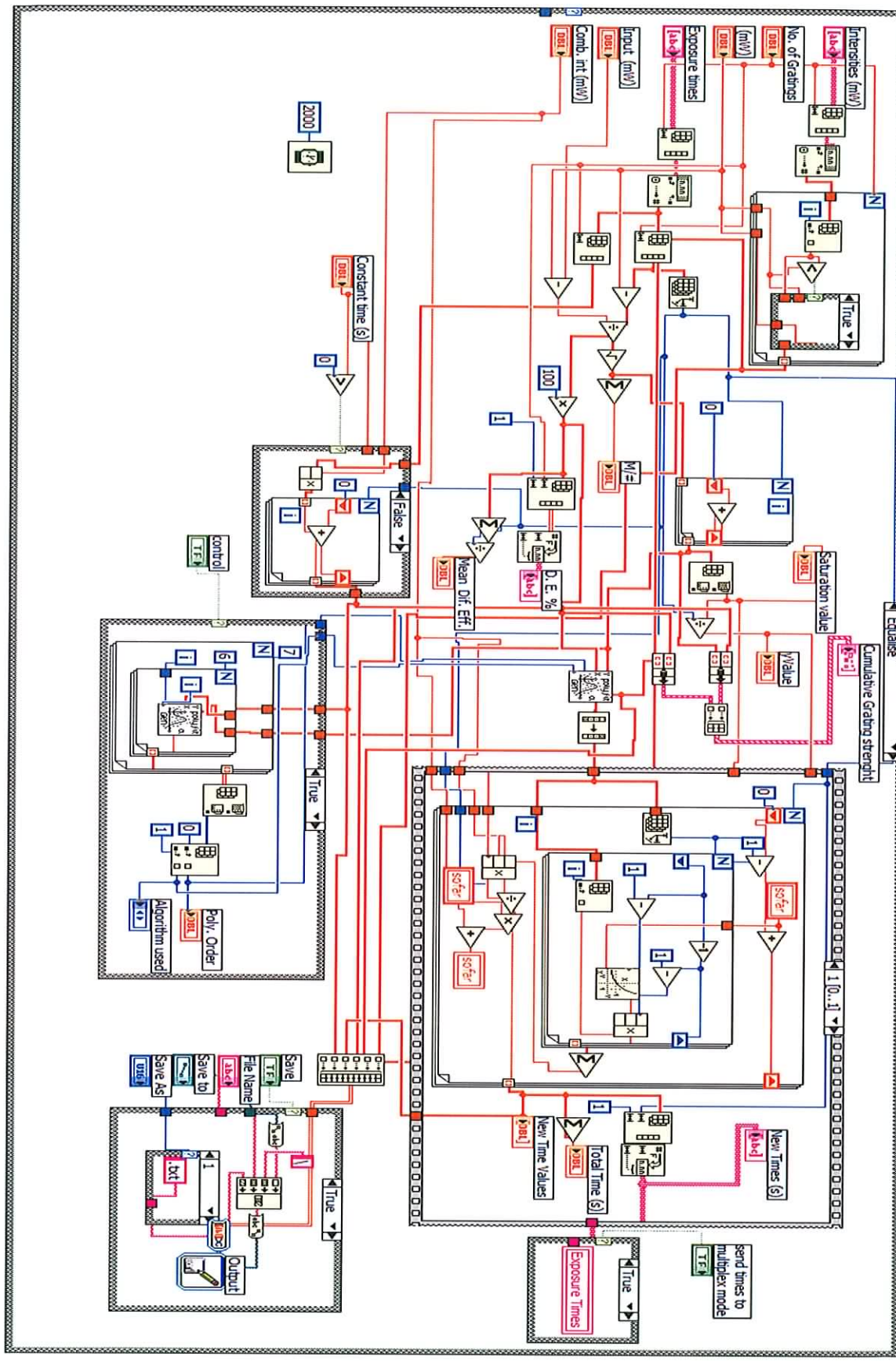

Figure B.10: Block diagram for *Equalise* mode.

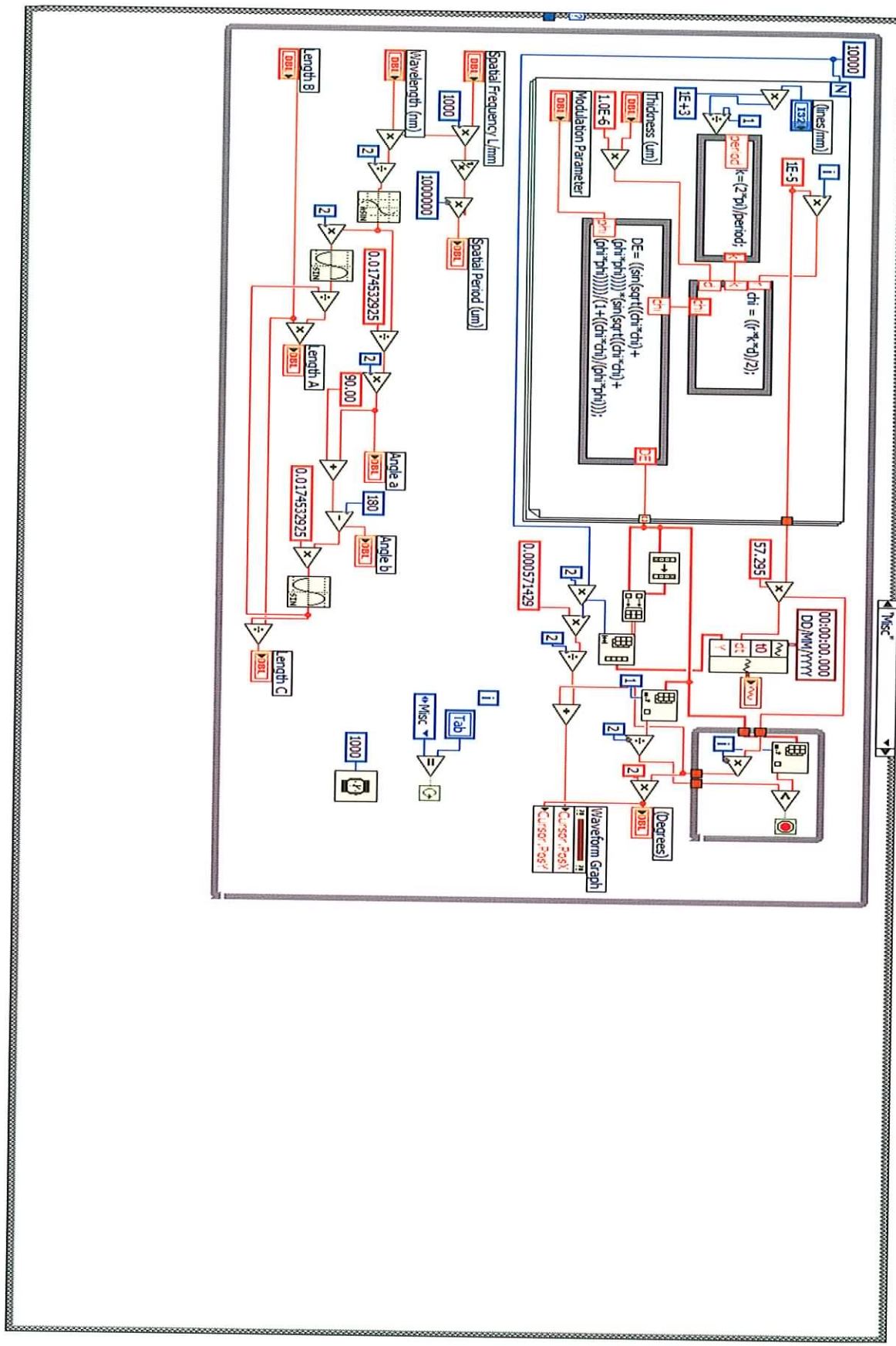

Figure B.11: Bragg condition modelling and setup configuration calculation code.

C. Publications

Journal Publications

- H. Sherif, I. Naydenova, S. Martin, C. McGinn, and V. Toal "Characterization of an acrylamide-based photopolymer for data storage utilizing holographic angular multiplexing", Journal of Optics A: Pure Applied Optics, 7, 255-260, 2005.

Conference Proceedings

- H. Sherif, I. Naydenova, S. Martin, C. McGinn, G. Berger, C. Denz, V. Toal, "Study of an acrylamide-based photopolymer for use as a holographic data storage medium", Proceedings of SPIE, Opto-Ireland, Dublin, April, 305 - 313, 2005.

- Naydenova, H. Sherif, S. Mintova, S. Martin, V. Toal, "Holographic recording in nanoparticle-doped photopolymer", International Conference on Holography, Optical Recording and Processing of Information, Varna, May 2005.

- E. Mihaylova, I. Naydenova, H. Sherif, S. Martin, V. Toal, Application of photopolymer holographic gratings in electronic speckle pattern shearing interferometry", Proceedings of SPIE, Vol. 5249, 318-326, 2003.

Poster Presentations

- H. Sherif, I. Naydenova, S. Martin, V. Toal, G. Berger, C. Denz, "Investigation of an acrylamide-based photopolymer in terms of data-page recording and temporal stability characteristics", IOP spring weekend meeting, Newbridge, March 2005.

- H. Sherif, I. Naydenova, S. Martin, C. McGinn, V. Toal, "Equalisation and analysis of angularly multiplexed holograms using an acrylamide-based photopolymer", IOP spring weekend meeting, Armagh, 2004.

- I. Naydenova, H. Sherif, S. Martin, V. Toal, S. Mintova, "Influence of Si-MFI nanoparticles on the holographic properties of acrylamide-based photopolymer" Scientific & Social Programme 29th Annual Microscopy Ireland, Dublin, September, 2005.

- H. Sherif, I. Naydenova, S. Martin, C. McGinn. V. Toal, "Study of an acrylamide-based photopolymer for use as a holographic data storage medium", SPIE's Opto-Ireland, Dublin, April 2005.

- H. Sherif, I. Naydenova, S. Martin, C. McGinn, V. Toal, "Equalisation and Analysis of Angularly Multiplexed Holograms using an Acrylamide-Based Photopolymer", Cost P8, "Materials and Systems for Optical data storage", meeting Ancona, Italy, 29-30 April.

- V. Toal, "Nanoparticle doped acrylamide-based photopolymer for optical data storage applications", Novel Optical Materials and Applications, Cetrara, Italy, 29 May – 04 June 2005. Presented without authors.

Abstract

- I. Naydenova, H. Sherif, S. Mintova, S. Martin, V. Toal, "Nanoparticle-doped photopolymer for holographic applications", Catalytic processes on advanced micro- and mesoporous materials 2-5 September 2005, Nesebar, Bulgaria.

- I. Naydenova, H. Sherif, S. Martin, V. Toal, S. Mintova, "Influence of Si-MFI nanoparticles on the holographic properties of acrylamide-based photopolymer" Scientific & Social Programme 29th Annual Microscopy Ireland, Dublin, September, 2005.